

VOLUME 4 / ISSUE 3 / 2021

PAGES 161-261

EXPERIMENTAL BIOMEDICAL RESEARCH

ISSN 2618-6454

[http:// www.experimentalbiomedicalresearch.com](http://www.experimentalbiomedicalresearch.com)

EXPERIMENTAL BIOMEDICAL RESEARCH

VOLUME 4 / ISSUE 3 / JUL-AUG-SEP / 2021

EDITOR-IN-CHIEF

Professor, M.D., Hayrettin Ozturk, Dept. Pediatric Surgery and Pediatric Urology, Bolu Abant Izzet Baysal University, Medical School, Bolu, Turkey

SECTION EDITORS

Associate Professor, M.D., Gulali Aktas, Dept. Internal Medicine, Bolu Abant Izzet Baysal University, Medical School, Bolu, Turkey

Professor, M.D., Yusuf Yagmur, Dept. General Surgery, Medical Park, Gaziantep, Turkey

Professor, M.D., Mete Kaya, Dept. Pediatric Surgery, Health Sciences University, Sevkett Yilmaz Education and Research Hospital, Bursa, Turkey

Associate Professor, M.D., Erkan Kilinc, Dept. Physiology, Bolu Abant Izzet Baysal University, Medical School, Bolu, Turkey

Assistant Professor, Ph.D., Muhammad Akhlaq, Dept. of Pharmaceutics, Faculty of Pharmacy, Gomal University, D.I.K Khyber Pakhtoonkhwah, Pakistan

Professor, M.D., Yalcin Karagoz, Dept. Biostatistics, Cumhuriyet University, Medical School, Sivas, Turkey

ASSOCIATE EDITORS

Assistant Professor, M.D., Emine Ozsari, Dept. Chest Diseases, Bolu Abant Izzet Baysal University, Medical School, Bolu, Turkey

Assistant Professor, M.D., Fatih Hilmi Cetin, Dept. Child and Adolescent Mental Health, Selcuk University, Medical School, Konya, Turkey

Associate Professor, M.D., Ummugul Uyeturk, Dept. Oncology, Bolu Abant Izzet Baysal University, Medical School, Bolu, Turkey

Specialist, M.D., Songul Peltek Ozer, Dept. Pathology, Bolu AIBU Training and Research Hospital, Bolu, Turkey

EDITORIAL BOARD MEMBERS

Professor, MBBS, DCH. M.D., Muslim Uddin Sabuj, Child Health Specialist, Head of the Department, Chattagram International Medical College (CIMC), Bangladesh

Professor, M.D., med. Amir Minovi, Chair and Director, Department of Otorhinolaryngology, St. Elisabeth-Krankenhaus Academic Teaching Hospital Cologne University Cologne, Germany

Professor, M.D., Turan Aslan, Dept. Infectious Diseases and Clinical Microbiology, Balikesir University, Medical School, Bolu, Turkey

Liping Li, M.D., Ph.D., Eunice Kennedy Shriver National Institute of Child Health and Human Development, National Institute of Health, Bethesda, MD, USA

Associate Prof., M.D., Nedaa Skeik, Vascular Medicine, Minneapolis Heart Instit., MN, USA

Professor, M.D., Fahri Yilmaz, Dept. Pathology, Sakarya University, Medical School, Sakarya, Turkey

Associate Prof., M.D., Serdar Ceylaner, Dept. Genetic, Intergen Genetic Diseases Diagnostic Research and Application Center, Ankara, Turkey

Associate Professor, M.D., Gulali Aktas, Dept. Internal Medicine, Bolu Abant Izzet Baysal University, Medical School, Bolu, Turkey

Associate Prof., M.D., Suleyman Ipekci, Dept. Endocrinology, Selcuk University, Faculty of Medicine, Konya, Turkey

Professor, M.D., Amir Hossain, Chattagram International Medical College (CIMC), Chittagong, Bangladesh

Professor, M.D., Kahraman Ozturk, Dept. of Hand Surgery, Health Sciences University, Istanbul, Turkey

Professor, M.D., Ahmet Ural, Department of Otorhinolaryngology, Bolu Abant Izzet Baysal University, Medical School, Bolu, Turkey

Associate Prof., M.D., Mukremin Uysal, Dept. Oncology, Afyon Kocatepe University, Medical School, Afyon, Turkey

Associate Prof., M.D., Mehmet Ozen, Dept. Hematology, Ufuk University, Medical School, Ankara, Turkey

Professor, M.D., Yasar Bukte, Dept. Radiology, Health Sciences University, Istanbul, Turkey

Professor, M.D., Nebil Yildiz, Dept. Neurology, Bolu Abant Izzet Baysal University, Medical School, Bolu, Turkey

Professor, M.D., Ramazan Topsakal, Dept. Cardiology, Erciyes University, Medical School, Kayseri, Turkey

Associate Prof., M.D., Hikmet Tekce, Dept. Internal Medicine-Nephrology, Bolu Abant Izzet Baysal University, Medical School, Bolu, Turkey

Professor, M.D., Hasan Orucoglu, Dept. Endodontics, Faculty of Dentistry, Bolu Abant Izzet Baysal University, Bolu, Turkey

Professor, M.D., Fuat Akpınar, Dept. Orthopedics and Traumatology, Istanbul Medeniyet University, Istanbul, Turkey

Associate Prof., M.D., Furkan Erol Karabekmez, Dept. Plastic and Reconstructive Surgery, Health Sciences University, Ankara, Turkey

Professor, M.D., Muhammed Guzel Kurtoglu, Dept. Microbiology, Bolu Abant Izzet Baysal University, Medical School, Bolu, Turkey

Associate Prof., M.D., Memis Hilmi Atay, Dept. Hematology, Ondokuz Mayıs University, Medical School, Samsun, Turkey

Professor, Ph.D., Erol Ayaz, Dept. Parasitology, Bolu Abant Izzet Baysal University, Medical School, Bolu, Turkey

Professor, M.D., Gokhan Kirbas, Dept. Chest Diseases, Dicle University, Medical School, Diyarbakir, Turkey

Associate Prof., M.D., Basri Cakiroglu, Dept. Urology, İstanbul Atlas University, Medical School, İstanbul, Turkey

Professor, M.D., Kemal Nas, Dept. Physical Medicine and Rehabilitation, Sakarya University, Medical School, Sakarya, Turkey

Professor, M.D., Huseyin Buyukbayram, Dept. Chest Diseases, Dicle University, Medical School, Diyarbakir, Turkey

Associate Professor, M.D., Akif Hakan Kurt, Dept. Pharmacology, Bolu Abant Izzet Baysal University, Medical School, Bolu, Turkey



AUTHOR GUIDELINES

INSTRUCTIONS FOR AUTHORS

Author Guidelines

Instructions for Authors

Experimental Biomedical Research publishes articles in English. Since the journal does not offer translation services, if the language of the manuscripts is not enough, the editors may refuse the manuscript or ask the author to seek language editorial services to bring the manuscript to minimum standards for the review process. If your manuscript is accepted it will be checked by our copyeditors for spelling and formal style before publication.

If you would like to submit a Review, please contact Editor-in Chief at info@experimentalbiomedicalresearch.com.

Online Submission

The articles must be submitted by the corresponding author via the Online Submissions System. If authors encounter technical problems with online submission, they may contact with support team at info@experimentalbiomedicalresearch.com.

Corresponding author

The corresponding author's must do: complete submission of manuscript files; storage of the article and all related documents and giving original data when necessary; contributions of the authors and explanations of conflict of interest disclosures; approval for submission; and the final proof control.

ORCID ID

[ORCID](#) IDs of the corresponding author and other authors must be submitted during the registration process. This section is mandatory.

As part of our commitment to ensuring an ethical, transparent and fair peer review process, Experimental Biomedical Research is a publisher who signed ORCID open letter. ORCID provides a unique and persistent digital identifier that distinguishes researchers from every other researcher, even those who share the same name, and, through integration in key research workflows such as manuscript and grant submission, supports automated linkages between researchers and their professional activities, ensuring that their work is recognized.

The collection of ORCID iDs from corresponding authors is now part of the submission process of this journal. If you already have an ORCID iD you will be asked to associate that to your submission during the online submission process. We also strongly encourage all co-authors to link their ORCID ID to their accounts in our online peer review platforms. It takes seconds to do: click the link when prompted, sign into your ORCID account and our systems are automatically updated. Your ORCID iD will become part of your accepted publication's metadata, making your work attributable to you and only you. Your ORCID iD is published with your article so that fellow researchers reading your work can link to your ORCID profile and from there link to your other publications.

If you do not already have an ORCID iD please follow this [link](#) to create one.

Author Declaration, Funding and Financial Conflicts of Interest

Authors should provide a cover letter declares: that the article submitted has not been published elsewhere and is not under review; that the submission has been approved by all co-authors and, if necessary, by the responsible authorities and the institute. The publisher will not be responsible in cases of any claims for compensation.

All authors should disclose commercial ties or consulting, stock or share interests or patent license arrangements that can be viewed as a conflict of interest in relation to the manuscript presented ([Author Declaration Form & Conflict Of Interest Statement](#)).

Permissions

Obtaining permission from the copyright owner/ owners is obligatory for figures, tables or texts that previously published elsewhere if the authors want to add them to their manuscripts. Without this evidence, any material used in the article will be deemed to be an original product of the authors.

Units of measurement

The *International System of Units* (SI) is the modern form of the metric system, and is the most widely used system of measurement. Therefore, units of measurement should be presented using the International System of Units in Experimental Biomedical Research.

Abbreviations

Abbreviations are defined at the first mention and are then used continuously. The authors should always be used standard abbreviations and generic names of the drugs. Additionally, the abbreviations presented in the Tables and Figures must be

compatible with SI. If registered trademarks are used, the name and country of the manufacturer must be given in parentheses following the generic name on the first use.

Preparation of Manuscript

Title Page

The title page should include: manuscript title, the name(s), the affiliation(s) and address (es) of the author(s).

The corresponding author information should include the e-mail address, the 16-digit ORCID ID, telephone number(s) and full mailing address.

Disclosure of conflict of interest, funding organizations and acknowledgments of people, grants, funds, etc. should be placed in the last section on the title page.

Abstract

Abstracts must not exceed 250 words. The abstract should describe with subheadings; *Aim, Method, Results, and Conclusions*. Abstracts should not contain any unexplained abbreviations or references. It is crucial that the abstract be an accurate summary of the contents of the paper.

Keywords

4 to 6 keywords are sufficient which can be recommended by the "[Index Medicus Subject Headings](http://www.nlm.nih.gov/mesh/meshhome.html)": **MeSH** (<http://www.nlm.nih.gov/mesh/meshhome.html>).

Main Text

The main text should describe with subheadings; *Introduction, Methods and Materials, Results, Discussion and Conclusions*.

Manuscripts should be submitted in Microsoft Office Word formats and arranged as 12-point Times New Roman for text.

References to literature, figures and tables should be placed in the order of their citation in the text. The Author(s) should not use italics, bold or underlined words in the texts. Please use only generic names of drugs.

Introduction: Introduction to a research report should provide a context for the study and specify the particular aims of the reported study. In this section, the emphasis should be on brevity, for the introduction is not meant to be a detailed review but merely a capsule summary that provides a rationale for the second and most important part which is a clear statement as to why the study was undertaken.

Methods and Materials : In this section, the researcher should clearly write the methods used. The materials section should contain the information requested when the reported results need to be expanded and elaborated. It is also important to carry out appropriate statistical tests and to state the sources of the drugs and chemicals used.

Results: In this section, the authors should clearly written information collected using the methods described to achieve the objectives of the study.

Discussion: The discussion section is critical, the information collected is evaluated in relation to the objectives of the study and the context in which the study begins, and any inconsistency between the results is explained and elaborated.

References: It is important that the authors cite appropriate and up-to-date articles for information and comments in the text.

Conflicts of Interest

Authors must declare all relevant interests that could be perceived as conflicting. Authors should explain why each interest may represent a conflict. If no conflicts exist, the authors should state this. Submitting authors are responsible for coauthors declaring their interests.

References

Number references in the order they are mentioned in the text; do not alphabetize. Reference citations in the text should be identified by numbers in square brackets. In listing references (Format AMA), follow NLM Style Guide, abbreviating names of journals according to Index Medicus. Indicate each author's family name followed by a space and initials closed up without periods. Author names should be separated with a comma, never using the conjunction "and" between entries. All authors must be listed for papers with 1 to 3 authors. For papers with more than 3 authors, only the first 3 authors must be listed, followed by et al.

For online journals or articles published online ahead of print, provide the DOI number, if possible, rather than the URL. URLs used in references will not be made hyperlinks.

Journal article

List the first three authors;

Bothra J, Shah H, Tiwar C. Classic Wilms' tumor with raised alpha-fetoprotein levels: A case report and literature review. *Pediatr Urol Case Rep.* 2017; 4(1):238-42.

More than three authors followed by et al.

Nondel B, Lazarus J, Howlett J, et al. Donated staghorn kidney stone in an HIV positive pediatric kidney transplant recipient. *Pediatr Urol Case Rep.* 2017; 4(4):350-55.

Chapter in a book

Luck H. Catalase. In: Bergmeyer HU, editor. *Methods of Enzymatic Analysis*. New York: Academic Press; 1971. p. 885-93.

Online document

Doe J. Title of subordinate document. In: *The dictionary of substances and their effects*. Royal Society of Chemistry. [cited 2016 Dec 27]. Available from: [http://www.rsc.org/dose/title of subordinate document](http://www.rsc.org/dose/title%20of%20subordinate%20document).

The authors are responsible for the accurate and in full presentation in accordance with the journal's style of references.

Preparation of Figures and Tables

The figures and tables should be uploaded electronically by a separate file and should be stated consecutively in the text. Each table should have an explanatory heading, and if numerical measurements are made, the units should be added to the column header. Figures should be presented in vector image formats (Illustrator, EPS, WMF, FreeHand, CorelDraw, PowerPoint, Excel etc.) or in bitmap formats (Photoshop, TIFF, GIF, JPEG, etc.). Bitmap images should be at least 300 dpi resolution.

Supplementary Materials

Authors can submit one file of supplementary material such as audio files, video clips, or datasets. A section titled "Supplementary Material" should be included before the references list with a concise description for each supplementary material file. Authors are responsible for providing the final supplementary materials files that will be published along with the article.

English Language Editing

Editors and reviewers should ensure the clarity of English language of the article in assessment of the manuscript.

If any help needed in writing in English one can consider the following:

- Ask for help from a co-worker who is a native English speaker in sake of clarity of the text.
 - Applying to a professional english language editing service to improve the quality of the language and grammar of the text.
- Authors should aware that the use of a language editing service does not warrant an article to be accepted for publication in this journal.

ETHICAL STANDARDS

Ethical Responsibilities of Authors

Experimental Biomedical Research journal will follow the **Committee on Publication Ethics (COPE)** guidelines on how to deal with potential acts of misconduct. For this reason, authors should protect the journal trust, the professionalism of the scientific authorship, and must refrain from misrepresenting the consequences of research that could destroy all scientific effort.

Plagiarism checking

Articles sent to Experimental Biomedical Research journal are checked for possible plagiarism by using an appropriate software (**iThenticate**). However, corresponding and co-authors are responsible for any fraud, intentional or unintentional malpractice.

Research involving human participants and/or animals

Experimental Biomedical Research adopt ICMJE Recommendations on Protection of Research Participants. For more information, [click here!](#)

In addition to ICMJE recommendations, we also support 3Rs principals (**Replacement, Reduction and Refinement**) for humans and animals usage in research. Briefly 3Rs are mentioned below, and more information can be [accessed here!](#)

Replacement: approaches which avoid or replace the use of animals

Reduction: approaches which minimise the number of animals used per experiment

Refinement: approaches which minimise animal suffering and improve welfare

All work should be done with the permission of local human subjects or animal care committees (institutional and national) and clinical trials should be registered to legislation. The official numbers from these committees must be found in the Materials and Methods section (or text describing the experimental procedures).

1) Statement of human rights

The studies involving human participants should state that the research has been endorsed by the institutional and / or national research ethics committee and that it is conducted in accordance with the ethical standards set out in the [Helsinki Declaration of 1964](#), and that subsequent changes are also met (1).

2) Statement on the welfare of animals

If you have done experimental research on animals, authors should indicate whether the international, national and / or institutional guidelines for the care and use of the animals are followed, and whether the work has been approved by an institutional research ethics committee.

Informed consent

If manuscripts report the results of an experimental research of human subjects, all authors must fulfill the **International Committee of Medical Journal Editors (ICMJE)** requirements on confidentiality and informed consent from patients and study participants. Therefore;

- 1- Informed consent is obtained from all participants before they are included in the work.
- 2- Distinguishing details of the participants examined (name, date of birth, identification numbers and other information) should not be published in print, photographs and genetic profiles.
- 3-Where someone is deceased, please make sure that you have written permission from the family or estate.
- 4-If the identification features are changed to protect anonymity as in genetic profiling, the authors should assure that the changes do not distort scientific meaning.

Authors may use this [Patient Consent Form](#), which sent to the journal if requested.

The journal reserve the right to reject manuscripts that do not comply with the above-mentioned guidelines.

Publication charges

There are no submission fees or page charges for Experimental Biomedical Research journal.

Copyright Policy

Articles published in *Experimental Biomedical Research* are open-access, distributed under the terms of the Creative Commons Attribution Non-Commercial License (<http://creativecommons.org/licenses/by-nc/4.0>), which permits unrestricted non-commercial use, distribution, and reproduction in any medium, provided the original work is properly cited. Upon acceptance of an article, authors will be asked to transfer copyright. This transfer will ensure the widest possible dissemination of information. A letter will be sent to the corresponding author confirming receipt of the manuscript. A form facilitating transfer of copyright will be provided. ([Copyright Transfer Agreement Form](#)).

If the article contains a figure or table produced from a book or other journal article, the authors must obtain permission from the copyright owner before submitting the manuscript and they will be entirely liable for legal and / or financial consequences if such authorization documents are not obtained.

If you wish to use PDF, HTML, XML files or any artwork published in this journal for any commercial purpose, please contact the publisher at info@experimentalbiomedicalresearch.com.

Proofs

Accepted articles are sent as portable document format (PDF) files, along with proof by e-mail to the relevant author for approval. Corrections to PDF evidence should be limited to posting errors only, and no significant additions / deletions should be made. Authors are responsible for all statements made in their work, including changes made by the copy editor and authorized by the author concerned. Authors are strongly advised to thoroughly examine the PDF evidence and return the proofs within 3 days.

Experimental Biomedical Research

E-mail: info@experimentalbiomedicalresearch.com

Completed authorship forms may be mailed to this address.

Reference

1-World Medical Association.Declaration of Helsinki: ethical principles for medical research involving human subjects. <http://www.wma.net/en/30publications/10policies/b3/index.html>. Accessed October 14, 2010.

Editorial Assessment and Peer Review Policy-Process

Experimental Biomedical Research is an online-only, international, peer-reviewed, open access journal and is committed to maintaining the high quality of the peer-review process. Additionally, the peer review process ensures that the articles published, meet the accepted standards of the discipline. Experimental Biomedical Research (Editor) reviews new submissions according to its guidelines. When they meet all criteria, they are sent to two referees (double blind) and all manuscripts are read by reviewers, and revisions to the manuscript may be required. If the decision conflicts between two reviewers, it will be send to third peer reviewer. The typical review will take in 2-4 weeks. When the manuscript is received from peer reviewer there will be one of the following outcome: 1) accepted manuscript without revisions, 2) invite authors to resubmit the manuscript after minor or major changes while the final decision is kept pending, 3) or reject the manuscript. When the manuscript is returned for revision prior

to acceptance, the revised manuscript must be submitted within 30 days after the author's receipt of the referee's reports. Editorial review again (re-peer review/accepted/rejected). The final decision is sent to the authors.

Double blinded peer review process

Manuscript Submission

- New submission via online system
- Cover letter, author and co-author details, manuscript and separate files

Pre- Quality Associate Editorial Assessment

- Plagiarism check
- Qualification in the English language editing
- Ensuring that the manuscript adheres to the stylistic and bibliographic requirements outlined in the Author Guidelines (Experimental Biomedical Research Submission and Publication Checklist)
- Sent back to author for approval of edits

Peer Review

- Double-blind peer review undertaken by experts in the field
- When the manuscript is received from peer reviewer there will be one of the following outcome: 1) accepted manuscript without revisions, 2) invite authors to resubmit the manuscript after minor or major changes while the final decision is kept pending, 3) or reject the manuscript.
- Revision made by authors on the basis of reviewer recommendations (revisions must be highlighted and accompanied by a letter in response to each comment by the reviewers)
- In case of revisions, the revised article will be send to the reviewers who will decide on a new recommendation for revision, acceptance or rejection.

Copy Editing

- Professional checking for the composition and organization (formatting) of the paper against the journal guidelines
- Reference styling and proof corrections
- Author's confirmation of the final edited manuscript before publication
- In this version, corrections to PDF evidence should be limited to posting errors only, and no significant additions / deletions should be made

Publishing

- Accepted article is sent for generating the galley proof
- Online publication of the manuscript

[Copyright Notice](#)

Copyright (c): Author(s)

Experimental Biomedical Research journal is licensed under a [Creative Commons Attribution-NonCommercial 4.0 International License](#).

[Privacy Statement](#)

The names and email addresses entered in this journal site will be used exclusively for the stated purposes of this journal and will not be made available for any other purpose or to any other party.



Experimental Biomedical Research is licensed under a [Creative Commons Attribution 4.0 International License](#)

Isolated effects of regional hyperthermic perfusion on the development of peritoneal metastasis and overall survival in rats with transplanted high-grade ovarian carcinoma

Iaroslav Gennadevich Murazov¹, Anna Sergeevna Artemyeva², Anna Olegovna Niuganen², Konstantin Yurjevich Senchik³

¹Scientific Laboratory of Cancer Chemoprevention and Oncopharmacology, FSBI «N.N. Petrov National Medical Research Center of Oncology» of the Ministry of Healthcare of the Russian Federation.

²Department of Pathology, FSBI «N.N. Petrov National Medical Research Center of Oncology» of the Ministry of Healthcare of the Russian Federation.

³Department of Soft Tissue and Bone Tumors, FSBI «N.N. Petrov National Medical Research Center of Oncology» of the Ministry of Healthcare of the Russian Federation.

ABSTRACT

Aim: To construct a perfusion circuit for experimental open hyperthermic intraperitoneal perfusion (HIPEP) and to evaluate the antitumor effects of regional hyperthermia in a model of advanced syngeneic high-grade ovarian carcinoma in vivo.

Method: 24 mature female Wistar rats underwent intraperitoneal transplantation of ascitic ovarian tumor 1×10^7 cells per rat. 48 hours after transplantation the animals were randomized into two groups: I. NIPEP group (12 rats) – normothermic intraperitoneal perfusion (NIPEP) with normal saline at room temperature during 45 minutes; II. HIPEP group (12 rats) – open hyperthermic intraperitoneal perfusion (HIPEP) with normal saline (40.5-41.5 °C) during 45 minutes. Endpoints included overall survival (OS), the total peritoneal cancer index (PCI), ascites weight and the grade of ascites hemorrhage.

Results: In both groups all animals survived the procedure, in the HIPEP group one rat died due to infectious complications on day 32. Compared with NIPEP group HIPEP with normal saline significantly increased the median OS from 19 to 39 days (log-rank test, $P=0.0013$), reducing the risk of death by 68% (HR=0.32; 95% CI 0.13-0.82). The open HIPEP without a cytostatic was associated with significantly lower total PCI (14 vs 5 points, $P=0.0155$). In the HIPEP group 3 of 12 animals had intrathoracic tumor spread with malignant pleural effusion without signs of peritoneal carcinomatosis and ascites.

Conclusion: The transplanted syngeneic tumor is a valid model that allows to quantitatively assess antitumor activity of intraperitoneal perfusion therapy. Our preclinical data confirmed the role of regional hyperthermia in the treatment of peritoneal carcinomatosis in ovarian tumors.

Key words: Ovarian cancer, peritoneal carcinomatosis, hyperthermia, peritoneal cancer index, HIPEC, preclinical study.

✉ Dr. Iaroslav Gennadevich Murazov,
Scientific Laboratory of Cancer Chemoprevention and
Oncopharmacology, FSBI «N.N. Petrov National
Medical Research Center of Oncology» of the Ministry
of Healthcare of the Russian Federation, Saint-
Petersburg, Russian Federation, 68, Leningradskaya

str., Pesochniy Settlement, Saint-Petersburg, 197758,
Russian Federation.
E-mail: yaroslav84@yandex.ru

Received: 2021-04-07 / Revisions: 2021-04-21

Accepted: 2021-04-23 / Published online: 2021-07-01

Introduction

Peritoneal surface malignancy may occur as a primary disease or as a metastatic tumor originating most often from gastrointestinal tract and gynecological cancers. Peritoneal carcinomatosis (PC) is an unfavorable prognostic factor associated with rapid disease progression, significant deterioration in the quality of life and high mortality of patients [1]. Thus, the 5-year OS of patients with epithelial ovarian cancer (EOC) and PC is about 29% [2]. Unfortunately, systemic chemotherapy has low efficacy against tumor deposits that have spread along the peritoneum, due to poor blood supply and the low ability of cytostatics to penetrate into intraperitoneal tumor nodules [3]. PC should be considered as a local disease that requires special approaches to treatment. The well-known synergism of the action of regional hyperthermia (40.5-43 °C) and chemotherapeutic agents has become the reason for a wide study and introduction into clinical practice of hyperthermic intraperitoneal chemotherapy (HIPEC) [4]. Technically HIPEC can be performed using an open, closed, semi-open, laparoscopic technique or using an expander. Hyperthermia not only enhances the antitumor activity of cytostatics, but also has antitumor activity itself. The direct cytostatic and cytotoxic effects of supranormal temperatures begin at 40-41 °C, while the synergism between hyperthermia and cytostatics begins at 39 °C and decreases at temperature above 43 °C. Temperature above 44 °C induce apoptosis in normal cells [3,5]. Currently, HIPEC is widely used in the treatment of PC in pseudomyxoma peritonei and peritoneal mesothelioma, peritoneal metastases of colorectal cancer. At the same time, for primary and recurrent EOC with PC the use of HIPEC is not recommended outside clinical trials [6,7]. This is due to the lack of

standardization of the HIPEC procedure (technique, antineoplastic drugs and their doses, carrier solutions, optimal temperature and duration of perfusion, flow rate of perfusate etc.), as well as the absence of developed algorithm for managing adverse events associated with the procedure. Moreover, current clinical data failed to isolate the curative effects of hyperthermia itself. Until more data are available from evidence-based studies, it is reasonable to conclude that a strategy of surgical cytoreduction and HIPEC is rational and interesting, though still an investigative approach in the management of advanced-stage epithelial ovarian cancer.

A critical stage in the investigation and standardization of perfusion technologies for the treatment of PC are preclinical studies on valid models *in vivo*. Commonly two types of EOC models are used for PC development in rodents: (1) cell lines and patient-derived xenografts of human tumors; (2) syngeneic models. In order to obtain intraperitoneal dissemination, the tumor can be transplanted intraperitoneally or orthotopically (under the ovarian bursa membrane) [8]. The use of immunodeficient animals for transplantation of human xenografts does not allow studying the interaction of a tumor with microenvironment in the context of the development of an immune response, inflammation, vascularization, and interaction with stromal components. Syngeneic models, on the contrary, make it possible to study the development of the antitumor immune response, epithelial-stromal interactions, and tumor vascularization. The use of immunocompetent animals provides a low incidence of infectious complications in comparison with immunodeficient animals. It should be noted that the hardware used for the experimental HIPEC is quite diverse. Each perfusion circuit is in fact a unique

multicomponent system [9-12]. Here we used an original peritoneal perfusion system, constructed from domestic devices.

The aim of our study is to assess the antitumor effect of open hyperthermic intraperitoneal perfusion (HIPEP) with normal saline (40.5-41.5°C) on the development of PC and OS in female Wistar rats with syngeneic high-grade ovarian carcinoma.

Materials and methods

Experimental design

A single intervention proceeded 48 h after intraperitoneal (IP) tumor transplantation. Animals were randomized into two groups: I. NIPEP group (12 rats) – normothermic intraperitoneal perfusion (NIPEP) with normal saline at room temperature during 45 minutes; II. HIPEP group (n = 12) - peritoneal cavity of the rats was perfused with heated normal saline according to "Coliseum" (open) technique (parameters are described below).

Animals

The study was approved by the local ethics committee (REC No 3/297-20) and carried out in accordance with the European Convention for the Protection of Vertebrate Animals used for Experimental and Other Scientific Purposes: Appendix A of the ETS 123 and Directive 2010/63/EU on the protection of animals used for scientific purposes. Twenty four outbred female mature Wistar rats with median weight 294 g (min-max 274-381 g) were purchased from "Rappolovo" animal nursery (Leningrad Region, Russia). Rats were housed in polypropylene cages in a conventional facility (temperature 20–24°C, relative humidity 50–60%, 12 h light/12 h dark cycle). Animals received standard laboratory crop (Moscow, Russia) and tap water ad libitum.

The ovarian cancer rat model

The tumor strain was obtained as a result of transplacental carcinogenesis using high doses of 7,12-dimethylbenzanthracene (DMBA). The initial histological type of tumor is metastatic papillary adenocarcinoma, at present it is an ascitic tumor [13]. Tumor strain is maintained in female Wistar rats. On days 7-9 after IP inoculation, ascitic fluid was collected and transplanted IP to experimental animals (1×10^7 cells in 0.5 ml of normal saline per rat).

Open intraperitoneal perfusion technique

Scheme of the experimental perfusion circuit is shown in Figure 1. Thirty minutes prior to and then twice a day on days 0-2 postoperatively, meloxicam («Renewal», Novosibirsk, Russia) was given subcutaneously 2 mg/kg for analgesia. Rats were anesthetized using isoflurane (Abbott Laboratories Limited, Queenborough, UK), 5% for induction and 2% for maintenance. No warming mattress was used during HIPEP, to avoid systemic hyperthermia. A midline laparotomy was performed with a 6-8 cm incision. A "Coliseum" was formed by hemming the edges of the abdominal wall with a surgical suture to a metal ring on a tripod. The inflow line was placed in the left subdiaphragmatic space and the outflow line in the right paracolic gutter. The parameters of the perfusion system were as follows: volume of perfusate (normal saline, "Slyvanskaya Apteka" LLC, Vladimir region, Russia) - 210 ml, flow rate - 30 ml/min, abdominal cavity temperature – 40.5-41.5 °C (for HIPEP group), perfusion time - 45 minutes. During perfusion the abdomen was massaged gently to achieve a uniform heat distribution. After completion of the perfusion, the abdominal wall was closed using 3/0 polyglactin sutures for the muscular layer and 3/0 non-absorbable polyester sutures for the skin. Additionally, the wound was strengthened

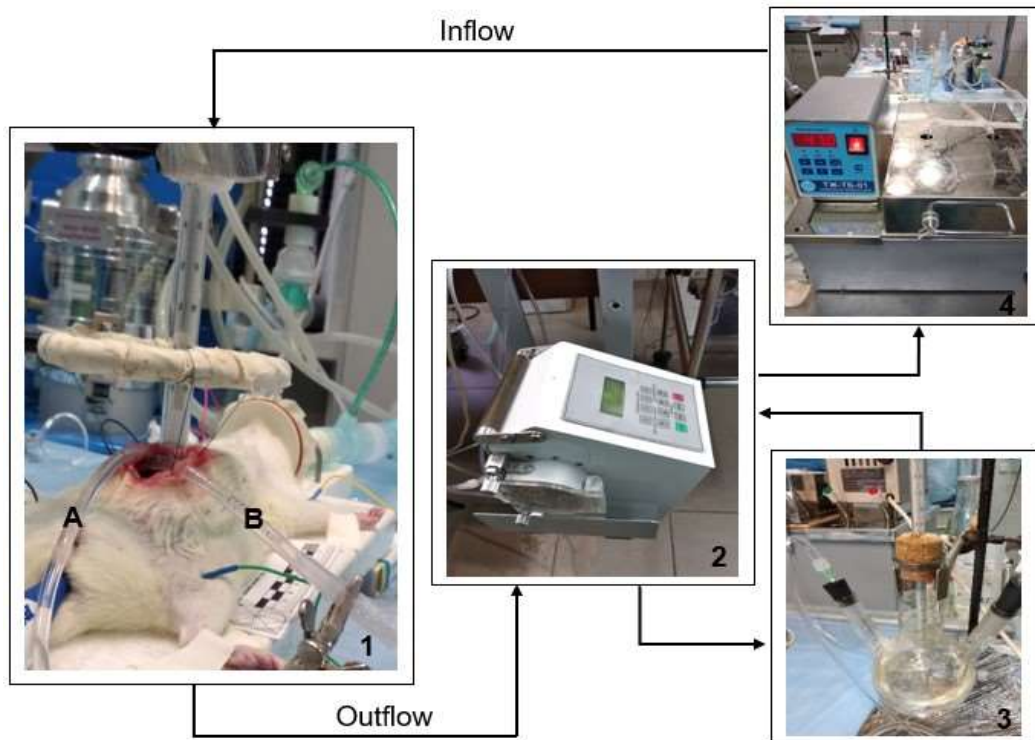


Figure 1. Scheme of the perfusion circuit for an experimental open NIPEP and HIPEP. 1 - position of the animal during the procedure: (A) – inflow line, (B) – outflow line, diameter 4 mm; 2 - perfusion roller pump (Russian State Scientific Center for Robotics and Technical Cybernetics, Saint-Petersburg, Russia); 3 - reservoir for perfusate; 4 - thermostatic water bath (Russian State Scientific Center for Robotics and Technical Cybernetics, Saint-Petersburg, Russia).

with BF-6 glue (JSC «Werteks», Saint-Petersburg, Russia). Immediately after wound closure rats were given with 10 ml saline subcutaneously for rehydration. Cefepime (JSC «Sintez», Kurgan, Russia) 60 mg/kg was injected intramuscularly after perfusion and then for next 4 days once daily. The animal was placed on the absorbent sheet in a plastic cage. A heating platform (set at 40 °C) was placed under the half of the cage in order to prevent hypothermia. To reduce stress, medium enrichment agents (minks) were placed into the cage. The first five days the postoperative wound was treated with Levomekol ointment (JSC "Nizhfarm", Nizhny Novgorod, Russia).

Follow-up. The animals were observed throughout the entire period of their life. OS was defined as time from the day of tumor transplantation to day of animal death. The total peritoneal cancer index (PCI), ascites weight

and its grade of haemorrhagia were determined at autopsy. The total PCI was determined according to the modified method of Y.L. Klaver. et al. [14]. After laparotomy, the abdomen was carefully examined for tumor growth at eight different sites (see Table 1). The tumor load at each site was scored semi quantitatively: 0 – no macroscopic tumor; 1 – limited tumor growth (diameter 1–2 mm); 2 – moderate tumor growth (diameter 2–4 mm); 3 – abundant (diameter more than 4 mm). In the case of multiple nodes in the organ, the node with the largest diameter was selected. The sum of scores from all sites represented the total PCI for that animal. The grade of ascites haemorrhagia was determined using a semi quantitative visual scale, where 0 - absence of hemorrhagic ascites; 1 - weak hemorrhagic ascites; 2- moderate hemorrhagic ascites; 3 - strong hemorrhagic ascites. Organs of the

reproductive system of all animals, as well as organs and tissues with macroscopic signs of PC, were subjected to standard histological examination by light microscopy after hematoxylin and eosin staining. Cytological smears of ascites and pleural effusion were examined after Pappenheim's stain.

Statistical Analysis

Statistical analysis was performed using GraphPad Prism version 8.0. Based on pilot preclinical study (data was not published) required sample size was 12 animals per group to reject the null hypothesis that survival in the NIPEP group and the HIPEP group are equal with power $(1-\beta)=80\%$ and $\alpha=0.05$ [15]. Nonparametric testing for the continuous data was performed using Mann-Whitney test. Comparison of categorical values was done using Fisher's exact test. All tests were two-sided; the level of statistical significance was set at a P value of <0.05 . Survival outcomes were analyzed and expressed using Kaplan–Meier curves and compared with the log-rank test. The Cox proportional-hazards model was used to obtain hazard ratio (HR) and its 95% confidence interval (95% CI).

Results

All animals in the NIPEP and HIPEP groups survived the procedure. On day 32 after HIPEP one of 12 rats died from infectious complications. Mean anesthesia time was 115 minutes (min-max: 100-142). The dynamics of intraperitoneal and rectal temperature during HIPEP is shown in Figure 2. The set temperature in the abdominal cavity was reached 10-17 minutes after the installation of the lines and the start-up of the circuit.

After IP transplantation tumor take rate achieved nearly 100% and led to haemorrhagic ascites formation and PC. Cancer-related

mortality in rats was nearly 100%. The autopsy revealed tumor lesions in mesentery, greater omentum, parietal peritoneum and diaphragm. High volume tumor implants were observed in ovaries, horns and body of uterus, perigonadal fat pads (Figure 3).

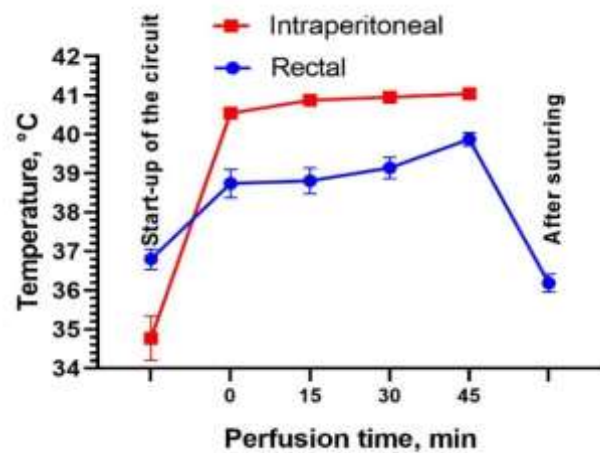


Figure 2. The temperature course during HIPEP in the abdomen and in the rectal cavity.



Figure 3. Macroscopic tumor view in rat with transplanted syngeneic ovarian carcinoma (NIPEP group). Tumor implants in mesentery, uterine horns and body with perigonadal fat pads, greater omentum and diaphragm.

The development of peritoneal metastasis was accompanied by hemorrhagic ascites. In smears

of ascitic fluid extensive focuses of high-grade serous carcinoma discretely lying among the fields of cells of the monocytic series were determined. Cells were polymorphic, sharply atypical with large nuclei with nucleoli and a high nuclear-cytoplasmic ratio (Figure 4).

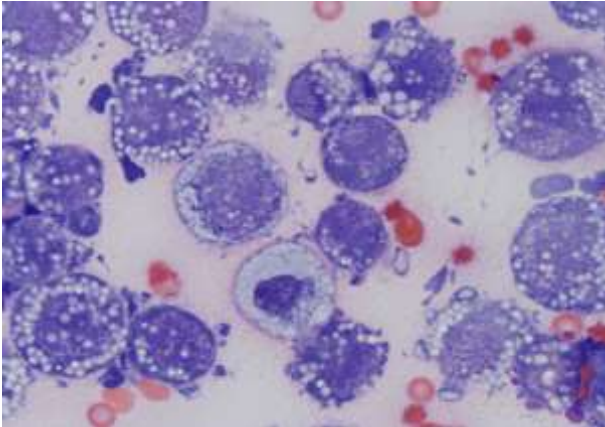


Figure 4. Smear of ascitic fluid, Pappenheim's stain, ×1000.

It is noteworthy, that 3 out of 12 rats in the HIPEP group had haemorrhagic malignant pleural effusion (confirmed by cytologic examination) with involvement of organs in thoracic cavity (lungs, pericardium, intrathoracic lymph nodes). Macroscopically it was no evidence of tumor growth in the peritoneal cavity and ascites.

Histological examination of autopsy material revealed invasive malignant tumor of a papillary-solid structure, consisting of rounded cells with scanty eosinophilic or optically empty cytoplasm, with large sharply atypical polymorphic nuclei, with a high nuclear-cytoplasmic ratio (Figure 5).

Kaplan–Meier's curves are shown in Figure 6. Median OS was 19 days in the NIPEP group, and 39 days in the HIPEP group. This

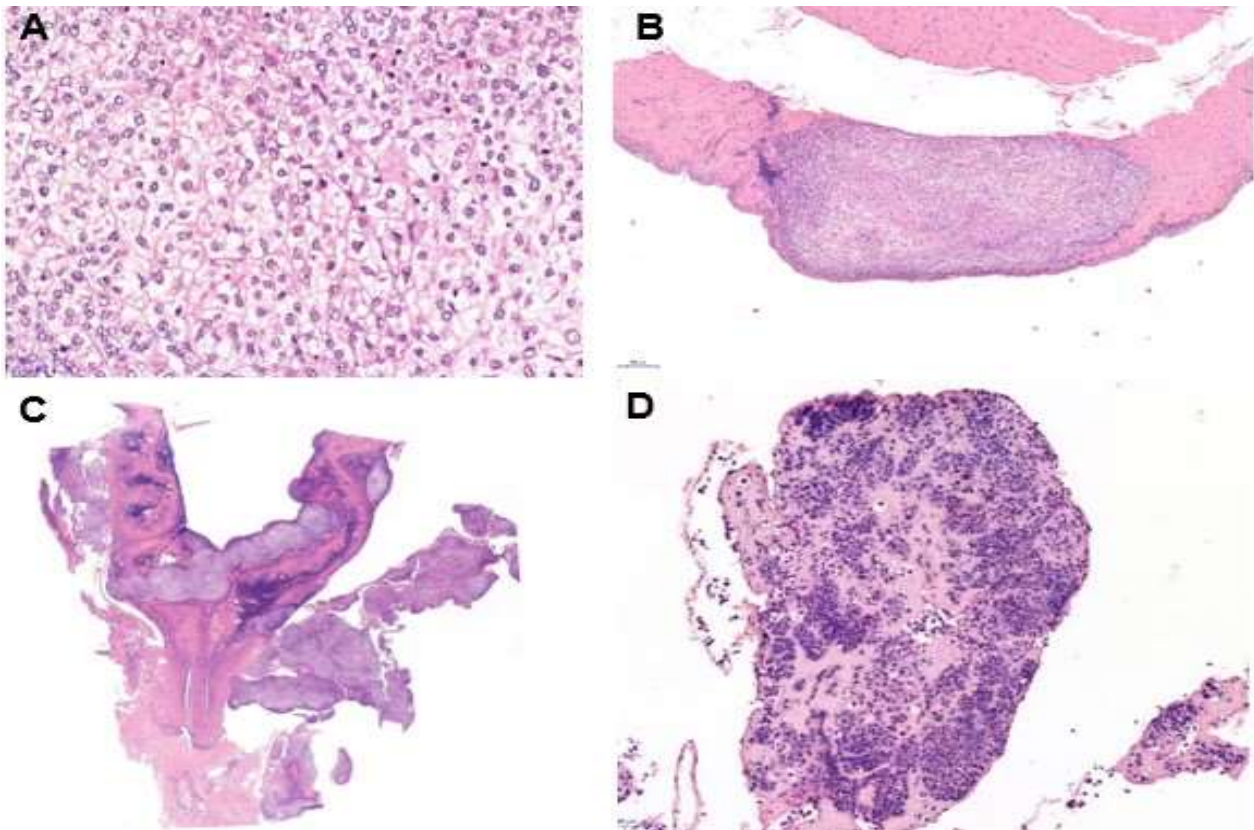


Figure 5. Microscopic tumor view. (A) – focus of serous high-grade carcinoma, haematoxylin and eosin, ×400; (B) – tumor nodule on the parietal peritoneum, haematoxylin and eosin, ×60; (C) – invasion of the tumor into the body of the uterus and uterine horns, haematoxylin and eosin, ×5; (D) – a fragment of the greater omentum with tumor infiltration, haematoxylin and eosin, ×40.

difference in survival outcome was significant, log-rank test $P=0.0013$; $HR=0.32$ (95% CI 0.13-0.82). One rat from the HIPEP group was sacrificed on day 138 after tumor transplantation without any signs of tumor growth (confirmed on autopsy).

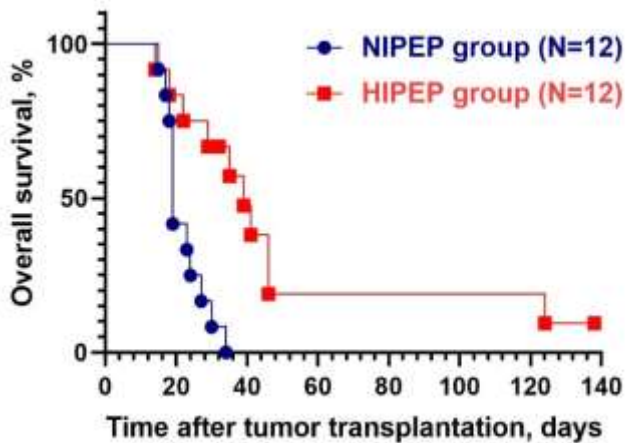


Figure 6. Kaplan–Meier analysis of survival curves of rats with transplanted ovarian carcinoma. NIPEP – normothermic intraperitoneal perfusion with normal saline; HIPEP – hyperthermic intraperitoneal perfusion with normal saline.

In NIPEP group all animals developed extensive intraperitoneal tumor growth at autopsy. Rats in the HIPEP group were found to have a significantly lower mean of the total PCI than rats in NIPEP group ($P=0.00155$). There was no significant difference in the ascites weight between groups owing to massive variation of this parameter. Although there was a trend towards a decrease in the HIPEP group. At the same time, ascites from HIPEP group had a more pronounced degree of haemorrhagia. Autopsy findings are shown in Table 1.

Discussion

The selective effects of hyperthermia on malignant cells as well as its ability to potentiate chemotherapy agents make it a

valuable adjunct to intraperitoneal chemotherapy in the management of PC [16]. It is supported by an increasing number of research data. But available clinical data failed to isolate the antitumor effects of hyperthermia itself. Currently, the role of HIPEP in the management of primary and recurrent EOC is still not clear [17]. One of the reasons for this is insufficient experimental data, including preclinical studies on adequate experimental models.

The chosen model of syngeneic ovarian carcinoma in Wistar rats resembles the clinical situation of advanced EOC (stage III-IV) in humans with the PC and ascites. The histological structure corresponded to the most common subtype of human ovarian tumor – high-grade serous carcinoma. The model resembles the microscopic disease before the emergence of visible nodules [18].

For our study we designed and tested a new peritoneal perfusion system in tumor bearing rats. We chose to use the “Coliseum” technique for NIPEP and HIPEP due to its advantages over the closed technique. It allows to achieve homogeneous temperature and better control of perfusate distribution within the peritoneal cavity, make the access to the entire cavity easier, prevents of bubble formation in the circuit and organ suction, possibility of debulking of large tumors before perfusion, easier circuit blockage corrections, and minimal risk of thermal damage of organs and tissues [12,19].

Here, we demonstrated that open HIPEP with saline only significantly increased the median survival of the animals from 19 to 39 days (log-rank test $P=0.0013$) and reduced the risk of death by 68% (HR for HIPEP group vs NIPEP group 0.32; 95% CI 0.13-0.82).

The exact mechanism of antitumor activity of hyperthermia is not fully understood. It is

Table 1. Influence of HIPEP with normal saline on the spread of transplanted ovarian carcinoma and the ascites weight on autopsy.

Tumor score per site^a	NIPEP group (N=12)	HIPEP group (N=12)^b	<i>P</i> value
Greater omentum	3 (3-3)	1 (0-3)	
Space between the liver and the diaphragm	3 (0-3)	0 (0-3)	
Liver hilum	3 (0-3)	0 (0-3)	
Mesentery	3 (0-3)	0 (0-3)	
Diaphragm	0 (0-3)	0 (0-3)	
Ovaries	1 (0-3)	0 (0-2)	
Parietal peritoneum	0 (0-2)	0 (0-3)	
Uterine horns and body with perigonadal fat pads	2,5 (0-3)	0 (0-3)	
Total PCI ^c	14 (2)	5 (2)	<i>Mann Whitney test, P=0.0155</i>
Ascites weight, g ^b	67.4 (31.5-100.5)	24.6 (11.1-80.1)	<i>Mann Whitney test, P=0.1206</i>
Grade of ascites haemorrhagia ^b	2 (2-2)	3 (2-3)	<i>Mann Whitney test, P=0.0379</i>
Intrathoracic tumor spread with malignant pleural effusion, n	0	3	<i>Fisher's exact test, P=0.0932</i>

^a Values are median (Q1-Q3) and ^c mean (SEM). ^b 3 animals with malignant pleural effusion and 1 rat with infectious complications were excluded from PCI calculation.

known that the cytotoxic effects of hyperthermia are caused by damage of cell membranes, nuclei, protein denaturation, and changes in the permeability to calcium ions. It disrupts mitotic processes of malignant and non-malignant cells too. In tumor cells, after exposure to hyperthermia, an increase in the number of lysosomes and the activity of lysosomal enzymes is established.

Microcirculation in tumor tissue is suppressed by hyperthermia, which leads to decrease in blood flow to the tumor or its complete stasis,

whereas in normal tissues the blood flow increases. These effects, along with a violation of cellular respiration processes, lead to the accumulation of lactic acid and acidification of the tumor microenvironment, which leads to an increase in the number and "fragility" of lysosomes, accompanied by increased death of tumor cells [20].

Noteworthy is the profile of the OS curve in the HIPEP group. The presence of such "tails" may be associated with the activation of antitumor immunity in immunocompetent animals with

transplanted syngeneic tumor. This profile resembles the OS curve of patients receiving checkpoint inhibitors with a long-term response to this therapy [21]. It is known that in addition to the direct cytotoxic effect on tumor cells, hyperthermia stimulates the production of heat shock proteins (HSPs) and their presentation in complex with the major histocompatibility complex class II, activates dendritic cells and natural killers, enhances the adhesive properties of T-cells and their traffic to peripheral tissues and promotes immune surveillance [22].

Locoregional intraperitoneal heating independently contributed to antitumor activity and reduced intraperitoneal tumor dissemination. In the HIPEP group the total PCI was significantly lower and a trend towards a decrease in the ascites weight was noticed. At the same time, ascites in animals from HIPEP group had a more pronounced degree of haemorrhagia. Probably, this was the main cause of death. An interesting observation from the study was that 3/12 rats in HIPEP group had haemorrhagic pleural effusion with malignant cells but without macroscopic evidence of tumor growth in peritoneal cavity and ascites. Such phenomenon may be due to tumor cells migration under conditions of high intraabdominal pressure and supranormal temperature during perfusion.

Conclusions

In conclusion, the model of syngeneic high-grade ovarian carcinoma in Wistar rats and the original experimental perfusion circuit can be used for further investigation of HIPEC after proper equipment of the operating room by setting general and local ventilation, which will provide a special microclimate during the procedure. Our preclinical results supplemented the data about the antitumor activity of local hyperthermia and its role in the perfusion treatment of PC in ovarian tumors.

Funding: The author(s) received no financial support for the research, authorship, and/or publication of this article.

Conflict of Interest: The authors declare that they have no conflict of interest.

Ethical statement: The study was approved by the local ethics committee (REC No 3/297-20) and carried out in accordance with the European Convention for the Protection of Vertebrate Animals used for Experimental and Other Scientific Purposes: Appendix A of the ETS 123 and Directive 2010/63/EU on the protection of animals used for scientific purposes.

Open Access Statement

This is an open access journal which means that all content is freely available without charge to the user or his/her institution under the terms of the Creative Commons Attribution Non-Commercial License (<http://creativecommons.org/licenses/by-nc/4.0>). Users are allowed to read, download, copy, distribute, print, search, or link to the full texts of the articles, without asking prior permission from the publisher or the author.

References

- [1]Helderman RFCPA, Löke DR, Kok HP et al. Variation in Clinical Application of Hyperthermic Intraperitoneal Chemotherapy: A Review. *Cancers (Basel)*. 2019; 11(1): 78.
- [2]Reid B.M., Permuth J.B., Sellers T.A. Epidemiology of ovarian cancer: a review. *Cancer Biol Med*. 2017; 14(1): 9–32.
- [3]Goodman MD, McPartland S, Detelich D et al. Chemotherapy for intraperitoneal use: a review of hyperthermic intraperitoneal chemotherapy and early post-operative intraperitoneal chemotherapy. *J Gastrointest Oncol*. 2016; 7(1): 45-57.

- [4] Sugarbaker PH, Graves T, DeBruijn EA, et al. Early postoperative intraperitoneal chemotherapy as an adjuvant therapy to surgery for peritoneal carcinomatosis from gastrointestinal cancer: pharmacological studies. *Cancer Res.* 1990; 50(18): 5790-94.
- [5] Hager E.D. Intracavitary Hyperthermic Perfusion. In: *Madame Curie Bioscience Database [Internet]*. Austin (TX): Landes Bioscience 2000-2013, <https://www.ncbi.nlm.nih.gov/books/NBK6059>.
- [6] Cortez AJ., Tudrej P, Kujawa KA et al. Advances in ovarian cancer therapy. *Cancer Chemother Pharmacol.* 2018; 81(1): 17-38.
- [7] Jewell A, McMahan M, Khabele D. Heated Intraperitoneal Chemotherapy in the Management of Advanced Ovarian Cancer. *Cancers (Basel).* 2018; 10(9): 296.
- [8] Murazov Ia.G., Niuganen A.O., Artemyeva A.S. Experimental modeling of ovarian carcinoma. *Laboratory Animals for Science.* 2020; 3. <https://doi.org/10.29296/2618723X-2020-03-05> (In Russian).
- [9] Pelz JO, Doerfer J, Hohenberger W et al. A new survival model for hyperthermic intraperitoneal chemotherapy (HIPEC) in tumor-bearing rats in the treatment of peritoneal carcinomatosis. *BMC Cancer.* 2005; 5:56.
- [10] Badrudin D, Sideris L, Perrault-Mercier C, et al. Comparison of open and closed abdomen techniques for the delivery of intraperitoneal pemetrexed using a murine model. *J Surg Oncol.* 2018; 117(6): 1318-22.
- [11] Park EJ, Ahn J, Gwak SW, et al. Pharmacologic Properties of the Carrier Solutions for Hyperthermic Intraperitoneal Chemotherapy: Comparative Analyses Between Water and Lipid Carrier Solutions in the Rat Model. *Ann Surg Oncol.* 2018; 25(11): 3185-92.
- [12] McCabe-Lankford E, Peterson M, McCarthy B. et al. Murine Models of Intraperitoneal Perfusion for Disseminated Colorectal Cancer. *J Surg Res.* 2019;233:310-22.
- [13] Pogogyants EE, Prigozhina EL, Egolina NA. Transplantable rat ovary ascitic tumor. *Vopr Oncol* 8: 29-36, 1962 (In Russian).
- [14] Klaver YL, Hendriks T, Lomme RM, et al. Intraoperative hyperthermic IP CT after CRS cytoreductive surgery for peritoneal carcinomatosis in an experimental model. *Br J Surg.* 2010; 97(12): 1874-80.
- [15] Schoenfeld DA, Richter JR. Nomograms for calculating the number of patients needed for a clinical trial with survival as an endpoint. *Biometrics.* 1982;38(1): 163-70.
- [16] Sticca RP, Dach BW. Rationale for hyperthermia with intraoperative intraperitoneal chemotherapy agents. *Surg Oncol Clin N Am.* 2003; 12(3):689–701.
- [17] Vergote I, Harter P, Chiva L. Is There a Role for Intraperitoneal Chemotherapy, Including HIPEC, in the Management of Ovarian Cancer? *J Clin Oncol.* 2019; 37(27): 2420-23.
- [18] Gremontprez F, Willaert W, Ceelen W. Intraperitoneal chemotherapy (IPC) for peritoneal carcinomatosis: review of animal models. *J Surg Oncol.* 2014; 109(2): 110-16.
- [19] González-Moreno S, González-Bayón LA, Ortega-Pérez G. Hyperthermic intraperitoneal chemotherapy: Rationale and technique. *World J Gastrointest Oncol.* 2010; 2(2):68-75.
- [20] Sticca RP, Dach BW. Rationale for hyperthermia with intraoperative intraperitoneal chemotherapy agents. *Surg Oncol Clin N Am.* 2003; 12(3): 689–701.
- [21] Harris SJ., Brown J, Lopez J et al. Immunology combinations: raising the tail of

the survival curve. *Cancer Biol Med.* 2016;
13(2): 171-93.

[22] Skitzki JJ., Repasky EA, Evans SS.
Hyperthermia as an immunotherapy strategy
for cancer. *Curr Opin Investig Drugs.* 2009;
10(6): 550-58.

The effect of COVID-19 infection on retinal nerve fiber layer and ganglion cell complex layer thicknesses

Sedat Ozmen¹, Burcin Cakir¹, Huseyin Dogus Okan², Nilgun Ozkan Aksoy¹, Ertugrul Guclu²

¹Department of Ophthalmology, Sakarya University Medical Education and Research Hospital, Sakarya, Turkey

²Department of Infection Diseases Sakarya University Medical Education and Research Hospital, Sakarya, Turkey

ABSTRACT

Aim: To evaluate the possible effects of SARS-CoV-2 infection on retinal nerve fiber layer (RNFL) and ganglion cell complex layer (GC-IPL) thicknesses.

Method: Patients who had been infected by SARS-CoV-2 and hospitalized because of severe pneumonia were found out from the database of COVID-19 pandemic hospital and formed the patient group. The control group was composed of non-COVID-19 age-matched subjects. The mean and fragmented RNFL and GC-IPL thicknesses were measured by optical coherence tomography (OCT), and compared between two groups, statistically.

Results: Patient group 34 eyes of 34 subjects (18 male, 16 female) and 31 eyes of 31 subjects (14 male, 17 female) in the control group were enrolled. The mean age and gender were not statistically different between groups (p:0.56, 0.57, respectively). A statistically significant difference was not found between groups in terms of mean, superior, inferior, temporal, nasal RNFL thicknesses and mean superior, inferior, temporal, and nasal GC-IPL thicknesses.

Conclusion: The mean and fragmented RNFL and GC-IPL thicknesses measured by OCT were not statistically different in patients who had moderate disease course and recovered from COVID-19 infection.

Key words: COVID-19 infection, retinal nerve fiber layer thickness, ganglion cell- internal plexiform layer thickness, optical coherence tomography.

✉ Dr. Sedat Ozmen,
Department of Ophthalmology, Sakarya University
Medical Education and Research Hospital, Sakarya,
Turkey.

E-mail: drsozmen@gmail.com

Received: 2021-02-19 / Revisions: 2021-03-27

Accepted: 2021-05-06 / Published online: 2021-07-01

Introduction

The novel Coronavirus disease (COVID-19) became a pandemic in the early months of 2020 [1]. We have already learned plenty of information about coronaviruses and the

disease. These viruses are enveloped positive-sense RNA viruses that primarily target the human respiratory system and commonly cause fever, cough, and fatigue [2,3]. Although clinical features revealed by a chest computer tomography scan present as pneumonia, the disease can also be manifested by extreme symptoms that may lead to death [4].

Ophthalmic manifestations in patients infected by a novel coronavirus (SARS-CoV-2) have been reported. Follicular conjunctivitis, conjunctival hyperemia, tender palpable

preauricular lymph nodes, and watery discharge were found to be common ocular findings in patients with active COVID-19 [5-7]. To the best of our knowledge, there are few studies about the possible effects of SARS-CoV-2 virus infection on the posterior segment of the eye, in the literature [8-10].

The hypothesis of this current study is the effect of possible microvascular changes and neuroinflammation on inner retinal layers. The current study aimed to evaluate the possible effects of SARS-CoV-2 infection on retinal nerve fiber layer (RNFL) and ganglion cell complex layer (GC-IPL) thicknesses measured by optical coherence tomography (OCT) in patients who recovered from COVID-19.

Materials and methods

This study was conducted at Sakarya University Education and Research Hospital. Prior approval was received from the Institutional Review Board (IRB number: 71522473/050.01.04/366), and written informed consent was obtained from each subject. The study was performed in adherence to the Declaration of Helsinki.

Patients who had been infected by SARS-CoV-2 and hospitalized because of severe pneumonia were found out from the database of COVID-19 pandemic hospital and these patients formed the patient group. The control group was composed of patients who applied to Ophthalmology polyclinic and who had no significant ocular disease which might affect OCT assessments.

In the patient group, all patients had positive real-time reverse transcription-polymerase chain reaction (RRT-PCR) tests obtained from nasopharyngeal and oropharyngeal swabs. Oral hydroxychloroquine treatment (200mg/day for 3 days) and anticoagulant therapy (enoxaparine 40 mg/day) was given to all patients. Absence

of symptoms and negative results of two consecutive nasopharyngeal and oropharyngeal swab RRT-PCR tests were considered recovery. Two months after the recovery of COVID-19, ophthalmic examination including RNFL and GC-IPL thickness assessment was done.

Exclusion criteria for both groups were: spherical equivalent above 3 diopter, choroidal atrophy, high myopia, age-related macular degeneration, central serous chorioretinopathy, any type of glaucoma, optic neuropathy, hereditary retinal diseases, demyelinating disorders, neurodegenerative disorders, and any other ocular disorders which might alter RNFL and GC-IPL thicknesses.

Cirrus EDI-OCT (Carl Zeiss Meditec, Dublin, CA, USA) was used for peripapillary RNFL and GC-IPL thickness measurements. RNFL thickness analysis was done by "Optical Disc Cube 200 * 200" method and ganglion cell analysis was done according to "Macular Cube 512 * 128" program.

Average, superior, inferior, temporal and nasal quadrant RNFL and GC-IPL thicknesses were compared between the patient and control groups.

Data were statistically evaluated by using IBM SPSS Statistics Software (Version 23.0). All data were reported as mean \pm standard deviation. The normality for the distribution of variables was determined by the Kolmogorov-Smirnov test. A student t-test was used for comparing independent samples. Any p-value of less than 0.05 was considered to be significant.

Results

Patient group 34 eyes of 34 subjects (18 male, 16 female) and 31 eyes of 31 subjects (14 male, 17 female) in the control group were enrolled. The mean ages of groups were 40.0 ± 16.6 years

and 42.2 ± 14.0 years in the patient and the control groups, respectively. The mean age and gender were not statistically different between groups ($P > 0.56$ and $P > 0.57$, respectively). Table 1 reveals characteristics of study group including additional systemic diseases, therapies, etc.

A statistically significant difference was not found between groups in terms of mean, superior, inferior, temporal, nasal RNFL thicknesses and mean superior, inferior, temporal, and nasal GC-IPL thicknesses. Table 2 reveals the details of these data.

Table 1. Characteristics of the study group.

Variables	Patients (N / %)
Systemic arterial HT	6/17
DM	2/5
Red eye during infection	13/38
Oxygen therapy requirement	18/52
Favipiravir requirement	12/35
Venous thrombosis	4/11
ICU admission	2/5
Corticosteroid requirement	8/23

HT: hypertension DM: diabetes mellitus ICU: intensive care unit.

Discussion

The main possible mechanism that might affect the posterior segment of the eye in COVID-19 disease might be micro-thrombotic events in the microvascular system of the eye [8]. This

type of damage to microvascular structures of the retina might cause alterations in the inner layers of the retina. Savastano et al. [8] investigated radial peripapillary capillary plexus (RPCP) perfusion density and flow index measured by OCT angiography in patients who recovered from COVID-19 disease. RPCP perfusion density was found to be lower in patients compared to controls. RNFL average thickness was linearly correlated to RPCP flow index and RPCP perfusion density within post-COVID-19 group. The RPCP perfusion density was previously found to be correlated to RNFL thickness in glaucoma patients [11,12]. The correlation between PRCP flow index and average RNFL thickness, found by Savastano et al. [8] is remarkable but they did not find statistical difference between study and control groups in terms of average RNFL and GC-IPL thicknesses. In our study, we also did not find any statistical difference. The percent of patients who required intensive care unit (ICU) administration was only 5% in our study and venous thrombosis were diagnosed in 11% of the patients in the study group. The low rate of thrombotic events might prevent micro-thrombotic events in the microvascular system of the eye. Patients who need ICU treatment and / or survive thrombotic events can be investigated in the future and can enlighten us on this issue. Paulo M et al. evaluated the retina layer of 12 patients with COVID-19 infection by using OCT in the first month of the disease and found that the patients had hyperreflective lesions in the retinal ganglion cell and inner plexiform layer, especially in the papillomacular band. In our study, we could not detect any changes in the retinal ganglion complex and retinal nerve fiber layer [13]. No retinal changes were detected in the patient group in our study.

Table 2. Comparison of the parameters obtained from OCT between the patient and the control groups.

Parameters	Patient group	Control group	<i>p-value</i>
mean RNFL thickness (μm)	92,85±12,49	89,58±8,40	0,224
Superior RNFL thickness (μm)	115,70±15,87	111,67±9,76	0,228
Inferior RNFL thickness (μm)	122,79±18,18	116,03±16,70	0,125
Temporal RNFL thickness (μm)	64,94±9,68	61,35±7,88	0,109
Nasal RNFL thickness (μm)	71,85±14,68	70,87±13,90	0,783
Mean GC-IPL thickness (μm)	82,64±4,91	82,22±5,38	0,743
Superior GC-IPL thickness (μm)	82,79±6,06	82,00±6,18	0,603
Inferior GC-IPL thickness (μm)	81,44±6,06	82,25±8,07	0,644
Temporal GC-IPL thickness (μm)	82,76±4,13	81,20±5,79	0,239
Nasal GC-IPL thickness (μm)	83,02±7,68	81,64±5,53	0,412

OCT: optical coherence tomography RNFL: retinal nerve fiber layer GC-IPL: ganglion cell-inner plexiform layer.

In their study, Burgos-Blasco et al. [14] found that patients who had COVID-19 infection with anosmia and headache during their disease period increased the thickness of the peripapillary RNFL and GC-IPL thicknesses in the early period compared to normal healthy individuals. They did not detect a difference with postcovid patients without anosmia and headache. They stated that anosmia and headache are associated with neurological involvement and that the early period of viral infection causing neuroinflammation caused an increase in RNFL and GCL [14]. In our study, we did not separate the patients into those with and without neurological findings. In the literature, there is a case report of increased

intraocular pressure and angle-closure glaucoma due to change in electrolyte level after COVID-19 infection. Krawitz et al. [15] detected angle-closure glaucoma after hyponatremia due to chlortalidone use in a 65 years old patient who had positive nasopharygeal swab test for COVID-19. Hyponatremia is the most common electrolyte disorder in COVID-19 disease and has been associated with high mortality. In COVID-19 patients, serum sodium level may decrease, consequently, aqueous serum gradient changes. The higher sodium level in the humor aqueous than the serum creates an osmotic pressure difference. Consequently, fluid transition to humor aqueous occurs from serum. Fluid

passage into humor aqueous causes increase in intraocular pressure [15]. Depending on the change in intraocular pressure, RNFL and GS-IPL may also become thinner. In our study, we found no difference between the patient group and the control group in RNFL and GC-IPL. Hyponatremia was not detected in our study. The absence of RNFL and GS-IPL changes can be explained by the absence of changes in intraocular pressure.

COVID-19 patients who are treated in intensive care with acute respiratory distress are given a prone position to regulate breathing, which can increase intraocular pressure. Nerlikar et al. [16] detected bilateral angle-closure in a 56-year-old diabetic and hypertensive patient who was placed in a prone position due to pneumonia due to SARS-Cov-2 infection. They stated that angle closure occurs because of the narrowing of the anterior chamber angle due to the prone position of the patient [16].

As a result, COVID 19 disease may cause changes in RNFL and GS-IPL by mechanisms such as ischemia due to microvascular occlusion in the retina and optic disc, neuroinflammation, and intraocular pressure change. Studies have shown that in COVID- 19 disease, optic nerve head RNFL and GS-IPL can be affected by different mechanisms.

There are a few studies about the effect of SARS-Cov-2 infection on inner retinal layers. In the current study, a statistically significant difference was not found in terms of RNFL and GC-IPL thicknesses between healthy controls and postcovid patients. In our opinion, more studies about the possible effect of SARS-Cov-2 infection on retinal layer thicknesses should be performed.

The limitations of our study were relatively small sample sizes in both groups and alterations in the therapies. On the other hand,

the severity of COVID-19 infection was moderate in all patients.

In conclusion, the mean and fragmented RNFL and GC-IPL thicknesses were not statistically different in patients who had moderate disease and recovered from COVID-19 infection.

Funding: *The author(s) received no financial support for the research, authorship, and/or publication of this article.*

Conflict of Interest: *The authors declare that they have no conflict of interest.*

Ethical statement: *The study was approved by the Local Ethics Committee of Sakarya University (Decision no: 71522473/050.01.04/366), and written informed consent was obtained from each subject.*

Open Access Statement

This is an open access journal which means that all content is freely available without charge to the user or his/her institution under the terms of the Creative Commons Attribution Non-Commercial License (<http://creativecommons.org/licenses/by-nc/4.0>). Users are allowed to read, download, copy, distribute, print, search, or link to the full texts of the articles, without asking prior permission from the publisher or the author.

References

- [1] Talevi D, Socci V, Carai M, et al. Mental health outcomes of the CoViD-19 pandemic. *Riv Psichiatr.* 2020;55(3):137-144.
- [2] Rothan HA, Byrareddy SN. The epidemiology and pathogenesis of coronavirus disease (COVID-19) outbreak. *J Autoimmun.* 2020;109:102433.
- [3] Wang W, Tang J, Wei F. Updated understanding of the outbreak of 2019 novel

- coronavirus (2019-nCoV) in Wuhan, China. *J Med Virol.* 2020;92(4):441–47.
- [4]Huang C, Wang Y, Li X, et al. Clinical features of patients infected with 2019 novel coronavirus in Wuhan, China. *Lancet.* 2020;395(10223):497–506.
- [5]Dockery DM, Rowe SG, Murphy MA, et al. The Ocular Manifestations and Transmission of COVID-19: Recommendations for Prevention. *J Emerg Med.* 2020;59(1):137-140.
- [6]Wu P, Duan F, Luo C, et al. Characteristics of Ocular Findings of Patients With Coronavirus Disease 2019 (COVID-19) in Hubei Province, China. *JAMA Ophthalmol.* 2020;138(5):575-78.
- [7]Öncül H, Öncül FY, Alakus MF, et al. Ocular findings in patients with coronavirus disease 2019 (COVID-19) in an outbreak hospital. *J Med Virol.* 2021;93(2):1126-32.
- [8]Savastano A, Crincoli E, Savastano MC, et al. Against Covid-Post-Acute Care Study Group. Peripapillary Retinal Vascular Involvement in Early Post-COVID-19 Patients. *J Clin Med.* 2020;9(9):2895.
- [9]Benito-Pascual B, Gegúndez JA, Díaz-Valle D, et al. Panuveitis and Optic Neuritis as a Possible Initial Presentation of the Novel Coronavirus Disease 2019 (COVID-19). *Ocul Immunol Inflamm.* 2020;28(6):922-25.
- [10]Cozzupoli GM, Savastano MC, Falsini B, et al. Possible Retinal Impairment Secondary to Ritonavir Use in SARS-CoV-2 Patients: A Narrative Systematic Review. *J Ophthalmol.* 2020;2020:5350494.
- [11]Jia Y, Simonett JM, Wang J, et al. Wide-Field OCT Angiography Investigation of the Relationship Between Radial Peripapillary Capillary Plexus Density and Nerve Fiber Layer Thickness. *Invest Ophthalmol Vis Sci.* 2017;58(12):5188-94.
- [12]Mansoori T, Sivaswamy J, Gamalapati JS, et al. Radial Peripapillary Capillary Density Measurement Using Optical Coherence Tomography Angiography in Early Glaucoma. *J Glaucoma.* 2017;26(5):438-43.
- [13]Marinho PM, Marcos AAA, Romano AC, et al. Retinal findings in patients with COVID-19. *Lancet.* 2020;395(10237):1610.
- [14]Burgos-Blasco B, Güemes-Villahoz N, Vidal-Villegas B, et al. Optic nerve and macular optical coherence tomography in recovered COVID-19 patients. *Eur J Ophthalmol.* 2021:11206721211001019.
- [15]Krawitz BD, Sirinek P, Doobin D, et al. The Challenge of Managing Bilateral Acute Angle-closure Glaucoma in the Presence of Active SARS-CoV-2 Infection. *J Glaucoma.* 2021;30(3):e50-e53.
- [16]Nerlikar RR, Palsule AC, Vadke S. Bilateral Acute Angle Closure Glaucoma after Prone Position Ventilation for COVID 19 Pneumonia. *J Glaucoma.* 2021. doi: 10.1097/IJG.0000000000001864.

Fournier's gangrene: etiology, treatment outcomes and factors affecting mortality in 38 patients

Murat Derebey¹, Ismail Alper Tarim¹, Ufuk Karabacak², Kadir Seker³, Gokhan Selcuk Ozbalci²

¹Department of General Surgery, Ondokuz Mayıs University, Faculty of Medicine, Samsun, Turkey

²Department of Surgical Oncology, Sivas Cumhuriyet University, Faculty of Medicine, Sivas, Turkey

³Department of General Surgery, Bafra State Hospital, Samsun, Turkey

ABSTRACT

Aim: Fournier's gangrene (FG) is a rare, rapidly progressing and life-threatening disease of the genital, perianal and perineal regions. We aimed to evaluate etiological parameters, accompanying diseases, current treatment methods and factors affecting mortality in patients with FG.

Method: The medical records of 38 patients who were operated by the same team with a diagnosis of FG from December 2015 to January 2021 were retrospectively reviewed. Those patients were divided into two groups: survivors (Group 1), and non-survivors (Group 2). Comparisons were made regarding clinical and demographic features; comorbid diseases; leukocyte count at first presentation; etiological factors; treatment outcomes; and mortality rates.

Results: Thirty-eight patients (24 males, 14 females) were evaluated; mean age was 60.2 ± 13.2 years. While 76.3% (n = 29) of these patients recovered with treatment, the total mortality rate was 23.7% (n = 9). The most common cause of the FG and comorbidity were anorectal diseases (n = 22; 57.9%) and type 2 diabetes mellitus (n = 21; 55.3%), respectively. Female gender, septic shock, necrosis, abdominal wall and lumbar region involvement, chronic renal failure, FG development secondary to postoperative complications and ostomy rates were higher in non-survivors. There were no significant differences between the two groups regarding leukocyte count at first presentation, number of debridement, dressing methods, reconstruction methods, and length of hospital stay.

Conclusions: Female gender, presence of septic shock and necrosis on physical examination, involvement of the abdominal wall and lumbar region in addition to the perianal region, chronic renal failure, disease secondary to postoperative complications and the necessity of ostomy play an important role in mortality.

Key words: Fournier's gangrene, etiology, therapy, outcome, mortality.

✉ Dr. Murat Derebey

Department of General Surgery, Ondokuz Mayıs University, Faculty of Medicine, Samsun, Turkey

E-mail: mderebey@gmail.com

Received: 2021-02-28 / Revisions: 2021-04-20

Accepted: 2021-04-29 / Published online: 2021-07-01

Introduction

In 1883, Dr Jean Alfred Fournier described an infection with unknown origin that led to rapid

necrosis of the scrotal skin in young healthy men [1]. This infection is now called Fournier's gangrene (FG), although other definitions have been proposed, such as necrotising fasciitis, as suggested by Wilson in 1952 [2]. The term FG is now more widely implemented to genital, perianal, perirectal and abdominal wall infections. Although the initial definition does not contain a known etiology, trauma and

infection of the perianal and genital areas seem to play an important role in this disease [3]. FG can occur after colorectal and urinary system pathologies, perineal infections, perianal or genital trauma and any surgical intervention in the above-mentioned areas. This disease, which appears suddenly and progresses rapidly, is mostly mortal if not it is under control with early treatment [4, 5]. It can affect both genders and individuals in all ages [6].

Predisposing factors include diabetes mellitus, hypertension, coronary and peripheral artery diseases, obesity, smoking, drug addiction, poor hygiene, chronic alcoholism, malignancies and immunosuppression [7, 8]. This disease, which is difficult to diagnose without necrosis or gangrene, can show a rapid course and lead to death [9]. Early diagnosis of FG and determining the correct treatment method are very important for survival. The emergency treatment of FG begins with surgical debridement and broad-spectrum antibiotic therapy [3]. After the initial comprehensive debridement, a series of repetitive debridement may be required. An effective dressing is very valuable in treatment. In recent years, negative pressure wound therapy (NPWT) has gained popularity and is widely used in wound management [10].

Despite the advancement of knowledge on etiology, diagnosis, treatment and intensive care techniques, the mortality rate of FG patients is still high. The incidence of FG is increasing especially in developed countries aging population. Therefore, it is important to understand the predisposing factors, pathophysiology and clinical course of this disease. In this study, we aimed to review our experiences of FG treatment and to evaluate the etiological parameters, accompanying diseases, current treatment methods and factors affecting mortality in patients with FG.

Materials and methods

Ethical approval was obtained from the Local Ethics Committee for this study (IRB approval number OMU: 2020/751). The medical records of 38 patients who were operated by the same team with a diagnosis of FG from December 2015 to January 2021 were retrospectively reviewed. The diagnosis of FG was established based on patient history, clinical symptoms, physical examination at presentation and radiological findings.

The patients were divided into two groups as follows: survivors (Group 1, n = 29) and non-survivors (Group 2, n = 9). Demographic characteristics of the patients, initial symptoms, involved areas, etiological factors, comorbidities, leukocyte count at first presentation, number of debridement, dressing methods (wet or negative aspiration system), the presence of a diverting ostomy, reconstruction methods, and length of hospital stay were recorded and compared between the two groups. The effect of these parameters on clinical results was investigated.

All data were analyzed by using SPSS (Statistical Package for Social Sciences) for Windows 15.0 program. In the comparison of qualitative data, descriptive statistical methods (mean or median and standard deviation) and Pearson's chi-square test were used. The Mann-Whitney U test and independent samples t-test were used for binary comparisons of continuous variables. A value of $p < 0.05$ was accepted as statistically significant.

Results

Thirty-eight patients who were operated by the same team for FG were included in this study. While 29 (76.3%) of these patients recovered with treatment, 9 (23.7%) patients were deceased. Data on patient age, gender, clinical features, leukocyte count at first presentation

Table 1. Patient demographics, clinical features, leukocyte count at first presentation and comorbid diseases

Parameters	Group I (n=29)	Group II (n=9)	Total (n=38)	P value
Age* (years)	59.5 (12.9)	62.5 (14.6)	60.2 (13.2)	.559
Gender				
Female	8 (27.6%)	6 (66.7%)	14 (36.8%)	.034
Male	21 (72.4%)	3 (33.3%)	24 (63.2%)	
Initial symptoms				
Perianal swelling	22 (75.9%)	2 (22.2%)	24 (63.2%)	.040
Perianal pain	20 (69%)	1 (11.1%)	21 (55.3%)	.002
Necrosis	9 (31%)	8 (88.9%)	17 (44.7%)	.002
Fever	11 (37.9%)	1 (11.1%)	12 (31.6%)	.130
Perineal pain	9 (31%)	1 (11.1%)	10 (26.3%)	.236
Crepitus	7 (24.1%)	3 (33.3%)	10 (26.3%)	.584
Septic shock	1 (3.4%)	6 (66.7%)	7 (18.4%)	<.001
Scrotal swelling	5 (17.2%)	2 (22.2%)	7 (18.4%)	.736
Vulvar swelling	3 (10.3%)	2 (22.2%)	5 (13.2%)	.689
Involved area				
Perianal	24 (82.8%)	4 (44.4%)	28 (73.7%)	.023
Genital	14 (48.3%)	4 (44.4%)	18 (47.4%)	.841
Perineal	14 (48.3%)	3 (33.3%)	17 (44.7%)	.431
Abdominal wall	4 (13.8%)	7 (77.8%)	11 (28.9%)	<.001
Lumbar region	4 (13.8%)	4 (44.4%)	8 (21.1%)	.049
Etiology				
Anorectal	19 (65.5%)	3 (33.3%)	22 (57.9%)	.088
Urogenital	3 (10.3%)	3 (33.3%)	6 (15.8%)	.098
Cutaneous	4 (13.8%)	0	4 (10.5%)	.239
Postoperative complication	1 (3.4%)	3 (33.3%)	4 (10.5%)	.011
Trauma	2 (6.9%)	0	2 (5.3%)	.418
COVID-19	1 (3.4%)	0	1 (2.6%)	.572
Leukocyte count at first presentation* (u/L)	17047 (7336)	16735 (8206)	16973 (7436)	.914
Comorbid disease				
Diabetes	17 (58.6%)	4 (44.4%)	21 (55.3%)	.455
Hypertension	7 (24.1%)	4 (44.4%)	11 (28.9%)	.241
Coronary artery disease	7 (24.1%)	2 (22.2%)	9 (23.7%)	.906
Malignancy	5 (17.2%)	3 (33.3%)	8 (21.1%)	.301
Chronic renal failure	2 (6.9%)	3 (33.3%)	5 (13.2%)	.040
Cerebrovascular disease	3 (10.3%)	2 (22.2%)	5 (13.2%)	.357

*Data is presented as mean (standard deviation), Bold values indicate statistical significance.

Table 2. The etiology of Fournier's gangrene.

Etiology	Group I	Group II	Total
Anorectal	19 (50%)	3 (7.9%)	22 (57.9%)
Perianal abscess	10 (26.5%)	1 (2.6%)	11 (29.1%)
Fistula to the rectum	1 (2.6%)	-	1 (2.6%)
Ischiorectal abscess	4 (10.5%)	-	4 (10.5%)
Perforated appendicitis	1 (2.6%)	-	1 (2.6%)
Rectum cancer	1 (2.6%)	-	1 (2.6%)
Perforated cecum tumor	-	1 (2.6%)	1 (2.6%)
Rectum perforation / foreign body	1 (2.6%)	-	1 (2.6%)
Diverticular perforation	1 (2.6%)	1 (2.6%)	2 (5.3%)
Urogenital	3 (7.9%)	3 (7.9%)	6 (15.8%)
Scrotal abscess	1 (2.6%)	1 (2.6%)	2 (5.3%)
Vulvar abscess	1 (2.6%)	2 (5.3%)	3 (7.9%)
Bartholin abscess	1 (2.6%)	-	1 (2.6%)
Cutaneous	4 (10.5%)	0	4 (10.5%)
Decubitus ulcer	2 (5.3%)	-	2 (5.3%)
Perineal soft tissue infection	2 (5.3%)	-	2 (5.3%)
Postoperative complication	1 (2.6%)	3 (7.9%)	4 (10.5%)
Haemorrhoidal disease	1 (2.6%)	-	1 (2.6%)
Intestinal anastomotic leak	-	2 (5.3%)	2 (5.3%)
Colostomy complication	-	1 (2.6%)	1 (2.6%)
Trauma	2 (5.3%)	0	2 (5.3%)
COVID-19	1 (2.6%)	0	1 (2.6%)

Table 3. Treatment outcomes for Fournier's gangrene.

Parameters	Group I (n=29)	Group II (n=9)	Total (n=38)	P value
Number of debridement*	3 (2-20)	3 (2-12)	3 (2-20)	.927
Dressing methods				
Wet-dressing	4 (13.8%)	0		.266
NPWT	25 (86.2%)	9 (100%)	34 (89.5%)	
Ostomy	8 (27.6%)	6 (66.7%)	14 (36.8%)	.034
Reconstruction				
Fasciocutaneous flap	4 (13.8%)	2 (22.2%)	6 (15.8%)	.203
Split-thickness skin graft	8 (27.6%)	0	8 (21.1%)	
Length of hospital stay (day)	23 (3-59)	20 (4-86)	22 (3-86)	.447

NPWT: negative pressure wound therapy, *Data is presented as median (min-max value), Bold value indicate statistical significance.

and comorbid diseases are presented in Table 1. The mean age was 60.2 ± 13.2 years and 63.2% of the population was male. Female gender was significantly higher in Group 2 ($p < 0.05$).

When the initial symptoms were compared, perianal swelling and perianal pain were significantly higher in Group 1, and septic shock and necrosis in Group 2 ($p < 0.05$). Perianal involvement was more common in Group 1 and abdominal wall and lumbar region involvement in Group 2 ($p < 0.05$).

Etiological origins are shown in Table 1 and Table 2, and the most common cause of Fournier's gangrene was a perianal or perirectal infection spreading to the perineum, external urogenital organs, abdominal wall, and lumbar region. FG developing secondary to postoperative complications was significantly higher in Group 2 ($p < 0.05$). There was no statistical difference between the groups in terms of leukocyte count at first presentation. The most common comorbid disease was diabetes mellitus (21 patients; 55.3%). 33% of the patients who died from Fournier's gangrene had chronic renal failure. In Group 1, Fournier's gangrene occurred in 1 patient during COVID 19 treatment and in 2 patients after blunt perineal trauma due to falling from height (Table 2).

There were no significant differences between the two groups regarding number of debridement, dressing methods, reconstruction methods, and length of hospital stay ($p > 0.05$). Ostomy was required in 8 (27.6%) patients in Group 1 and 6 (66.7%) patients in Group 2 due to anal sphincter defect or surgical wound contamination. Stoma rate was higher in Group 2 ($p < 0.05$) (Table 3).

Discussion

Fournier's gangrene (FG) is a rare but serious and progressive infection that can affect the

genital area, perineum and lower abdominal wall separately or together [3]. As the causative microorganisms multiply, the infection spreads to the anatomical fascial planes. The pathognomonic histological findings on FG are necrosis of the superficial and deep fascial planes, fibrin deposition within and around the arterioles [11]. FG predominantly occurs in individuals aged between 30 and 60 [12]. In a recent study, although this disease is detected at all ages, it has been reported mostly in individuals in their fifties [13]. This aggressive disease process is associated with a high mortality rate of 20-30% [14]. There are different results in the literature regarding age as a prognostic factor for death. Sorensen et al. [15] emphasized that the prognosis worsens with increasing patient age, while Yenyol et al. [16] found no statistical difference in age between survivors and non-survivors. The mean age of the patients in the present study was 60.2 years and the mortality rate was 23.7%. We did not observe any significant difference in age among groups. While FG has been known to be a predominantly male disease since scrotal involvement was used as the key component of the original FG definition, the definition has expanded with the presentation of this disease also in women [17]. Although FG was observed less frequently in women in our study, the mortality rate was found to be significantly higher. Similarly, Czymek et al. [18] stated that female gender is a prognostic factor for mortality. On the other hand, this result may be due to the fact that the study was conducted with a smaller number of patients.

Patients usually come to the emergency service within a few days after the onset of complaints such as purulent rectal discharge, perineal edema or pain. Infectious sources are mostly anorectal diseases, urological diseases, intraperitoneal events or traumatic injuries, and

in some cases the cause may not be determined [19, 20]. In this study, the main patient complaints were perianal swelling, perianal pain, and necrosis around the anus. The mortality rate was significantly higher in patients who had symptoms of necrosis and septic shock at presentation, and accompanying abdominal wall and lumbar region involvement in addition to perianal involvement. Although many diseases have been reported to be positively associated with FG, especially diabetes mellitus is the most important predisposing factor among them [3, 21]. On the other hand, the relationship between diabetes mellitus and mortality is still controversial. Some studies report an association with both incidence and mortality, while others only show a relationship with incidence. In our study, 55.3% of the patients had diabetes mellitus; however, there was no significant association between diabetes mellitus and mortality. In a recent study, FG with extensive soft tissue necrosis and pre-existing chronic kidney disease was associated with poor prognosis [22]. Similarly, chronic renal failure was statistically more common in non-survivors in this study.

Previously, FG was generally known as a urological disease, but now it is mainly of concern to general surgeons as the most common etiology is colorectal-derived diseases. Stephens et al. found a higher mortality in patients with colorectal-derived FG compared to other etiologies [23]. Necrotizing soft tissue infections caused by intestinal perforation can occur in an atypical fashion with significant morbidity and mortality rates [24]. When anorectal etiologies and postoperative colorectal surgery complications were evaluated together, it was seen that they constituted 68.4% of the total etiology in our study. Moreover, mortality rate was high in FG

cases developing secondary to postoperative colorectal surgery complications. Fournier's gangrene was detected in a 76-year-old female patient who was followed up in the intensive care unit due to respiratory failure secondary to COVID-19. COVID-19, which suppresses the immune system, has emerged as another etiological factor. The above mentioned patient, who underwent emergency and aggressive debridement along with COVID-19 treatment, was discharged on the 7th week of hospitalization. It has been reported that a high mean leukocyte count at first presentation is a prognostic factor for mortality [25]. On the contrary, no significant difference was found among the groups in terms of leukocyte count in our study.

Early diagnosis, urgent debridement and adequate administration of broad-spectrum antibiotics are the most essential component of treatment [26]. In this study, aggressive debridement and broad-spectrum antibiotic therapy were performed to all patients. Serial debridement was continued until necrotic lesions disappeared at the wound site. The median amount of debridement for both groups was 3 and there was no statistically significant difference between the groups. A conventional wet-to-dry dressing is a well-known, popular, inexpensive and accepted method with many advantages such as keeping the wound clean. NPWT is a widely used another method of wound treatment [27]. Once the necrosis is eliminated, NPWT helps the wound heal physiologically. The negative pressure leads to increased blood flow and the migration of inflammatory cells to into the wound site [28]. NPWT requires less frequent change compared to traditional dressings and is a less painful procedure. This also prevents bacterial contamination and accelerates the formation of granulation tissue with the removal of exudates

[29,30]. NPWT treatment was used in 89.5% of all patients, and there was no statistically significant difference between the groups in terms of wound therapy.

The debridement area usually carries the risk of faecal contamination [31]. Therefore, a faecal diversion is an important attempt at FG treatment. Loop colostomy is often used in patients with severe perineal involvement and wounds close to the anus [32]. The literature has shown that patients requiring ostomy has a poor prognosis [15]. 36.8% of the patients required ostomy and there was statistically significant association between ostomy and prognosis. Stoma rate was statistically higher in non-survivors. Early closure of tissue defects is an important part of treatment. Various reconstructive methods are available for good functional and cosmetic results. There is no consensus on the best method of reconstruction. The reconstructive treatment should be based on the patient's clinical characteristics, patient preference, and surgeon's judgment [33]. We preferred either fasciocutaneous flap or split-thickness skin graft in wounds with large tissue defects that did not close with secondary healing after NPWT treatment. Major wounds caused by debridement in FG patients usually take a long time to heal and thus require a long hospital stay. Although Ersay et al. [20] have determined that longer hospital stay was a factor affecting survival, there was no statistically significant difference between the groups in terms of hospital stay in our study.

The limitation of this study was associated with the disadvantages caused by the retrospective design. Although the data were collected in a five-year period, the sample size was small. Another limitation was that when the patient data were analyzed retrospectively, we could not reach all the necessary laboratory values to calculate the FGSI score. Therefore, we could

not use this parameter to compare between groups. FG with diffuse soft tissue necrosis is associated with poor prognosis and complex patient management. Rapid recognition of disease spread and patient's poor prognostic factors is essential to reduce mortality and establish a management plan for this disease. In spite of development in medical treatment and intensive care procedures, FG is still a mortal disease.

Conclusion

Fournier's gangrene is a serious surgical emergency with a high mortality rate. Female gender, presence of septic shock and necrosis on physical examination, involvement of the abdominal wall and lumbar region in addition to the perianal region, chronic renal failure, disease secondary to postoperative complications and the necessity of ostomy play an important role in mortality.

Funding: *The author(s) received no financial support for the research, authorship, and/or publication of this article.*

Conflict of Interest: *The authors declare that they have no conflict of interest.*

Ethical statement: *The study was approved by the Local Ethics Committee of Ondokuz Mayıs University (IRB approval number OMU: 2020/751), and written informed consent was obtained from each subject.*

Open Access Statement

This is an open access journal which means that all content is freely available without charge to the user or his/her institution under the terms of the Creative Commons Attribution Non-Commercial License (<http://creativecommons.org/licenses/by-nc/4.0>). Users are allowed to read, download, copy, distribute, print, search, or link to the full

texts of the articles, without asking prior permission from the publisher or the author.

References

- [1]Fournier JA. Jean-Alfred Fournier 1832-1914. Gangrène foudroyante de la verge (overwhelming gangrene). Sem Med 1883. Diseases of the colon and rectum. 1988;31(12):984-88.
- [2]Wilson B. Necrotizing fasciitis. The American surgeon. 1952;18(4):416-31.
- [3]Morpurgo E, Galandiuk S. Fournier's gangrene. The Surgical clinics of North America. 2002;82(6):1213-24.
- [4]Korhonen K. Hyperbaric oxygen therapy in acute necrotizing infections with a special reference to the effects on tissue gas tensions. Annales chirurgiae et gynaecologiae Supplementum. 2000(214):7-36.
- [5]Eke N, Echem RC, Elenwo SN. Fournier's gangrene in Nigeria: a review of 21 consecutive patients. International surgery. 2000;85(1):77-81.
- [6]Oguz A, Gümüş M, Turkoglu A, et al. Fournier's Gangrene: A Summary of 10 Years of Clinical Experience. International surgery. 2015;100(5):934-41.
- [7]Hejase MJ, Simonin JE, Bihrl R, et al. Genital Fournier's gangrene: experience with 38 patients. Urology. 1996;47(5):734-39.
- [8]Benizri E, Fabiani P, Migliori G, et al. Gangrene of the perineum. Urology. 1996;47(6):935-39.
- [9]Jeong HJ, Park SC, Seo IY, et al. Prognostic factors in Fournier gangrene. International journal of urology : official journal of the Japanese Urological Association. 2005;12(12):1041-44.
- [10]Pour SM. Use of negative pressure wound therapy with silver base dressing for necrotizing fasciitis. Journal of wound, ostomy, and continence nursing : official publication of The Wound, Ostomy and Continence Nurses Society. 2011;38(4):449-52.
- [11]Vick R, Carson CC, 3rd. Fournier's disease. The Urologic clinics of North America. 1999;26(4):841-49.
- [12]Sockkalingam VS, Subburayan E, Velu E, et al. Fournier's gangrene: prospective study of 34 patients in South Indian population and treatment strategies. Pan African medical journal. 2018;12(31):110.
- [13]Bilton BD, Zibari GB, McMillan RW, et al. Aggressive surgical management of necrotizing fasciitis serves to decrease mortality: a retrospective study. The American surgeon. 1998;64(5):397-400.
- [14]Singh A, Ahmed K, Aydin A, et al. Fournier's gangrene. A clinical review. Archivio italiano di urologia, andrologia : organo ufficiale [di] Societa italiana di ecografia urologica e nefrologica. 2016;88(3):157-64.
- [15]Sorensen MD, Krieger JN, Rivara FP, et al. Fournier's gangrene: management and mortality predictors in a population based study. The Journal of urology. 2009;182(6):2742-47.
- [16]Yeniyol CO, Suelozgen T, Arslan M, et al. Fournier's gangrene: experience with 25 patients and use of Fournier's gangrene severity index score. Urology. 2004;64(2):218-22.
- [17]Smith GL, Bunker CB, Dinneen MD. Fournier's gangrene. British journal of urology. 1998;81(3):347-55.
- [18]Czymek R, Frank P, Limmer S, et al. Fournier's gangrene: is the female gender a risk factor? Langenbecks Arch Surg. 2010;395(2):173-80.

- [19] Shyam DC, Rapsang AG. Fournier's gangrene. *The surgeon : journal of the Royal Colleges of Surgeons of Edinburgh and Ireland*. 2013;11(4):222-32.
- [20] Ersay A, Yilmaz G, Akgun Y, et al. Factors affecting mortality of Fournier's gangrene: review of 70 patients. *ANZ journal of surgery*. 2007;77(1-2):43-48.
- [21] Taviloglu K, Yanar H. Necrotizing fasciitis: strategies for diagnosis and management. *World Journal of Emergency Surgery*. 2007;2(1):19.
- [22] Hahn HM, Jeong KS, Park DH, et al. Analysis of prognostic factors affecting poor outcomes in 41 cases of Fournier gangrene. *Annals of surgical treatment and research*. 2018;95(6):324-32.
- [23] Enriquez JM, Moreno S, Devesa M, et al. Fournier's syndrome of urogenital and anorectal origin. A retrospective, comparative study. *Diseases of the colon and rectum*. 1987;30(1):33-37.
- [24] Kumar D, Cortés-Penfield NW, El-Haddad H, et al. Bowel Perforation Resulting in Necrotizing Soft-Tissue Infection of the Abdomen, Flank, and Lower Extremities. *Surgical infections*. 2018;19(5):467-72.
- [25] Villanueva-Sáenz E, Martínez Hernández-Magro P, Valdés Ovalle M, et al. Experience in management of Fournier's gangrene. *Techniques in coloproctology*. 2002;6(1):5-10.
- [26] Norton KS, Johnson LW, Perry T, et al. Management of Fournier's gangrene: an eleven year retrospective analysis of early recognition, diagnosis, and treatment. *The American surgeon*. 2002;68(8):709-13.
- [27] Ozturk E, Ozguc H, Yilmazlar T. The use of vacuum assisted closure therapy in the management of Fournier's Gangrene. *American journal of surgery*. 2009;197(5):660-65.
- [28] Arslan E, Ozturk OG, Aksoy A, et al. Vacuum-assisted closure therapy leads to an increase in plasma fibronectin level. *International wound journal*. 2011;8(3):224-28.
- [29] Assenza M, Cozza V, Sacco E, et al. VAC (Vacuum Assisted Closure) treatment in Fournier's gangrene: personal experience and literature review. *La Clinica terapeutica*. 2011;162(1):e1-5.
- [30] Czymek R, Schmidt A, Eckmann C, et al. Fournier's gangrene: vacuum-assisted closure versus conventional dressings. *American journal of surgery*. 2009;197(2):168-76.
- [31] Ozkan OF, Altýnlý E, Koksall N, et al. Combining Flexi-Seal and negative pressure wound therapy for wound management in Fournier's gangrene. *International wound journal*. 2015;12(3):364-5.
- [32] Ozkan OF, Koksall N, Altinli E, et al. Fournier's gangrene current approaches. *International wound journal*. 2016;13(5):713-16.
- [33] Insua-Pereira I, Ferreira PC, Teixeira S, et al. Fournier's gangrene: a review of reconstructive options. *Central European journal of urology*. 2020;73(1):74-79.

Dual effect of epigallocatechin gallate on the pathology of Alzheimer's: Cholinesterases and amyloidogenesis

Eda Ozturan Ozer 

Department of Medical Biochemistry, Baskent University, Faculty of Medicine, Ankara, Turkey

ABSTRACT

Aim: To evaluate the dual inhibitory effect of epigallocatechin gallate on Alzheimer's pathogenesis.

Methods: Cholinesterase inhibition studies were performed by kinetic Ellman methods and also the inhibitory effect of molecule on amyloid fibrillation is determined by dye binding thioflavin T method.

Results: Epigallocatechin gallate inhibited both types of cholinesterases and amyloid fibrillation. The inhibition of acetylcholinesterase indicated an uncompetitive inhibition whereas butyrylcholinesterase inhibition had an unique pattern. Compound inhibited butyrylcholinesterase with two types of inhibition in a dose related manner. Fibrillation destabilization is also observed by the compound.

Conclusion: Our results indicated that epigallocatechin gallate may be accepted as a candidate molecule as the dual effective drugs for neurodegenerative diseases.

Key words: Cholinesterase, amyloid, epigallocatechin gallate, Alzheimer's disease.

✉ Dr. Eda Ozturan Ozer

Department of Medical Biochemistry, Baskent University, Faculty of Medicine, Ankara, Turkey

E-mail: eozer@baskent.edu.tr

Received: 2021-04-07 / Accepted: 2021-04-29

Published online: 2021-07-01

Introduction

Catechins are polyphenols that belong to plant-derived flavonoid family. Antioxidant effects are the well-known effects and their prooxidant behavior is also reported depending on the dose and route of administration [1,2]. Dietary sources, tea and especially green tea is a fundamental source of catechins for human. The major active component of the polyphenolic content of green tea is epigallocatechin gallate (EGCG). Besides antioxidant effects, some other beneficial roles of EGCG are reported as antiatherogenic, anticarcinogenic, antiapoptotic and its

importance in neurodegenerative diseases is widely emphasized in experimental *in vivo* studies [3,4]. Many studies of human clinical trials showed to have an augmented healing effect on the cognitive dysfunction by the use of flavanol compounds.

Alzheimer's disease (AD) is a deteriorative neurological disorder characterized by loss of memory and mental functions, behavioral disorders and also impairment of cholinergic neurotransmission. Although the etiology of AD is not clarified definitely yet, there are some well accepted features about the basis of disease. Aggregation of amyloid peptides is reported as the most common reason in the onset and progression. Amyloid peptides are the proteolytic cleavage products of amyloid precursor protein (APP). Although this cleavage is a physiological process, the activity of specific enzymes results with the formation

of fragments (amyloid beta 1-40, amyloid beta 1-42) that form toxic aggregates (amyloid plaques) in the brain. The inhibition of aggregation is accepted as the main strategy for the treatment of the disease and there are several *in vitro* reports dealing with this approach [5-9].

Another well-known fact about the pathology and progress of the AD is the attenuation of cholinergic response. Whether it is caused by the apoptosis of cholinergic neurons or the decreased activity of acetylcholinesterase; it is mainly reported that the diminished acetylcholine levels has an important role in the severe symptoms of AD. Cholinesterase inhibitors are widely used medications to overcome this problem on the symptomatic treatment of the disease for an improved quality of lifetime. Cholinesterases are the serine hydrolases responsible for the cholinergic metabolism. Acetylcholinesterase (AChE; E.C.3.1.1.7) and butyrylcholinesterase (BChE; E.C.3.1.1.8) may use acetylcholine as the substrate with different affinities and both known to have roles in the maintenance of acetylcholine levels. Besides the enzymatic activity, many *in vitro* studies report another function of AChE in the molecular pathology of AD. Experiments show that, the peripheral anionic site (PAS) of the AChE interacts with amyloid peptides behaving as a core for promoting fibril aggregation [10].

Upon these observations experiments mainly focus on the generation and development of the dual effective cholinesterase inhibitors that target both the enzymatic activity and self-fibrillation [11,12].

There are several reports dealing with the inhibitory effects of flavonoids on the cholinesterases [13]. Our study is aimed to determine the inhibitory parameters of EGCG on cholinesterases and to evaluate the possible

destabilization of amyloidogenesis within the determined pharmacological concentrations obtained by kinetic analysis. Based on our hypothesis EGCG may be nominated as a member of dual effective drugs family for Alzheimer's treatment.

Materials and methods

Chemicals

Human recombinant AChE, Equine serum BChE, amyloid peptides 1-40/1-42, epigallocatechin-3-gallate (EGCG), acetylthiocholineiodide (ATCh), butyrylthiocholineiodide (BTCh) and Thioflavin T (ThT) were purchased from Sigma-Aldrich (MO, USA). All biochemical studies were performed in triplicate and data were expressed as mean \pm SEM.

Enzymatic Analysis

Enzyme activities (AChE and BChE) were assayed by the Ellman Method with/without various concentrations of inhibitor (EGCG). The tubes having zero concentrations of EGCG are used as the control. The activity medium was containing 100 mM MOPS pH 8.0, 0.05–0.5 mM ATCh or BTCh as the substrate, 0.125 mM dithiobisnitrobenzoic acid (DTNB) and inhibitor. Reactions were initiated by the addition of enzyme(s) (0.02 U/mL) and the absorbance change at 412 nm was monitored spectrophotometrically against the sample blank (Shimadzu-1601, Japan) at 25 °C [14].

Amyloid peptide fibrillation

The inhibitory effect of EGCG on the amyloid aggregation is tested by Thioflavin T fluorescence method. ThT is a dye giving a characteristic fluorescence upon binding to peptides/polypeptides and also aggregates [15]. Due to characteristics of the binding, the

increase in the fluorescence with respect to control, is accepted as the increase of fibrillation (aggregation). Commercially available peptides were dissolved in 100 mM potassium phosphate buffer pH 7.2 and incubated with/without 50 μM of EGCG for 24 hours. The fluorescence intensities were recorded and expressed as arbitrary unit (A.U.) at the time intervals given on the figure. ThT fluorescences were obtained using 8 μM ThT in 100 mM sodium phosphate buffer, pH 7.4, by spectrofluorometer (Shimadzu RF-5301, Japan) at wavelengths Ex: 442 and Em: 482. Rifampicin was used as the standard for fibril destabilization [16].

Results

Kinetic Analysis

In order to estimate the probable inhibitory effect of EGCG on cholinesterase activities and perform further kinetic evaluation, IC_{50} values were determined as $55 \pm 1,3 \mu\text{M}$ for AChE and $63 \pm 1,1 \mu\text{M}$ for BChE. Inhibitor types and kinetic properties for both enzymes were determined by Lineweaver-Burk plots with secondary reciprocals. As shown in Figure 1 the inhibition of AChE by EGCG was uncompetitive (Figure 1). EGCG inhibited BChE in a dose related manner. The inhibition type was uncompetitive at low inhibitor concentrations (25,50 μM)

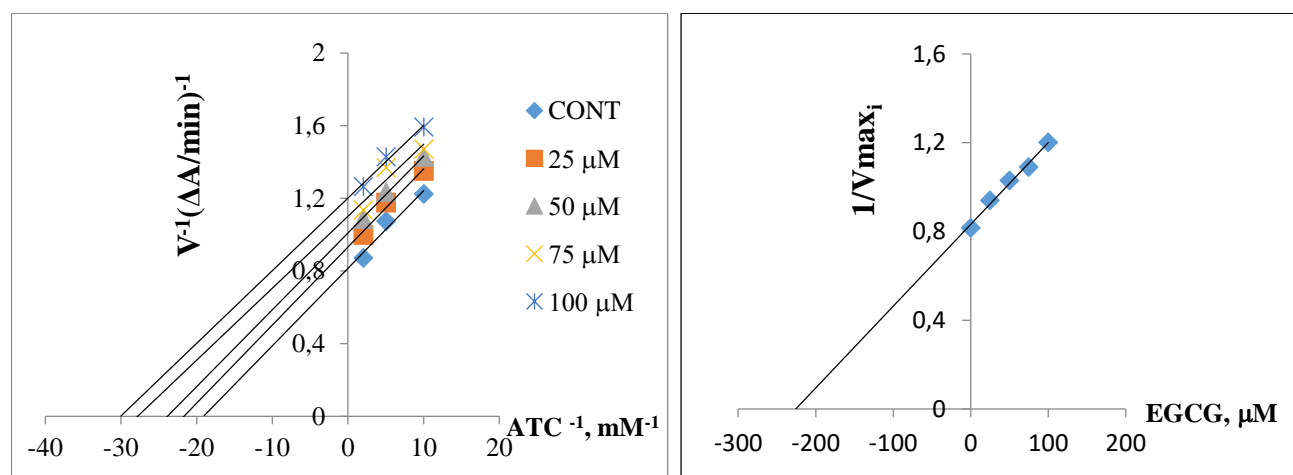


Figure 1. The Lineweaver-Burke (A) and reciprocal (B) plot of AChE inhibition by EGCG. Each point is the average of three determinations.

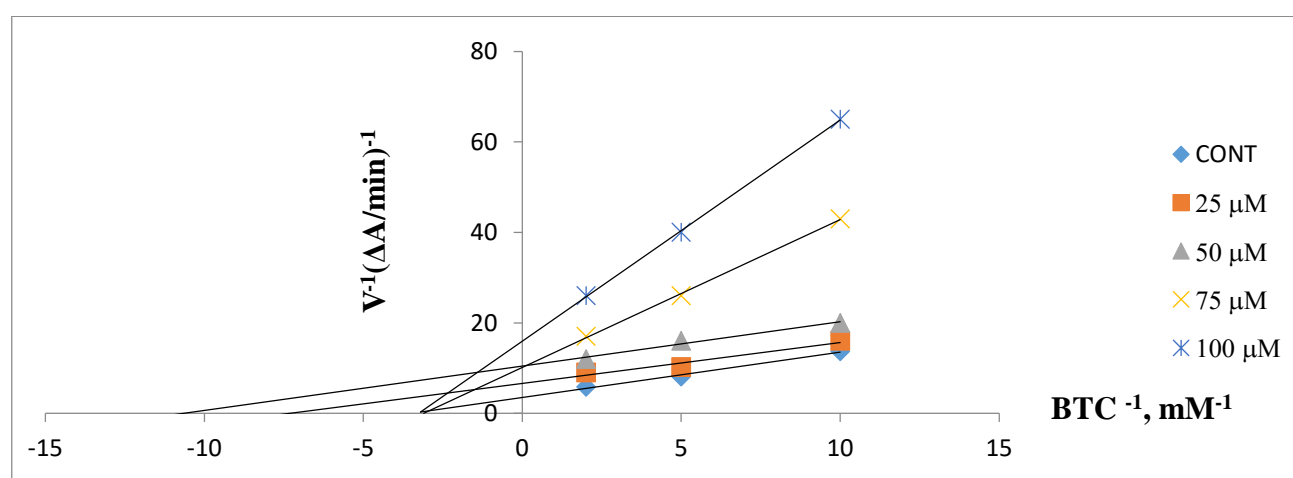


Figure 2. The Lineweaver-Burk plot of BChE inhibition by EGCG. Each point is the average of three determinations.

whereas at high inhibitor concentrations (75,100 μM) inhibition was noncompetitive (Figure 2). The reciprocal plots for each are given respectively in Figure 3 A and B.

The types of inhibitions and inhibitor-enzyme dissociation constant (K_i) values were given in Table 1.

Amyloid Destabilization

The inhibitory effect of EGCG on three forms

of fibrillation (1-40-140, 1-42-1-42 and 1-40-42) was tested with the ThT fluorescence method. As shown in Figure 4 EGCG inhibited the formation of all types of fibril aggregation from the fourth hour of experiment. Rifampicin which is a well-known standard destabilizing agent was used in our experiment for the same purpose [16].

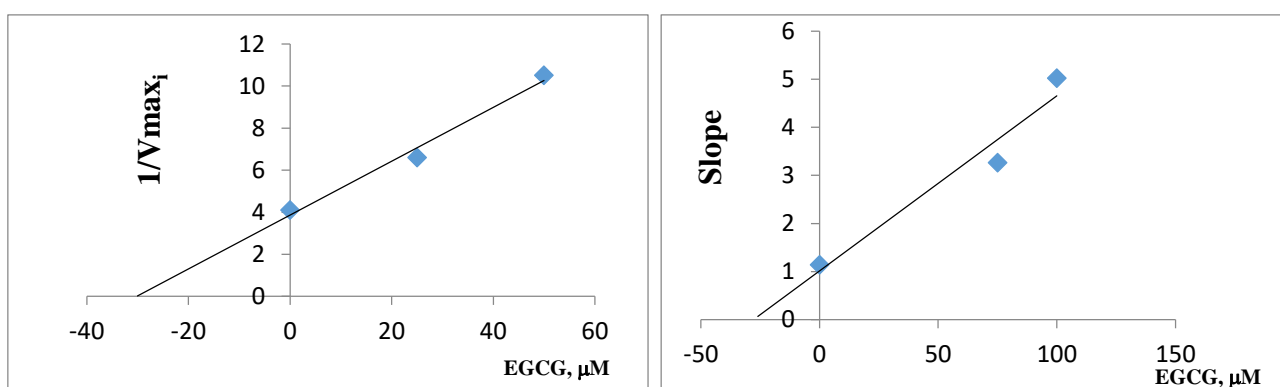


Figure 3. The reciprocal plots for (A) uncompetitive (B) noncompetitive inhibition of BChE inhibition by EGCG. Each point is the average of three determinations.

Table 1. The kinetic data of inhibitory parameters of EGCG on cholinesterases. Values are expressed as mean \pm SEM.

Enzyme	Inhibition type	K_i (μM)
AChE	Uncompetitive	222.3 ± 1.25
BChE	Uncompetitive	28.1 ± 0.33
25-50 μM EGCG	Noncompetitive	32.3 ± 0.46
75-100 μM EGCG		

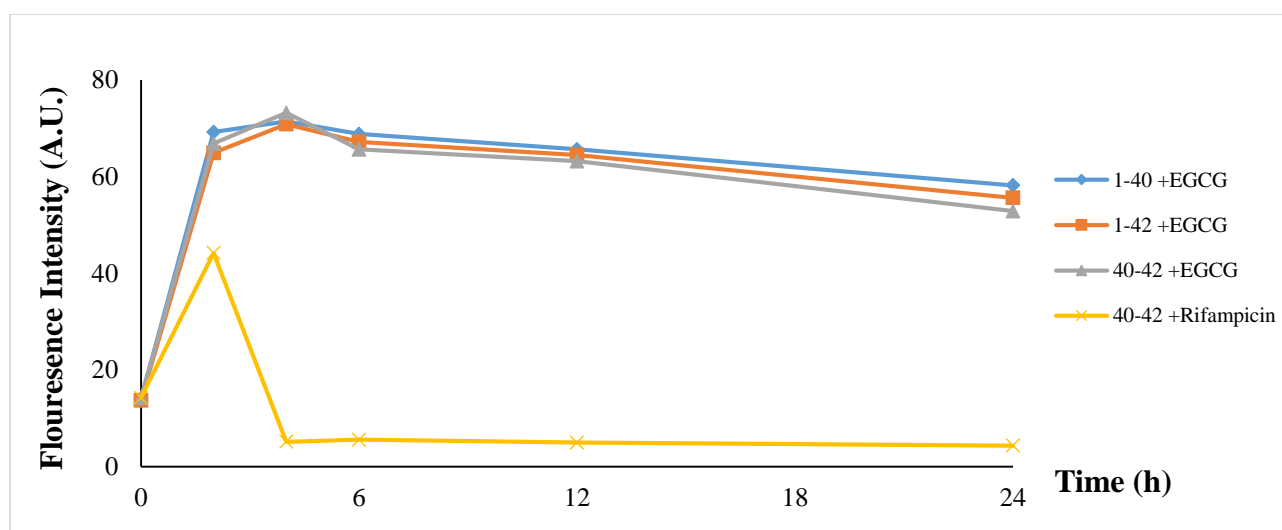


Figure 4. Inhibitory effect of EGCG on amyloid peptide aggregation. Each point is the average of three determinations.

Discussion

In our study EGCG is found to inhibit both types of cholinesterases and also amyloid aggregation. Although the calculated IC_{50} 's were not promising when compared to the values of donepezil (23.1 nM for human recombinant AChE and 7.4 nM for BChE) the discovery of dual inhibitory effect was satisfactory [17].

The plots indicated an uncompetitive inhibition of AChE and a dose related inhibition pattern for BChE.

Due to its physiological importance, AChE is one of the most investigated enzymes for the *in vivo* and *in vitro* effects of herbal medicines. There are several reports indicating the roles of ginsenosides [18], flavanoids [19], and other types of plant-based sources on the activity of cholinesterases.

The active site of cholinesterases (active gorge) has five different regions for proper catalysis. The amino acid content of these sites differ for AChE and BChE and contribute to the differences in catalytic activities and their behavior against the inhibitors. It is mainly known that the gorge of AChE is smaller than the active gorge of BChE by the replacement of 14 aromatic amino acids with the aliphatic ones. The common catalytic site is a catalytic triad having Ser-His-Glu residues [20].

In our model, the uncompetitive inhibition of AChE indicates an interaction of EGCG with a site other than the catalytic triad of the enzyme. The smaller gorge of AChE may block the entrance of EGCG to active site and EGCG is captured by the PAS. The peripheral anionic site (PAS) which is placed on the entry of active gorge has Asp and Tyr amino acids. EGCG is a polyphenolic substance having free hydroxyl residues in its structure. Due to the probable hydrogen bond formation between Asp/Tyr amino acids with these polyhydroxyls an

uncompetitive inhibition is caused by EGCG [21].

The inhibition of BChE with EGCG showed an interesting pattern. At concentrations below IC_{50} values the inhibition was uncompetitive whereas noncompetitive inhibition was observed at concentrations greater than 50 μ M. These results implied a multi-site interaction of molecule with the enzyme. In order to prove our assumption Hill plot was constructed [22]. By the plot, inhibitor binding sites were calculated as 1.9 and 2.4 at low and high concentrations respectively having an average 2.15. The n values greater than 1 obtained by Hill plot indicates more than one binding sites for inhibitor – enzyme relationship and this data clarified dose related inhibition pattern. Also findings were in accordance with the previous studies dealing with this type of inhibitions [17,23]. This observation is generally reported due to conformational change at the active site of BChE by increasing concentrations of inhibitor. Several reports mention the importance of Leu and Val residues of acyl bonding pocket of BChE for the binding of large molecules [24,25]. We postulate that this change of inhibition type is caused by the binding of EGCG to PAS at low concentrations and the increased concentrations predominating interaction with the second site, acyl pocket.

EGCG also inhibited the amyloid fibril aggregation in a time course manner. Previous studies report [26] the destabilizing effect of EGCG on Ab42 fibrillation but we investigated all types of fibrillation processes. All types of fibril formations was observed to increase by the two hours of experiment and EGCG destabilized the fibrillation from fourth hours. Rifampicin which is a well-accepted fibrillation destabilizer inhibited fibril formation by 90.9% in 24 h and EGCG is inhibited only by 7%. The selected

concentration of EGCG was only 50 μ M in order to sustain and mimic IC₅₀ levels and we conclude that the fibrillation inhibitions may be repeated in dose dependent manner.

Conclusion

The dual inhibitory effect on both cholinesterases and amyloidogenesis is a well investigated effect of molecules for the treatment of AD and depending on this approach our findings add a new insight to known beneficial effects of EGCG on neurodegenerative diseases.

Ethical statement and Funding: *This study is funded by Başkent University after the approval of Başkent University Institutional Review Board and Ethics Committee and also supported by Başkent University Research Fund (DA16/06 and DA20/27).*

Conflict of Interest: *The authors declare that they have no conflict of interest.*

Open Access Statement

This is an open access journal which means that all content is freely available without charge to the user or his/her institution under the terms of the Creative Commons Attribution Non-Commercial License (<http://creativecommons.org/licenses/by-nc/4.0>). Users are allowed to read, download, copy, distribute, print, search, or link to the full texts of the articles, without asking prior permission from the publisher or the author.

References

[1] Ryan P, Hynes MJ. The kinetics and mechanisms of the complex formation and antioxidant behaviour of polyphenols EGCG and ECG with iron. *J Inorganic Biochem.* 2007; 101(4): 585-93.

- [2] Ren-You G, Hua-Bin L, Zhong-Quan Su, et al. Absorption, metabolism, anti-cancer effect and molecular targets of epigallocatechin gallate (EGCG): An updated review. *Crit. Rev. Food Sci Nutr.* 2018; 58(6): 924–41.
- [3] Kumarn VS, Arulmahti K, Srividhya R et al. Repletion of antioxidant status by EGCG and retardation of oxidative damage induced macromolecular anomalies in aged rats. *Exp Gerontol.* 2007; 43(3): 176-83.
- [4] Okello EJ, Mather J. Comparative Kinetics of Acetyl- and Butyryl-Cholinesterase Inhibition by Green Tea Catechins|Relevance to the Symptomatic Treatment of Alzheimer's Disease. *Nutrients.* 2020;12(4): 1090-2013.
- [5] Uddin S, Kabir T, Niaz K, et al. Molecular Insight into the Therapeutic Promise of Flavonoids against Alzheimer's Disease. *Molecules.* 2020;25(6): 1267-96.
- [6] Maltsev AV, Bystryak S, Galzitskaya OV. The role of β -amyloid peptide in neurodegenerative diseases. *Ageing Res Rev.* 2011; 10(4): 440–52.
- [7] Parihar, MS, Hemnani T. Alzheimer's disease pathogenesis ve therapeutic interventions. *J Clin Neurosci.* 2004; 11(5): 46–67.
- [8] Clippingdale AB, Wade JD, Colin W. The amyloid- β -peptide ve its role in Alzheimer disease. *J Pept Sci.* 2001; 7(5): 227–49.
- [9] Selkoe DJ. Physiological production of the β -amyloid protein ve the mechanism of Alzheimer's disease. *Trends Neurosci.* 1999;16(10): 403–409.
- [10] Ferrari GV, Canales MA, Shin I, et al. A structural motif of acetylcholinesterase that promotes amyloid beta-peptide fibril formation. *Biochemistry-US.* 2001; 40(45):10447-457.

- [11] Luo W, Li YP, He Y. Design, synthesis and evaluation of novel tacrine-multialkoxybenzene hybrids as dual inhibitors for cholinesterases and amyloid beta aggregation. *Bioorg Med Chem*. 2001; 19(2): 63–770.
- [12] Morgana C, Colombres M, Nunez MT, and Inestrosa NC. Structure and function of amyloid in Alzheimer's disease. *Prog Neurobiol*. 2004; 74(6): 323–49.
- [13] Yanbei T, Chuanhai W, Yunyao K, et al. Bioactivity-guided identification of flavonoids with cholinesterase and β -amyloid peptide aggregation inhibitory effects from the seeds of *Milletia pachycarpa*. *Bioorg Med Chem Lett*. 2019; 29(10): 1194-98.
- [14] Ellman, GL, Courtney KD, Veres VJr, et al. A new and rapid colorimetric determination of acetylcholinesterase activity. *Biochem Pharmacol*. 1961; 7: 88-95.
- [15] Groenning M, Olsen L, Van-de-Weert M, et al. Study on the binding of Thioflavin T to β -sheet-rich and non- β -sheet cavities. *J Struct Biol*. 2007; 158(3): 358-69.
- [16] Takami T, Akira S, Ken-ichiro K, et al. Inhibition of Amyloid beta Protein Aggregation and Neurotoxicity by Rifampicin: Its possible function as a hydroxyl radical scavenger *J Biol Chem*.1996; 271(12): 6839–44.
- [17] [17] Kimura M, Akasofu S, Ogura H, and Sawada K. Protective effect of donepezil against A β (1-40) neurotoxicity in rat septal neurons. *Brain Res*. 2005; 1047: 72-84.
- [18] Özturan Özer E, Ünsal Tan O and Türkoglu S. The structural diversity of ginsenosides affects their cholinesterase inhibitory potential. *Turkish J Biochem*. 2019; 45(2):1-9.
- [19] Mahmud T, Hassan K, Orhan FS. et al. Cholinesterase inhibitory activities of some flavonoid derivatives and chosenxanthone and their molecular docking studies. *Chem-Biol Interact*.2009; 181(3):383–89.
- [20] Çokuğraş AN. Butyrylcholinesterase: Structure and physiological importance. *Turkish J Biochem*. 2003; 28:54-61.
- [21] Mason P, Xie W, Froment MT. et al. Interaction between the peripheral site residues of human butyrylcholinesterase, D70 and Y332, in binding and hydrolysis of substrates *Biochim Biophys Acta*. 1999; 1433(1-2): 281-93.
- [22] Chou TC. Derivation and properties of Michaelis-Menten type and Hill type equations for reference ligands. *J Theor Biol*. 1976; 59(2): 255-76.
- [23] Ozturan Ozer E, Unsal Tan O, Keriman Ozadali et al. Synthesis, molecular modeling and evaluation of novel N0-2-(4-benzylpiperidin-/piperazin-1-yl) acylhydrazone derivatives as dual inhibitors for cholinesterases and A beta aggregation. *Bioorg Medicin Chem Lett*. 2013; 23(2): 440–43.
- [24] Radić Z, Pickering NA, Vellom DC, et al. Three distinct domains in the cholinesterase molecule confer selectivity for acetyl- and butyrylcholinesterase inhibitors. *Biochemistry*. 1993; 32(45): 12074-084.
- [25] Larik FA, Shakil Shah M, Saeed A, et al. New cholinesterase inhibitors for Alzheimer's disease: structure activity relationship, kinetics and molecular docking studies of 1-butanoyl-3-arylthiourea derivatives. *Int J Biol Macromol*. 2018; 116:144-150.
- [26] Park G, Xue C, Wang H, et al. Distinguishing the Effect on the Rate and Yield of A β 42 Aggregation by Green Tea

Polyphenol EGCG. ACS Omega 2020;
5(34):21497–505.

The predictive role of neutrophil-to-lymphocyte ratio and platelet-to-lymphocyte ratio in children with simple febrile seizures

Meyri Arzu Yoldas¹, Fatma Hanci², Gokce Kaya Dincel¹, Mervan Bekdas¹

¹Department of Pediatrics, Bolu Abant Izzet Baysal University, Faculty of Medicine, Bolu, Turkey

²Department of Pediatric Neurology, Bolu Abant Izzet Baysal University, Faculty of Medicine, Bolu, Turkey

ABSTRACT

Aim: To evaluate the predictive roles of biochemical and complete blood count parameters in the diagnosis of febrile seizures by comparing these between patients with simple febrile seizures and febrile patients without seizures.

Methods: One hundred fifty-two children (66 girls and 86 boys), aged 6-60 months presenting with fever symptoms presenting to our hospital's pediatric emergency department between January 2015 and January 2020 were included in the study. Demographic data, complete blood count parameters and biochemical parameter levels were compared between the two groups. These were divided into a patient group with simple febrile seizures (n = 74) and a febrile control group without seizures (n = 78).

Results: Comparison of biochemical parameters revealed significantly higher glucose, CRP, and ALT levels in the febrile seizure group, while Ca and Na were significantly lower. Comparison of complete blood count parameters revealed significantly higher white blood cell (WBC), neutrophil, red cell distribution width, neutrophil-to-lymphocyte ratio (NLR), and platelet-to-lymphocyte ratio (PLR) values in the febrile seizure group, while hemoglobin, hematocrit, mean corpuscular volume, lymphocytes, and mean platelet volume were significantly lower.

Conclusions: We think that in addition to markers such as WBC, leukocytes, and CRP for evaluating inflammation in patients with febrile seizures, simple, easily available, and inexpensive tests such as NLR and PLR can also be useful for assessing inflammation.

Key words: Febrile seizure, child, leukocyte count, lymphocytes, platelet count.

✉ Dr. Meyri Arzu Yoldas

Department of Pediatrics, Bolu Abant Izzet Baysal University, Faculty of Medicine, Bolu, Turkey

E-mail: m.arzuyoldas@gmail.com

Received: 2021-04-08 / Revisions: 2021-04-29

Accepted: 2021-05-04 / Published online: 2021-07-01

Introduction

Febrile seizure (FS) is seen in 2-5% of infants and children, and is the most common

convulsive event in the pediatric age group. The American Academy of Pediatrics (AAP) defines febrile seizures as those accompanied by fever (>38° using any measurement technique) in neurologically healthy infants and children (aged between six and 60 months) with no signs of intracranial infection or metabolic disturbance, or history of afebrile seizures. Febrile seizure, the most common form of

seizure in the pediatric age group, was defined as a seizure associated with febrile illness with no known other cause of acute symptomatic seizure, including such as central nervous system infection or acute electrolyte imbalance [1].

Febrile seizures are also classified as either simple or complex. Complex febrile seizure was defined as either focal or multiple seizures, or seizures with a duration exceeding 15 min, or both. Simple febrile seizure was defined as a single generalized episode occurring within 24 h and seizures with a duration less than 15 min. Although the etiology of these seizures is still not fully understood, studies have shown the involvement of inflammation [2,3].

Complete blood count parameters currently used in studies for evaluating several conditions, such as acute and chronic inflammatory states, infectious diseases, and malignancies are simple and popular parameters in differential diagnosis. Systemic inflammation and febrile seizure are closely related entities. Various inexpensive and easily accessible laboratory parameters are available for evaluating the severity of systemic inflammation, including the neutrophil:lymphocyte ratio (NLR) and platelet:lymphocyte ratio (PLR). Changes in the proportions of white blood cells (neutrophilia and lymphopenia) represent the immune system's physiological response to an inflammatory process, injury or stress[4], also reflected by NLR and PLR. Some complete blood count parameters have been reported as novel inflammatory markers in Guillain-Barre syndrome and venous thrombosis [5,6].

Studies in recent years have shown that inflammation and hypoxia affect some complete blood count parameters and are associated with seizures [7]. The purpose of this study was to evaluate the predictive roles of

biochemical and complete blood count parameters in the diagnosis of febrile seizures by comparing these between patients with simple febrile seizures and febrile patients without seizures.

Materials and methods

One hundred fifty-two children aged 6-60 months presenting with fever symptoms to our hospital's pediatric emergency department between January 2015 and January 2020 were included in the study. Patients aged between six months and sixty months and meeting the definition of simple febrile seizure were included in the study. Patient data were analyzed retrospectively.

Patients meeting AAP diagnostic criteria were divided into a patient group (=Group 1) with simple febrile seizures (n = 74) and Group 2 with fever but no seizures (n = 78). Patients with previous histories of epilepsy or cerebral palsy, neuromotor retardation, chronic illness, head trauma, or diagnosed with meningitis or encephalitis within the previous month or concurrently, were excluded from the study. The data collected included demographics (date of birth, sex), and complete blood count parameters and blood biochemistry values were also compared between the groups.

Complete blood count parameters in blood collected at time of initial presentation included white blood cell (WBC) count, red blood cell (RBC) count, hemoglobin (Hb), mean erythrocyte volume (MCV), hematocrit (HCT), erythrocyte distribution width (RDW), platelet count (PLT), mean platelet volume (MPV), the neutrophil:lymphocyte ratio (NLR), and the platelet:lymphocyte ratio (PLR). NLR was calculated as the ration of lymphocytes to neutrophils, and PLR as that of platelets to lymphocytes (XN-1000-Hematology-Analyzer, Sysmex Corporation, Kobe, Japan).

Blood biochemistry parameters included sodium (Na), potassium (K), calcium (Ca), aspartate aminotransferase (AST), alanine aminotransferase (ALT), and C-reactive protein (CRP) Automatic Biochemistry Analyzer Abbott Architect c8000, Abbott Laboratories, Abbott Park, IL, USA). The study protocol was approved by the local human research committee (protocol number 2905 2020/179), and the study was conducted in compliance with the Declaration of Helsinki.

Statistical analysis

Continuous data were expressed as mean \pm SD (min-max) in both study groups, and categorical variables as frequency and percentage. The Kolmogorov-Smirnov test was first applied to assess normality of distribution of the study variables. Normally distributed variables were analyzed using the independent samples t-test, while categorical variables were analyzed using Pearson's chi-square test and Fisher's exact test. The results were assessed within 95% reliance, with $p < 0.05$ being considered statistically significant. All analyses were performed on Statistical Package for Social Sciences 25.0 for Windows software

(SPSS Inc., Chicago, IL, USA).

Results

One hundred fifty-two patients were included in the study. Mean ages (months) in group 1 with febrile seizures were 42 months (56.8) among boys and 32 months (43.2) in girls, compared to 44 months (56.4) in boys and 34 months (43.6) in girls in the group 2 ($p=0.96$). Boys constituted 42 (56.8%) of the group 1, while 34 (43.6%) of the group 2 were girls. No statistically significant difference was determined between the groups in terms of demographic data (Table 1).

In terms of biochemical parameters, CRP, glucose and ALT values were significantly higher in the group 1 than in the group 2, while Na and Ca were lower in the group 1 (Table 2). No significant difference was observed between the groups' serum AST and serum K levels.

Comparison of complete blood count parameters revealed significantly higher WBC, neutrophil, RDW, NLR and PLR values in the group 1 compared to the group 2, while MCV, HB, HCT, and MPV were lower ($p < 0.05$) (Table 3).

Table 1. Demographic characteristics of the study groups.

Parameters	Group 1 (n=74)	Group 2 (n=78)	<i>p</i> value
Age (months), mean \pm SD	41,64 \pm 18	36.2 \pm 19,9	0.078 ^a
Gender, n (%)			0.96 ^b
Male	42(56.8)	44(56.4)	
Female	32(43.2)	34(43.6)	

SD: Standard deviation. Data expressed as n (%). *p* values indicate statistical significance at 0.05.

^a Independent samples *t*-test, ^b Pearson's chi-square test.

Table 2. Biochemical parameters of the study groups

Parameters	Group 1 (n=74)	Group 2 (n=78)	p value
CRP, mg/L	10.8 (0.1-68.7)	4.5 (0.1-49.6)	0.003^a
Calcium, mg/L	9.5 (8.3-10.8)	9.8 (8.8-10.8)	0.01^a
AST, U/L	37.5 (11-160)	32.7 (19-58)	0.1^a
ALT, U/L	20.3 (7-100)	16.4 (10-33)	0.006^a
Serum glucose, mg/L	92.9 (38-174)	85.8 (63-127)	0.007^a
Sodium, mmol/L	137.1 (131-145)	138.8 (134-144)	0.011^a
Potassium, mmol/L	4.47 (3.5-5.5)	4.49 (3.8-5.5)	0.78^a

AST aspartate aminotransferase, ALT alanine aminotransferase, CRP C-reactive protein, SD standard deviation. Data expressed as mean (min-max). Bold p values indicate statistical significance at 0.05. ^a Independent samples t-test.

Table 3. Comparison of hematological parameters in the two groups.

Parameters	Group 1 (n=74)	Group 2 (n=78)	p value
WBC, × 10 ⁹ /L	9.9(4-27.3)	8.6(4.2-16.9)	0.022^a
Neutrophil, × 10 ⁹ /L	6.7(0.7-7.8)	2.8(0.4-7.8)	0.003^a
Lymphocyte, × 10 ⁹ /L	3.7(0.7-11.3)	4.7(0.8-10.8)	0.007^a
PLT, × 10 ⁹ /L	323.3(171-578)	349.2(291-575)	0.08 ^a
Hemoglobin, g/L	11.7(8.5-14.9)	12.4(10.2-14.7)	0.045^a
Hematocrit	35.2±3.38	37.5±2.5	0.02^a
MCV	76.9±6.6	78.9±5.5	0.047^a
RDW	16.8±2.02	13.4±1.7	0.04^a
MPV	7.16±3.6	9.3±1.2	0.039^a
NLR	3.35±8.1	0.77±0.67	0.008^a
PLR	119.9±83.8	88.1±45.9	0.005^a

WBC white blood cell, NLR neutrophil to lymphocyte ratio, PLR platelet to lymphocyte ratio, SD standard deviation, MPV mean platelet volume, PLT platelet count, RDW red cell distribution width, MCV mean corpuscular volume, MPV mean platelet volume, Data expressed as mean(min-max) or mean±SD. Bold p values indicate statistical significance at 0.05. ^a Independent samples t-test.

Discussion

The laboratory parameters of CRP, ALT, and glucose values were significantly higher in the febrile seizure group in the present study, while Na and Ca values were lower. In terms of

complete blood count parameters, WBC, neutrophil, RDW, NLR and PLR values were significantly higher in the simple febrile seizure group, while lymphocytes, MCV, HB, HCT, and MPV were lower. Inflammatory cells and

proinflammatory cytokines are known to play an important role in the etiopathogenesis of febrile seizure. Inflammation is thought to lower the seizure threshold and to increase stimulability in the brain [8].

CRP is an acute phase reactant and a highly important marker associated with inflammation levels independently of age, sex, and physical factors [9]. Yiğit et al. compared CRP levels in children with simple and complex febrile seizures and reported higher levels in patients with complex seizures [8]. Additionally, Romanowska et al. reported higher CRP levels in a febrile patient group without seizures compared with a group with febrile seizures [10]. CRP levels were also significantly higher in the simple febrile seizure group in the present study. The higher CRP in the febrile seizure group in the present research may indicate a role of inflammation in the etiopathogenesis of febrile seizure.

Na and Ca electrolyte and blood sugar level irregularities are known to play an important role in the etiology of seizures. Acute symptomatic seizures may be seen in children in case of Na levels lower than 115 to 120 mmol/L or higher than 145 mmol/L. It has been suggested that hyponatremia can lower the seizure threshold in febrile seizures [11]. In their comparison between children with febrile and afebrile acute gastroenteritis-related seizures, Wu YZ et al. reported lower Na levels in the afebrile group [12]. Zifman et al. reported lower Na values in a febrile patient group in children with acute gastroenteritis-related seizures [13]. In the present study, serum Na levels were significantly lower in the febrile seizure group. However, the focus of infection in our groups was upper respiratory tract infection.

Ca levels are also important in the seizure etiopathogenesis. Paresthesia and muscle

cramps can be seen in mild hypocalcemia, while a Ca level below 5 mg/dl is reported to cause seizures [14]. Yousefichaijan P et al. examined 549 cases of simple febrile seizure and observed low Ca levels in a small number of patients [15]. Serum Ca levels in the present study were significantly lower in the simple febrile seizure group compared to the febrile illness without seizure group.

AST is abundantly expressed in non-hepatic tissue, while ALT concentrations in non-hepatic tissues are low. High hepatic transaminase levels may represent not only liver damage, but also inflammation, fever, or non-specific tissue damage. Wu YZ et al. reported higher AST and ALT in a patient group with febrile seizure [12]. No significant difference was observed in AST levels in the present study, but ALT levels were significantly higher in the febrile seizure group. In contrast, blood sugar levels below 40 mg/dl or above 400 mg/dl are thought to cause neuronal over-stimulation and to trigger seizures [14]. Costea et al. compared serum glucose levels in patients with febrile seizure, and reported four-fold higher levels in patients with complex febrile seizure [16]. Similarly in the present study, glucose levels were higher in the simple febrile seizure group compared to the febrile illness without seizure group. Febrile seizures may be one of the risk factors for stress hyperglycemia in children, and further studies are now needed on this subject.

Iron deficiency is known to play a role in the development of febrile seizures [17]. The relationship between iron deficiency anemia and febrile seizure is still the subject of investigation. A Sherjil et al. reported that iron deficiency anemia increased the risk of febrile seizure two-fold [18]. Iron concentrations in blood could not be analyzed in the present study since the test was not routinely requested. One

previous study comparing types of febrile seizure determined statistically significantly lower Hb, Htc and MCV values in patients with complex febrile seizure [19]. Similarly in the present study, we also observed significantly lower Hb, Htc and MCV values in the febrile convulsion group. In addition, RDW is employed for evaluating the etiology of anemia, exhibits positive correlation with inflammation in some diseases, and is thought to be a potential inflammatory marker [20]. Türey et al observed significantly higher RDW in febrile seizure recurrence [21]. Örnek et al. observed higher mean RDW in their complex febrile seizure group, but the difference was not statistically significant [19]. RDW was significantly higher in the simple febrile seizure group in the present study.

Previous studies have investigated the relationship between MPV, reflecting the proportion and size of platelets produced from bone marrow, and severity of inflammation in various diseases [22]. One study comparing children with febrile seizures reported significantly increased MPV values in a complex febrile seizure group [23], while another study observed no significant difference [24]. MPV values in the present study were lower in the simple febrile seizure group.

Leukocyte, neutrophil, and lymphocyte counts, and the ratios thereof, are an important parameter that can be easily used to show the severity of disease in systemic inflammatory conditions [25]. Gontko-Romanowska et al. compared patients with febrile seizures and febrile patients without seizures and reported significantly higher neutrophil levels and significantly lower lymphocyte levels in their febrile seizure group [10]. Similarly in the present study, neutrophil levels were significantly higher in the febrile seizure group,

while lymphocyte rates were significantly lower. Yousefichaijan et al. reported significantly higher leukocyte counts in febrile children compared to children with febrile seizures [15]. Leukocyte counts were also significantly higher in the febrile seizure group in the present study.

NLR and PLR have recently been recognized as markers of systemic inflammation, and are used as predictive indicators in some diseases [4]. Studies have reported significantly higher NLR values in complex febrile seizure groups among patients with febrile seizures [8,26]. Another study reported significantly elevated NLR and PLR values [19]. NLR and PLR values were also significantly higher in the simple febrile seizure group in the present study.

The principal limitations of the present study are its retrospective nature, the low patient number, and the fact that only patients with upper respiratory tract infections were included. Further prospective studies with larger patient numbers are now needed.

Conclusion

Inflammation marker elevation must be carefully considered in patients with febrile seizures. We think that markers such as leukocyte count and CRP are simple, readily available and inexpensive tests. NLR and PLR values can also be employed as predictive indicators.

Funding: *The author(s) received no financial support for the research, authorship, and/or publication of this article.*

Conflict of Interest: *The authors declare that they have no conflict of interest.*

Ethical statement: *The study was approved by the Local Ethics Committee of Bolu Abant İzzet Baysal University (Date and Decision no: 2020-05-12/112), and written informed consent was obtained from each subject.*

Open Access Statement

This is an open access journal which means that all content is freely available without charge to the user or his/her institution under the terms of the Creative Commons Attribution Non-Commercial License (<http://creativecommons.org/licenses/by-nc/4.0>). Users are allowed to read, download, copy, distribute, print, search, or link to the full texts of the articles, without asking prior permission from the publisher or the author.

References

- [1] Subcommittee on Febrile Seizures; American Academy of Pediatrics. Neurodiagnostic evaluation of the child with a simple febrile seizure. *Pediatrics*. 2011;127(2):389-94.
- [2] Güneş M, Büyükgöl H. Relationship between generalized epileptic seizure and neutrophil/lymphocyte ratio, platelet/lymphocyte ratio, and neutrophil mediated inflammation. *Int J Neurosci*. 2020; 130(11): 1095-100.
- [3] Aronica E, Bauer S, Bozzi Y, et al. Neuroinflammatory targets and treatments for epilepsy validated in experimental models. *Epilepsia*. 2017; 58 (Suppl 3): 27-38.
- [4] Zahorec R. Ratio of neutrophil to lymphocyte counts--rapid and simple parameter of systemic inflammation and stress in critically ill. *Bratisl Lek Listy*. 2001; 102(1): 5-14.
- [5] Ozdemir HH. Analysis of the albumin level, neutrophil-lymphocyte ratio, and platelet-lymphocyte ratio in Guillain-Barré syndrome. *Arq Neuropsiquiatr*. 2016; 74(9): 718-22.
- [6] Artoni A, Abbattista M, Bucciarelli P, et al. Platelet to Lymphocyte Ratio and Neutrophil to Lymphocyte Ratio as Risk Factors for Venous Thrombosis. *Clin Appl Thromb Hemost*. 2018; 24(5): 808-14.
- [7] Eroglu T, Aydin Turkoglu S, Bolac ES, et al. Hemogram parameters in epilepsy may be indicators of chronic inflammation and hypoxemia. *J Neurol Clin Neurosci*. 2017; 1(1): 17–20.
- [8] Yigit Y, Yilmaz S, Akdoğan A, et al. The role of neutrophil-lymphocyte ratio and red blood cell distribution width in the classification of febrile seizures. *Eur Rev Med Pharmacol Sci*. 2017; 21(3): 554-59.
- [9] Bilgir O, Bilgir F, Calan M, et al. Comparison of pre- and post-levothyroxine high-sensitivity c-reactive protein and fetuin-a levels in subclinical hypothyroidism. *Clinics (Sao Paulo)*. 2015; 70(2): 97-101.
- [10] Gontko-Romanowska K, Żaba Z, Panieński P, et al. The assessment of laboratory parameters in children with fever and febrile seizures. *Brain Behav*. 2017; 7(7): e00720.
- [11] Kiviranta T, Airaksinen EM. Low sodium levels in serum are associated with subsequent febrile seizures. *Acta Paediatr*. 1995; 84(12): 1372-74.
- [12] Wu YZ, Liu YH, Tseng CM, et al. Comparison of Clinical Characteristics Between Febrile and Afebrile Seizures Associated With Acute Gastroenteritis in Childhood. *Front Pediatr*. 2020; 8: 167.
- [13] Zifman E, Alehan F, Menascu S, et al. Clinical characterization of gastroenteritis-related seizures in children: impact of fever and serum sodium levels. *J Child Neurol*. 2011; 26(11): 1397-1400.
- [14] Karceski S. Acute symptomatic seizures and systemic illness. *Continuum (Minneapolis, Minn)*. *Neurology of Systemic Disease*. 2014; 20(3): 614-23.
- [15] Yousefichaijan P, Dorreh F, Abbasian L, et al. Assessing the prevalence distribution of

- abnormal laboratory tests in patients with simple febrile seizure. *J Pediatr Neurosci.* 2015; 10(2): 93-97.
- [16] Costea RM, Maniu I, Dobrota L, et al. Stress Hyperglycemia as Predictive Factor of Recurrence in Children with Febrile Seizures. *Brain Sci.* 2020; 10(3): 131.
- [17] Akbayram S, Cemek M, Büyükben A, et al. Major and minor bio-element status in children with febrile seizure [published correction appears in *Bratisl Lek Listy.* 2012; 113(9): 572.
- [18] Sherjil A, Saeed Z, Shehzad S, et al. Iron deficiency anaemia-a risk factor for febrile seizures in children. *J Ayub Med Coll Abbottabad.* 2010; 22(3): 71-73.
- [19] Örmek Z, Kardeş H, Pişkin İE, et al. Comparison of hemogram parameters in febrile seizures types. *Duzce Med J.* 2020; 22(1): 1-6.
- [20] Lippi G, Targher G, Montagnana M, et al. Relation between red blood cell distribution width and inflammatory biomarkers in a large cohort of unselected outpatients. *Arch Pathol Lab Med.* 2009; 133(4): 628-32.
- [21] Turay, S., Hanci, F., & Ozde, S. (2021). An overview of vitamin B12 and iron deficiencies as a risk factors in children with febrile seizure etiology. *Exp Biomed Res.* 2021; 4(2): 154-63.
- [22] Yıldız Y, Cakmak S, Calapoğlu T, et al. Mean platelet volume can be used as a hospitalization criteria in pediatric patients diagnosed with acute bronchiolitis. *Acta Medica Mediterranea.* 2018; 34(6): 1997-2000.
- [23] Özkale M, Erol İ, Özkale Y, et al. Association between platelet indices and febrile seizures in children. *Cukurova Med J.* 2016; 41(4): 695-701.
- [24] Nikkhah A, Salehiomran MR, Asefi SS. Differences in mean platelet volume and platelet count between children with simple and complex febrile seizures. *Iran J Child Neurol.* 2017; 11(2): 44-47.
- [25] Zahorec R. Ratio of neutrophil to lymphocyte counts-- rapid and simple parameter of systemic inflammation and stress in critically ill. *Bratisl Lek Listy.* 2001; 102(1): 5-14.
- [26] Liu Z, Li X, Zhang M, et al. The role of Mean Platelet Volume/platelet count Ratio and Neutrophil to Lymphocyte Ratio on the risk of Febrile Seizure. *Sci Rep.* 2018; 8(1): 15123.

Comparison of ^{18}F FDG PET / CT, MRI (DWI + DCE) and MRI + ^{18}F FDG PET/CT in the detection of axillary metastatic lymph nodes in patients with newly diagnosed breast cancer

Hasan Gundogdu¹,  Osman Kupik² 

¹Department of Radiology, Recep Tayyip Erdoğan University, Faculty of Medicine, Rize, Turkey

²Department of Nuclear Medicine, Sıtkı Koçman University, Faculty of Medicine, Muğla, Turkey

ABSTRACT


Aim: We visually and quantitatively investigated the success of using 2-deoxy-2-[fluorine-18] fluoro-D-glucose integrated with computed tomography (^{18}F -FDG PET/CT) and magnetic resonance imaging (MRI) [Dynamic contrast enhancement (DCE) and diffusion weighted imaging (DWI)] separately and together in detecting axillary lymph node metastasis in patients with newly diagnosed breast cancer.

Methods: One hundred and thirteen patients who underwent ^{18}F FDG PET/CT were evaluated, 102 patients of these patients had also MRI (DEC + DWI). Primary tumour size (Tsize), SUVmax of primary tumour (SUVmaxT), short diameter of largest axillary lymph node on PET/CT (LnDPET/CT), SUVmax of axillary lymph node (SUVmaxLn), metabolic tumour volume of the primary tumour (MTV), short diameter of largest axillary lymph node on MRI (LnDMRI), the presence of fatty hilum absence and apparent diffusion coefficient (ADC) were evaluated.

Results: In visual analysis, sensitivity and specificity values of ^{18}F FDG PET/CT, MRI and MRI+ ^{18}F FDG PET/CT were 78.85, 94% – 72.27%, 96.15 – 83.87%, 98.04%, respectively. In the quantitative evaluation, $\text{ADC} \leq 1.2 \times 10^{-3} \text{ mm}^2/\text{sec}$ (OR = 6.665, $p = 0.001$, 95CI%: 2.181–20.370) and $\text{LnSUVmax} > 2$ (OR = 15.2, $p < 0.001$, 95CI%: 4.587–50.376) were independent predictors in detecting axillary lymph node metastasis.

Conclusion: $\text{LnSUVmax} > 2$ and $\text{ADC} \leq 1.2 \times 10^{-3} \text{ mm}^2/\text{sec}$ can be used as independent predictors of detecting axillary lymph node metastasis in patients with newly diagnosed breast cancer.

Key words: Breast neoplasms, lymphatic metastasis, fluorodeoxyglucose F18, PET / CT, MRI.

 Dr. Hasan Gundogdu

Department of Radiology, Recep Tayyip Erdoğan University, Faculty of Medicine, Rize, Turkey

E-mail: hasangundogdu@gmail.com

Received: 2021-02-08 / Revisions: 2021-04-10

Accepted: 2021-04-12 / Published online: 2021-07-01

Introduction

The presence of axillary lymph node metastasis (ALNM) is important for the prognosis of breast cancer and has an impact on treatment management [1]. Sentinel lymph node biopsy (SLNB) has become the standard axilla staging procedure in patients with early stage breast

cancer due to its lower morbidity rate and similar accuracy compared to axillary lymph node dissection (ALND) [2]. However, SLNB requires preoperative lymphoscintigraphy and a detailed pathological examination. In addition, it is a time-consuming complicated process [3]. Although SLNB has high sensitivity and specificity values in detecting axillary metastatic lymph node in breast cancer patients [4], it has also been reported to give false negative results [5-7]. It is an invasive procedure with complications such as infection, lymphedema and seroma [8]. For these reasons,

it is important to evaluate the axillary lymph node metastasis status by non-invasive imaging methods before surgery in patients with breast cancer [9, 10].

In addition to detecting the presence of distant organ metastasis in patients with breast cancer, 2-deoxy-2-[fluorine-18] fluoro-D-glucose integrated with computed tomography (^{18}F FDG PET/CT), which shows the glucose metabolism of the tissue, provides valuable information in detecting axillary lymph node metastasis. High sensitivity and specificity values have been reported for the success of ^{18}F FDG PET/CT in detecting metastatic lymph nodes in the axilla in patients with breast cancer [9, 11, 12].

Another non-invasive imaging method, magnetic resonance imaging (MRI), which is applied with dynamic contrast enhancement (DCE) and the diffusion-weighted imaging (DWI) technique, is used to evaluate the presence of axilla lymph node metastasis in patients with breast cancer [13, 14]. High sensitivity and specificity values of MRI applied with these two techniques have been reported in detecting axillary metastatic lymph nodes in breast cancer patients [15-17].

In this study, we investigated the success of each and their combined use of ^{18}F FDG PET/CT and DCE/DWI-MRI in detecting axillary metastatic lymph nodes in patients with newly diagnosed breast cancer

Materials and methods

The Clinical Research Ethics Committee of our institute reviewed and approved this retrospective study (2019/136). As this was a retrospective study, it was exempt by the institutional review board from the need for informed consent. All procedures performed in studies involving human participants were in accordance with the Helsinki declaration.

Patient selection: We retrospectively reviewed the data of patients diagnosed with breast cancer between March 2017 and January 2019 and who underwent ^{18}F FDG PET/CT and MRI before treatment. We included 113 patients who underwent ^{18}F FDG PET/CT, 102 of these patients also had MRI. We did not include patients who received neoadjuvant therapy. All patients had undergone SLNB or ALND. We included patients with invasive ductal carcinoma.

Surgical method: SLNB was applied to 60 patients who were clinically and radiologically axillary lymph node metastasis free; ALND was applied to 79 patients. Axillary dissection was performed in 53 of these patients whose axilla was clinically and radiologically metastatic. In 9 of these patients, the frozen result was positive for metastasis, while the frozen result was suspicious in terms of metastasis in 3 of them. In 3 patients, ALND was performed due to the detection of suspicious lymph nodes intraoperatively and in 11 patients due to the absence of sentinel lymph nodes (N = 26).

Nuclear medicine method (lymphoscintigraphy) was not used for SLNB. After the injection of "isosulfan blue" into/around the tumour or around the nipple, the lymph nodes which were stained blue in the axilla were excised.

^{18}F -FDG PET/CT procedures: A PET/CT scanner Biograph mCT (Siemens Healthcare, Erlangen, Germany) was used. After at least 4 hours of fasting, patients with a blood glucose level of < 200 mg/dl were administered a FDG injection at an approximate dose of 3.7 MBq/kg. After median 61 minutes [min-max 52-81 minutes], imaging was performed in the supine position with arms up. The PET imaging was adjusted to 2 minutes per bed position. Low-dose CT parameters were as follows:

voltage, 120 kV, CARE Dose 4D mA tube current and slice thickness 5.00 mm.

¹⁸F-FDG PET/CT parameters: We evaluated the long diameter of the primary tumour (Tsize), the maximum standardised uptake value of the primary tumour normalised to body weight (SUVmaxT), the short diameter of the axillary lymph node (LnDPET/CT), the maximum standardised uptake value of the axillary lymph node normalised to body weight (SUVmaxLn), the metabolic tumour volume of the primary tumour according to the 40% threshold of the SUVmaxT (MTV) and the presence of multifocality of the primary tumour.

¹⁸F FDG PET/CT image analyses: The Siemens Healthineers Syngo.via VB30 workstation, MM Oncology, post-processing unit was used for analyses. All analyses were performed by a Nuclear Medicine Specialist (O.K.) with 9 years of PET/CT experience.

MRI procedure: Magnetic Resonance imaging was performed on a 3 Tesla MR (Discovery w750, GE Healthcare, United States) device with an 8-channel breast coil in the prone position. Following conventional images, diffusion-weighted images and pre-contrast images, dynamic images were obtained by intravenous injection of contrast material through the antecubital vein.

For all patients, T2-weighted (FSE-IDEAL) axial section (time to repetition (TR)/TE: 7127/85 ms; section thickness 3.5 mm; field of view (FOV) 400 mm), T1-weighted (FSE) axial section (TR/TE: 838 ms/12 ms; slice thickness 3.5 mm; FOV: 400 mm), STIR axial section (TR/TE: 7673 ms/32 ms; TI: 180 ms; slice thickness 3.5 mm; FOV: 400 mm) were obtained.

The DWI was obtained at two different b values (50 s/mm², 800 s/mm²) with the echo-planar SE T2 weighted sequence (TR/TE: 6193 ms/18 ms;

cross sectional area 4 mm; FOV: 400 mm) in the axial plane. For DCE, gadobutrol (Gadovist; Bayer Schering Pharma, Berlin, Germany) was administered intravenously at a dose of 0.1 mmol/kg with an automatic injector at a speed of 3 ml/sec, and high-resolution T1-weighted oil-suppressed TSE axial and sagittal section (TR/TE: 5 ms /2.3 ms; slice thickness 0.8 mm; FOV: 360 mm, flip angle: 10) images were obtained. The DCE sequence was performed by axial imaging obtained at 70, 130, 190, 250 and 310 seconds in pre-contrast and post-contrast dynamic series.

MRI parameters: We evaluated the short diameter of axillary lymph nodes and the presence of fatty hilum absence. The ADC values were measured.

MRI image analysis: The MRI images of the patients were evaluated without knowing the pathology results and PET/CT findings. All analyses were performed by a Radiologist (H.G.) with 8 years of MRI experience.

ADC measurement technique: Lymph nodes with contrast enhancement in DCE and higher signal intensity in DWI were detected in the axilla. We then manually drew ROIs from 3 sections with a standard area of 0.25-0.35 mm² on the relevant region on the ADC map and obtained the mean ADC values.

The median time between ¹⁸F FDG PET/CT and MRI was 3 days [min: 0, max: 10]. There was a median of 11 days (minimum: 2, maximum: 29) between MRI and axillary surgery and a median of 9 days (min: 3, max: 22) between ¹⁸F FDG PET/CT and axillary surgery.

Statistical analysis: Continuous demographic data were analysed according to normality tests. Parametric data were reported as mean ± standard deviation and non-parametric data as median (min-max). Differences between groups were analysed using Student's t-test in

parametric data and Mann-Whitney U tests in non-parametric data. Discontinuous variables were shown as frequency. We used receiver operating characteristic (ROC) curve analysis to evaluate the diagnostic performance of the methods and to determine the threshold value. Univariate and multivariate logistic regression analyses were used to determine the relationship of test parameters of the patients at risk for axillary lymph node metastasis. Statistical significance value was accepted as 0.05. The software package SPSS v. 25 (Chicago, USA) was used for statistical analysis.

Results

In total, 113 female patients (mean age: 55.6 standard deviation (SD): 13.36) who were diagnosed with breast cancer and underwent ^{18}F FDG PET/CT were evaluated. One hundred and two of these patients also had MRI. Of these, 97 patients were luminal, 6 patients were Her2-positive, and 10 patients were in the triple negative (TN) receptor subgroup. The presence of axillary lymph node metastasis was confirmed histopathologically in 58 patients. Axillary lymph node metastasis was not detected in 55 patients. Patient and tumour characteristics are given in Tables 1 and 2.

Visual analysis: We performed visual analysis in 102 patients who underwent both ^{18}F FDG PET/CT and MRI. Histopathological metastasis was detected in 52 of these patients; metastasis was not detected in 50 patients. The ^{18}F FDG PET/CT detected 41 (79%) of 52 patients with axillary lymph node metastasis and failed to detect axillary lymph node metastasis in 11 patients (21%). The mean value of the short diameter in the lymph nodes of 11 patients in whom ^{18}F FDG PET/CT could not detect axillary lymph node metastasis was 5.14 ± 0.9 mm [min: 4 mm, max: 7 mm].

Table 1. Mean-median values of parameters evaluated by MRI and ^{18}F FDG PET/CT.

Parameters	Mean \pm SD	Median [Min-Max]
ADC (mm ² /sec)	1.18 \pm 0.27	1.21 (0.65-2.1)
LnDMRI (mm)	9 \pm 5	8 (4-32)
LnDPET/CT (mm)	8 \pm 5	7 (3-32)
LnSUVmax	3.63 \pm 4.46	1.40 (0.50-19.3)
MTV (cm ³)	6.07 \pm 7.63	3.70 (0.40-55)
SUVmaxT	9.49 \pm 9.11	6.95 (1.30-73.5)
Tsize (mm)	23 \pm 11	21 (8-60)

ADC, apparent diffusion coefficient; MTV, metabolic tumour volume; LnDMRI, short diameter of the largest axillary lymph node measured by MRI; LnDPET/CT, short diameter of the largest axillary lymph node measured by PET/CT; LnSUVmax, SUVmax of the axillary lymph node; SUVmaxT, SUVmax of the primary tumour; Tsize, long diameter of the primary tumour.

Table 2. Tumour characteristics.

Parameters		N / %
ALNM	No	55/49
	Yes	58/51
Multifocality	No	83/73
	Yes	30/27
Receptor Subtype	Luminal	97/86
	HER2+	6/5
	Triple negative	10/9
Fatty Hilum Absence	No	33/32
	Yes	69/68

ALNM, Axillary lymph node metastasis status

The ^{18}F FDG PET/CT was false positive in 3 of 50 patients (6%) without axilla lymph node metastasis. In 47 patients (94%), ^{18}F FDG PET/CT was able to detect no axillary lymph node metastasis. For the axillary lymph node short diameter > 6 mm, we found a 79% sensitivity of ^{18}F FDG PET/CT to detect the presence of metastasis, with a specificity of 70.9% (AUC = 0.821, $p < 0.001$) (Figure 1).

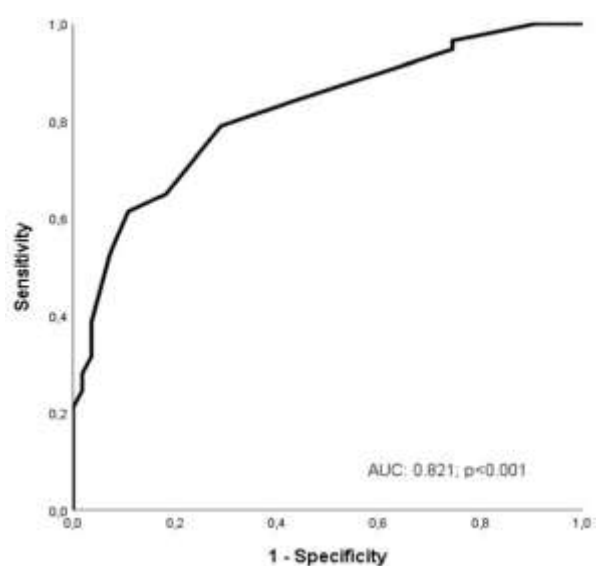


Figure 1. ROC curve showing the success of ^{18}F FDG PET/CT in detecting axillary metastatic lymph nodes when adopting a 6-mm threshold value for lymph node short diameter.

Magnetic resonance imaging (DCE + DWI) was performed in 102 patients and detected 30 (57.7%) of 52 patients with lymph node metastasis. The short-diameter mean value of lymph nodes of 22 patients in whom MRI could not detect lymph node metastasis was $7.1\text{mm} \pm 1.16$ [min: 5 mm, max: 9 mm]. The MRI detected 48 (96%) of 50 patients without axillary lymph node metastasis and was false positive in only 2 patients (4%).

When ^{18}F FDG PET/CT and MRI results were evaluated together ($n = 102$), ^{18}F FDG PET/CT + MRI detected 42 (81%) of 52 patients with

axillary lymph node metastasis, but could not detect 10 patients (19%). Short-diameter mean values of lymph nodes in these 10 patients were 5 ± 0.9 mm and 6.5 ± 0.85 mm for ^{18}F FDG PET/CT and MRI, respectively. The $\text{MR}^1 + ^{18}\text{F}$ FDG PET/CT detected 49 (98%) of 50 patients without axillary lymph node metastasis, with a false positive result in only 1 patient. The efficiency of the ROC curve of ^{18}F FDG PET/CT, MRI and $\text{MR}^1 + ^{18}\text{F}$ FDG PET/CT in detecting axillary metastatic lymph nodes is given in Figure 2. The sensitivity, specificity, accuracy, positive predictive values and negative predictive values of each of the ^{18}F FDG PET/CT, MRI, ^{18}F FDG PET/CT + MRI in detecting axillary metastatic lymph nodes are given in Table 3.

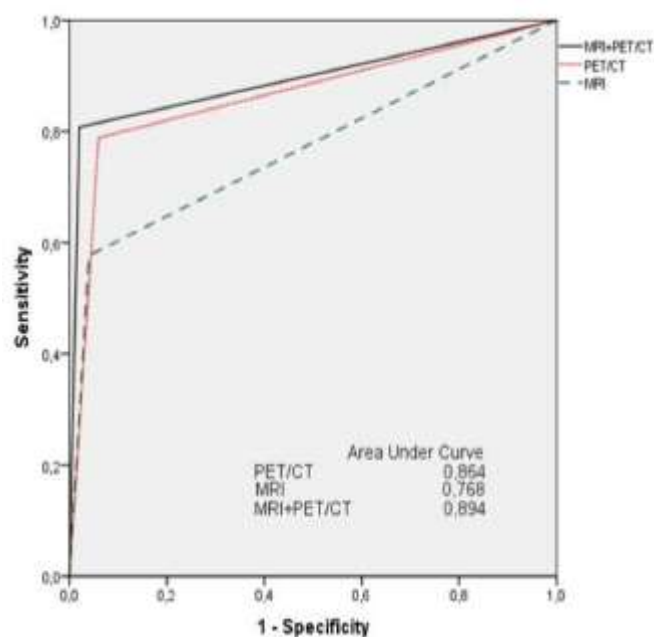


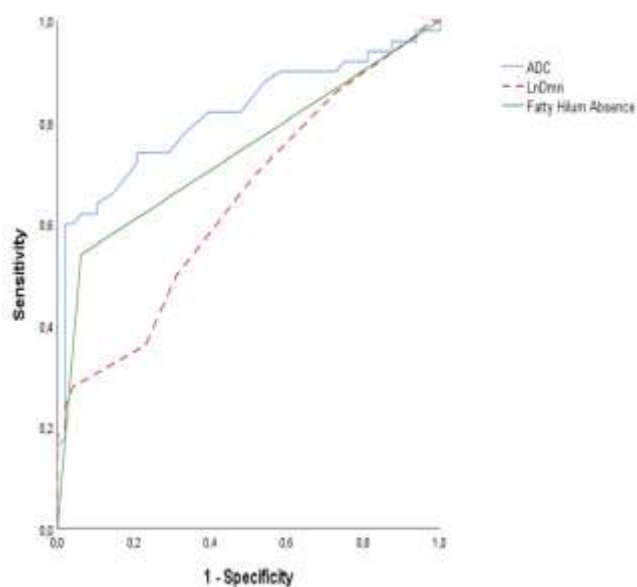
Figure 2. ROC curve demonstrating the success of ^{18}F FDG PET/CT, MRI and $\text{MR}^1 + ^{18}\text{F}$ FDG PET/CT in detecting axillary metastatic lymph nodes.

Quantitative analysis: We evaluated the MRI parameters [ADC, LnDMRI, fatty hilum absence] of 102 patients in univariate logistic regression analysis. In detecting lymph node metastasis, we performed ROC analysis and set

Table 3. Sensitivity, specificity, accuracy, positive predictive value, negative predictive values of ^{18}F FDG PET/CT, MRI and ^{18}F FDG PET/CT + MRI.

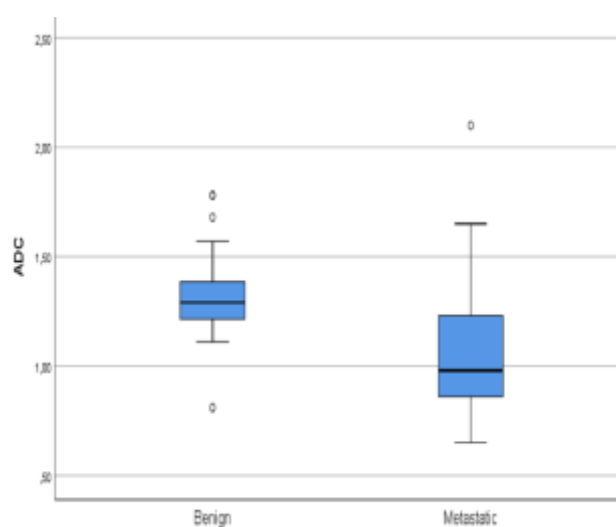
Parameters	^{18}F FDG PET/CT	MRI	^{18}F FDG PET/CT + MRI
Sensitivity (%)	78.85 (65.3-88.94)	70.27 (58.52-80.34)	83.87 (72.33-91.98)
Specificity (%)	94 (83.45-98.74)	96.15 (86.79-99.53)	98.04 (89.55-99.95)
Positive predictive value (%)	93.18 (81.89-97.64)	96.3 (86.89-99.03)	98.11 (88.16-99.73)
Negative predictive value (%)	81.03 (71.56-87.89)	69.44 (61.46-76.41)	83.33 (73.89-89.93)
Accuracy (%)	86.27 (78.04-92.29)	80.95 (73-87.4)	90.27 (83.25-95.04)

a threshold value of $1.2 \times 10^{-3} \text{ mm}^2/\text{sec}$ to obtain optimal sensitivity and specificity values for ADC. In univariate analysis, LnDMRI (Odds Ratio (OR) = 1.254, $p = 0.01$, 95% CI: 1.056-1.489), $\text{ADC} \leq 1.2 \times 10^{-3} \text{ mm}^2/\text{sec}$ (OR = 10.815, $p < 0.001$, 95% CI: 4.223-27.701) and lymph node fatty hilum absence (OR: 18, $p < 0.001$, 95% CI: 4.937-65.623) were statistically significant predictors for detecting axillary lymph node metastasis (Figure 3).

**Figure 3.** ROC curve demonstrating the success of MRI parameters in detecting axillary metastatic lymph nodes.

Multivariate logistic regression analysis showed that, $\text{ADC} \leq 1.2 \times 10^{-3} \text{ mm}^2/\text{sec}$ (OR = 4.472, $p = 0.008$, 95% CI: 1.484-13.479) and fatty hilum absence (OR = 6.703, $p = 0.011$, 95% CI: 1.537-29.228%) were independent predictors for detecting axillary lymph node metastasis.

We found a statistically significant difference between the mean ADC values of metastatic and benign lymph nodes (benign group mean ADC value: 1.31 ± 0.17 , metastatic group mean ADC value: 1.05 ± 0.27 , $p < 0.001$) (Figure 4).

**Figure 4.** Boxplot graph showing ADC values in metastatic and non-metastatic lymph nodes.

We evaluated the success of ^{18}F FDG PET/CT in detecting axillary lymph nodes in 113 patients with univariate logistic regression analysis. The parameters, Tsize (OR = 1.068, $p = 0.002$, 95CI 1.025-1.113%), MTV (OR = 1.082, $p = 0.034$, 95CI 1.006-1.163%), ^{18}F FDG PET/CT-multifocality (OR = 2.625, $p = 0.036$, 95CI 1.063-6.478%), LnDPET/CT (OR = 1.520, $p < 0.001$, 95CI%: 1.269-1.820), SUVmaxLn (OR = 2.213, $p < 0.001$, 95CI 1.533-3.193) were statistically significant predictors in detecting axillary metastatic lymph nodes, whereas SUVmaxT (OR = 1.011, $p = 0.608$, 95 CI 0.969-1.055) was not a reliable indicator in univariate analysis. We performed ROC analysis to obtain optimal sensitivity and specificity values of SUVmaxLn in detecting axillary lymph node metastasis and determined the threshold value 2 for SUVmaxLn. We created the model with the Backward LR method for multivariate logistic regression by including the parameters at $p < 0.2$ as a result of univariate analysis. In the multivariate logistic regression analysis, among the ^{18}F FDG PET/CT parameters, only SUVmaxLn > 2 (OR = 33.077, $p < 0.001$, 95CI%: 10.911-100.270) was an independent predictor in detecting axillary metastatic lymph nodes.

We included DCE-DWI MRI and ^{18}F FDG PET/CT parameters with $p < 0.2$ in the multivariate analysis as a result of univariate analysis. Multivariate logistic regression analysis showed that, $\text{ADC} \leq 1.2 \times 10^{-3} \text{ mm}^2/\text{sec}$ (OR = 6.665, $p = 0.001$, 95CI%: 2.181-20.370) and $\text{LnSUVmax} > 2$ (OR = 15.2, $p < 0.001$, 95CI%: 4.587-50.376) were independent predictors in detecting axillary metastatic lymph nodes. The sensitivity of SUVmaxLn > 2 was 73.7%, with a specificity of 92.7 (AUC = 0.845, $p < 0.001$). For $\text{ADC} \leq 1.212 \times 10^{-3} \text{ mm}^2/\text{sec}$, sensitivity was 74% and specificity was 79.2 (AUC: 0.814, $p < 0.001$) (Figure 5).

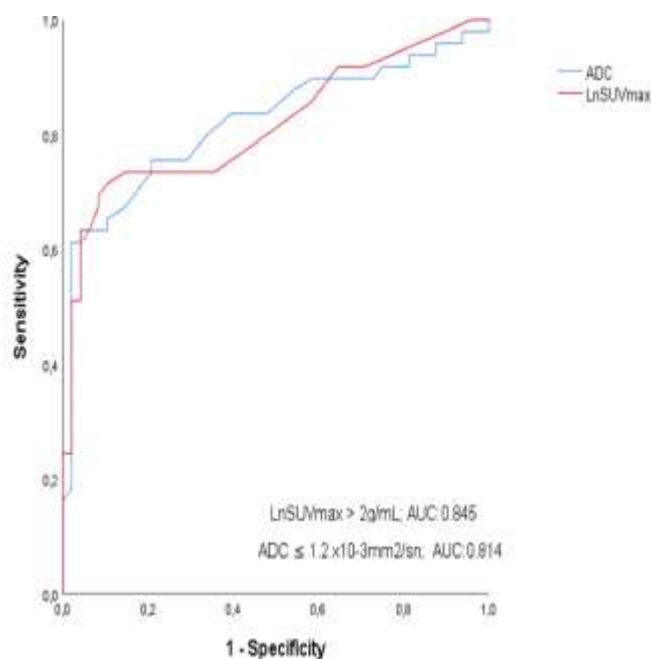


Figure 5. ROC curve showing success in detecting the presence of axillary lymph node metastasis for SUVmaxLn > 2 and $\text{ADC} \leq 1.2 \times 10^{-3} \text{ mm}^2/\text{sec}$.

We performed Cohen's kappa analysis between visual analysis results of ^{18}F FDG PET/CT and MRI. We observed a satisfactory value of agreement between the modalities (kappa: 0.669, $p < 0.001$). We also found a good agreement between the total result of MRI + ^{18}F FDG PET/CT visual evaluation and histopathological results (kappa: 0.785, $p < 0.001$).

Discussion

In this study, we visually and quantitatively evaluated the success of using ^{18}F FDG PET/CT, (DCE+DWI) MRI and a combination of them in detecting axillary lymph node metastasis in patients with newly diagnosed breast cancer.

In the visual analysis, we found a sensitivity of 78% and a specificity of 94% for ^{18}F FDG PET/CT; a sensitivity of 70% and a specificity of 96% for MRI. In the meta-analysis of 21 studies in 1,905 patients, the sensitivity of ^{18}F FDG PET/CT was 40 to 89% (pooled 64%),

with a specificity of 84 to 94% (pooled 93%). The sensitivity of MRI was 40 to 100% (pooled: 82%), with a specificity of 44 to 100% (pooled 94%) [18]. We observed an increase in sensitivity and specificity values when MRI and ^{18}F FDG PET/CT were used together (sensitivity: 83.8%, specificity: 98%). In another study in which 215 patients were evaluated, the total sensitivity of MRI and ^{18}F FDG PET/CT used together was 72.3, with a specificity of 92.4. Higher sensitivity and specificity values were obtained when used together than when used separately (sensitivity and specificity for MRI: 67.5 and 78%, for ^{18}F FDG PET/CT: 62.7 and 88.6%) [19].

Primary tumour MTV, Tsize, multifocality, LnDPET/CT, SUVmaxLn were statistically significant ^{18}F FDG PET/CT parameters for the presence of axillary lymph node metastasis in the univariate analysis. In the multivariate analysis, only SUVmaxLn was an independent parameter for the presence of axillary lymph node metastasis. In a study with 173 patients, only MTV was associated with the presence of axillary lymph node metastasis in T2 and T3 tumours, while MTV in T1 tumours was not associated with axillary lymph node metastasis [20]. In another study, only total lesion glycolysis (TLG) was an independent marker for the presence of axillary lymph node metastasis among primary tumour parameters [21]. In a study with 671 patients who were classified according to receptor subtypes as ER-positive/HER2-negative and HER2-positive, primary tumour SUVmax (> 4.25) and tumour size was associated with the presence of axillary lymph node metastasis. In patients of the triple negative (TN) receptor subgroup, primary tumour characteristics were not associated with the presence of axillary lymph node metastasis [22]. When we determined a threshold value of 2 for SUVmaxLn, we found

a sensitivity of 73.7%, and a specificity of 92.7%. In a study that included 196 patients, axillary lymph node SUVmax was associated with metastasis; when the authors took SUVmax threshold value as "1", they found a sensitivity of 53.8% and a specificity of 93.9% [23].

In this study, ADC values of metastatic axillary lymph nodes were lower than those of non-metastatic lymph nodes, similar to previous findings [16, 24]. For an ADC value of $1.2 \times 10^{-3} \text{ mm}^2/\text{sec}$, we found satisfactory values of sensitivity and specificity in detecting axillary lymph node metastasis. In a study involving 110 patients, the authors found a threshold value of $0.90 \times 10^{-3} \text{ mm}^2/\text{sec}$ for ADC, with a sensitivity of 100% and a specificity of 83.3%. We assumed that one of the reasons for this difference may be the fact that not all of the patients' imaging was performed with 3T MRI [24]. In another study performed with 3Tesla MRI in 52 patients, the sensitivity was 72.4% and the specificity was 79.6% for the ADC value of $0.812 \times 10^{-3} \text{ mm}^2/\text{sec}$. [25].

We found a significant relationship between the absence of fatty hilum in lymph nodes and the presence of axillary lymph node metastasis. In a study with 56 patients, the authors found a significant relationship between the absence of fatty hilum in lymph nodes and metastasis [26]. The main limitation of our study is that it is single-centred and retrospective. Although all our patients had IDC, we the patient group was not enough to analyse according to the hormone receptor status. We could not assess the cortical thickness parameter of the lymph nodes although it was an important criterion for axillary lymph node metastasis.

In conclusion, $\text{LnSUVmax} > 2$ and $\text{ADC} \leq 1.2 \times 10^{-3} \text{ mm}^2/\text{sec}$ were independent predictors in detecting axillary lymph node metastasis in patients with newly diagnosed breast cancer.

Funding: The author(s) received no financial support for the research, authorship, and/or publication of this article.

Conflict of Interest: The authors declare that they have no conflict of interest.

Ethical statement: The study was approved by the Local Ethics Committee of Recep Tayyip Erdogan University (Date and Decision no: 2019/136), and written informed consent was obtained from each subject.

Open Access Statement

This is an open access journal which means that all content is freely available without charge to the user or his/her institution under the terms of the Creative Commons Attribution Non-Commercial License (<http://creativecommons.org/licenses/by-nc/4.0>). Users are allowed to read, download, copy, distribute, print, search, or link to the full texts of the articles, without asking prior permission from the publisher or the author.

References

- [1]Carter CL, Allen C, Henson DE. Relation of tumor size, lymph node status, and survival in 24,740 breast cancer cases. *Cancer*. 1989; 63(19):181-87.
- [2]Crane-Okada R, Wascher RA, Elashoff D, et al. Long-term morbidity of sentinel node biopsy versus complete axillary dissection for unilateral breast cancer. *Ann Surg Oncol*. 2008; 15(7):1996-2005.
- [3]Purushotham AD, Upponi S, Klevesath MB, et al. Morbidity after sentinel lymph node biopsy in primary breast cancer: results from a randomized controlled trial. *J Clin Oncol*. 2005; 23(19):4312-21.
- [4]Veronesi U, Paganelli G, Viale G, et al. A randomized comparison of sentinel-node biopsy with routine axillary dissection in breast cancer. *N Engl J Med*. 2003; 349(6):546-53.
- [5]Monzawa S, Adachi S, Suzuki K, et al. Diagnostic performance of fluorodeoxyglucose-positron emission tomography/computed tomography of breast cancer in detecting axillary lymph node metastasis: comparison with ultrasonography and contrast-enhanced CT. *Ann Nucl Med*. 2009; 23(10):855-61.
- [6]McMasters KM, Tuttle TM, Carlson DJ, et al. Sentinel lymph node biopsy for breast cancer: a suitable alternative to routine axillary dissection in multi-institutional practice when optimal technique is used. *J Clin Oncol*. 2000; 18(13):2560-66.
- [7]Krag DN, Anderson SJ, Julian TB, et al. Technical outcomes of sentinel-lymph-node resection and conventional axillary-lymph-node dissection in patients with clinically node-negative breast cancer: results from the NSABP B-32 randomised phase III trial. *Lancet Oncol*. 2007; 8(10):881-88.
- [8]Wilke LG, McCall LM, Posther KE et al. Surgical complications associated with sentinel lymph node biopsy: results from a prospective international cooperative group trial. *Ann Surg Oncol*. 2006; 13(4):491-500.
- [9]Heusner TA, Kuemmel S, Hahn S, et al. Diagnostic value of full-dose FDG PET/CT for axillary lymph node staging in breast cancer patients. *Eur J Nucl Med Mol Imaging*. 2009; 36(10):1543-50.
- [10]Kvistad K, Rydland J, Smethurst H-B, et al. Axillary lymph node metastases in breast cancer: preoperative detection with dynamic contrast-enhanced MRI. *Eur Radiol*. 2000; 10(9):1464-71.
- [11]Ahn J-H, Son EJ, Kim J-A, et al. The role of ultrasonography and FDG-PET in axillary lymph node staging of breast cancer. *Acta Radiol*. 2010; 51(8):859-65.

- [12] Peare R, Staff RT, Heys SD. The use of FDG-PET in assessing axillary lymph node status in breast cancer: a systematic review and meta-analysis of the literature. *Breast Cancer Res Treat.* 2010; 123(1):281-90.
- [13] Zhang Y, Qin Q, Li B, et al. Magnetic resonance imaging for N staging in non-small cell lung cancer: A systematic review and meta-analysis. *Thorac Cancer.* 2015; 6(2):123-32.
- [14] Plana MN, Carreira C, Muriel A, et al. Magnetic resonance imaging in the preoperative assessment of patients with primary breast cancer: systematic review of diagnostic accuracy and meta-analysis. *Eur Radiol.* 2012; 22(1):26-38.
- [15] Kim EJ, Kim SH, Kang BJ, et al. Diagnostic value of breast MRI for predicting metastatic axillary lymph nodes in breast cancer patients: diffusion-weighted MRI and conventional MRI. *J Magn Reson Imaging.* 2014; 32(10):1230-36.
- [16] Fornasa F, Nesoti MV, Bovo C, et al. Diffusion-weighted magnetic resonance imaging in the characterization of axillary lymph nodes in patients with breast cancer. *J Magn Reson Imaging.* 2012; 36(4):858-64.
- [17] Kamitani T, Hatakenaka M, Yabuuchi H, et al. Detection of axillary node metastasis using diffusion-weighted MRI in breast cancer. *Clin. Imaging.* 2013; 37(1):56-61.
- [18] Liang X, Yu J, Wen B, et al. MRI and FDG-PET/CT based assessment of axillary lymph node metastasis in early breast cancer: a meta-analysis. *Clin Radiol.* 2017; 72(4):295-301.
- [19] An Y-S, Lee D, Yoon J-K, et al. Diagnostic performance of 18F-FDG PET/CT, ultrasonography and MRI. *Nuklearmedizin.* 2014; 53(3):89-94.
- [20] An Y-S, Kang DK, Jung Y, et al. Volume-based metabolic parameter of breast cancer on preoperative 18F-FDG PET/CT could predict axillary lymph node metastasis. *Medicine.* 2017; 96(45):e8557.
- [21] Yoo J, Kim BS, Yoon H-J. Predictive value of primary tumor parameters using 18 F-FDG PET/CT for occult lymph node metastasis in breast cancer with clinically negative axillary lymph node. *Ann Nucl Med.* 2018; 32(9):642-48.
- [22] Kim JY, Lee SH, Kim S, et al. Tumour 18 F-FDG uptake on preoperative PET/CT may predict axillary lymph node metastasis in ER-positive/HER2-negative and HER2-positive breast cancer subtypes. *Eur Radiol.* 2015 ;25(4):1172-81.
- [23] Sun WY, Choi YJ, Song Y-J. Prediction of Axillary Nodal Status according to the Axillary Lymph Node to Primary Breast Tumor Maximum Standardized Uptake Value Ratio on 18 F-fluorodeoxyglucose Positron Emission Tomography/Computed Tomography. *J Breast Dis.* 2016; 4(2):92-99.
- [24] Chung J, Youk JH, Kim J-A, et al. Role of diffusion-weighted MRI: predicting axillary lymph node metastases in breast cancer. *Acta Radiol.* 2014; 55(8):909-16.
- [25] Rautiainen S, Könönen M, Sironen R, et al. Preoperative axillary staging with 3.0-T breast MRI: clinical value of diffusion imaging and apparent diffusion coefficient. *PLoS One.* 2015; 10:e0122516.
- [26] Mortellaro VE, Marshall J, Singer L, et al. Magnetic resonance imaging for axillary staging in patients with breast cancer. *J Magn Reson Imaging.* 2009; 30(2):309-12.

Evaluation of the anatomical and electrical axis of the heart after pneumonectomy

Mehmet Sait Altintas¹, Ahmet Oz¹, Suleyman Cagan Efe¹, Hasan Akin², Ali Cevat Kutluk², Taskin Rakici³, Turgut Karabag¹

¹Department of Cardiology, Health Sciences University, İstanbul Training and Research Hospital, İstanbul, Turkey

²Department of Chest Surgery, Health Sciences University, Yedikule Training and Research Hospital, İstanbul, Turkey

³Department of Radiology, Health Sciences University, İstanbul Training and Research Hospital, İstanbul, Turkey

ABSTRACT

Aim: To investigate the position of the heart after pneumonectomy and, also to find out how the changes in the electrical axis of the heart contribute for the possible electrocardiographic and echocardiographic changes.

Methods: Ninety-eight patients with pneumonectomy were included to this observational study. To calculate the rotation of the heart and angle measurement two perpendicular lines, one septal and another atrioventricular, were drawn on the images acquired from thoracic computed tomography. Thoracic CT were taken at every 3 months for the first two years. On electrocardiograms net QRS vectors, amplitudes of p waves, findings of right and left ventricular hypertrophy, and other possible changes were recorded.

Results: The mean age of all patients was 55.51 ± 8.9 . Right pneumectomy was performed in 40 (57%) and left pneumonectomy in 30 cases (43%) cases. There was no significant change regarding both the angle of rotation and the amount of pleural effusion between the findings of the second and first year after the operation. The QRS shift was significantly more pronounced in patients with left pneumonectomies than right pneumonectomies. On echocardiography these cases showed right ventricular hypertrophy and increased pulmonary artery pressures in the second year when compared to the preoperative period.

Conclusions: The current study showed that many significant changes occurred in the electrocardiographic and echocardiographic parameters of the heart after pneumonectomy.

Key words: Pneumonectomy, heart, anatomy, electrical axis, computed tomography, electrocardiography, and echocardiography.

✉ Dr. Mehmet Sait Altintas

Department of Cardiology, Health Sciences University,
İstanbul Training and Research Hospital, İstanbul,
Turkey

E-mail: dr.mehmetsait@hotmail.com

Received: 2021-02-14 / Revisions: 2021-03-03

Accepted: 2021-05-01 / Published online: 2021-07-01

Introduction

Pneumonectomy is the removal of the whole lung in the ipsilateral hemithorax due to any cause such as malignancy, tuberculous or non-specific infections, and trauma [1,2]. It was first

performed by Graham and Singer in 1933 and has been the routine procedure until 1950 for the treatment of lung cancer [3]. A lot of changes occur after pneumonectomy including mediastinal shift and elevation of the hemidiaphragm in the ipsilateral hemithorax that lead to change of the heart, great vessels, liver, spleen, and stomach [4]. The process takes months to years to occur due to the production of fibrotic tissue in the empty pleural space, intrathoracic pressure changes, with elevation of the diaphragm and

overdistension of the remaining lung, the heart and mediastinum shift to the side that was operated on [5,6].

The effects of pneumonectomy on the anatomical and the electrical axis of the heart have not been studied much. The current study aims to investigate the position of the heart after right or left pneumonectomy and, also to find out how the changes in the electrical axis of the heart contribute for the possible electrocardiographic and echocardiographic changes.

Materials and methods

The study was conducted at Istanbul Training and Research Hospital, Turkey. The current study was approved by the Hospital Ethical Committee (Date and decision no: 2019/1660). Written consent of the participants was obtained.

Study population

In this observational study, 98 consecutive patients who had pneumonectomy due to lung cancer, bronchiectasis, aspergillosis or trauma were analyzed. All cases had thorough physical examinations and routine laboratory tests. Lung spirometry tests were performed in all cases to document forced expiratory volume in 1 second (FEV1), vital capacity (VC) and maximum oxygen uptake during exercise (VO₂max) was calculated. After double lumen endotracheal intubation standard posterolateral thoracotomy was performed and routine right or left pneumonectomy was achieved.

Computerized tomography of thorax (CTT) was performed for all cases preoperatively. All CTT were evaluated by a specialized chest radiologist. Patients were routinely examined by a staff cardiologist, and electrocardiograms and echocardiography were analyzed. At the follow-up visits (every 3 months for the first

two years) physical examinations and routine blood tests were performed, and thoracic CT (every 3 or 6 months for the first two years, on the basis of the etiology) were taken routinely.

Computerized Tomography Evaluation

All CTT both before and after the operation were taken by the same 64-slice CT scanner (Aquilion 64, Toshiba Medical Systems Europe, The Netherlands). The characteristics of the pictures were 0.5/0.3 collimation, 120 kv, 150 mA, pitch 0.75, 240 mm FOV, and 512 matrices. Tera-Recon Aquarius (San Mateo, California) processed the acquired data and calculated the axis angles, shift and rotation of the heart, and the amount of epicardial fat tissue and pleural effusion.

To calculate the rotation and angle measurement two perpendicular lines, one septal and another atrioventricular, were drawn on the images acquired from thoracic CT without contrast medium. The intercept of the two lines was accepted as the middle point (Figure 1A). Another line was drawn from the middle of the sternum to the spinous processes posteriorly (sterno-spinous line). The angle between the sterno-spinous line and septal line was the rotation line (Figure 1B). The distance between sterno-spinous line and the middle point was considered as the amount of shift (Figure 1C). All calculations were performed by RadiAnt Dicom Viewer application (Poznan, Poland). The measurements of a patient are presented in figure 2 as an example.

Electrocardiographic and echocardiographic evaluation

The preoperative and postoperative electrocardiographs (ECG) were recorded and evaluated by an experienced cardiologist. On ECG's net QRS vectors, amplitudes of p waves, findings of right and left ventricular

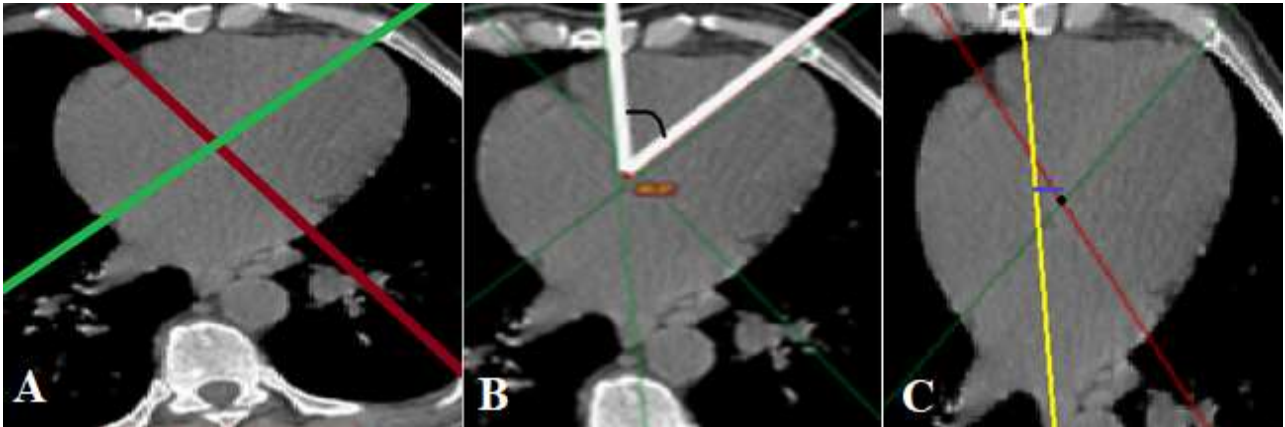


Figure 1. A) Drawing of two perpendicular lines, one septal and another atrioventricular. The intercept of the two lines was accepted as the middle point. B) Sterno-spinous line drawn from the middle of the sternum to the spinous processes posteriorly. The angle between the sterno-spinous line and septal line was the rotation line. C) The distance between sterno-spinous line and the middle point was considered as the amount of migration.

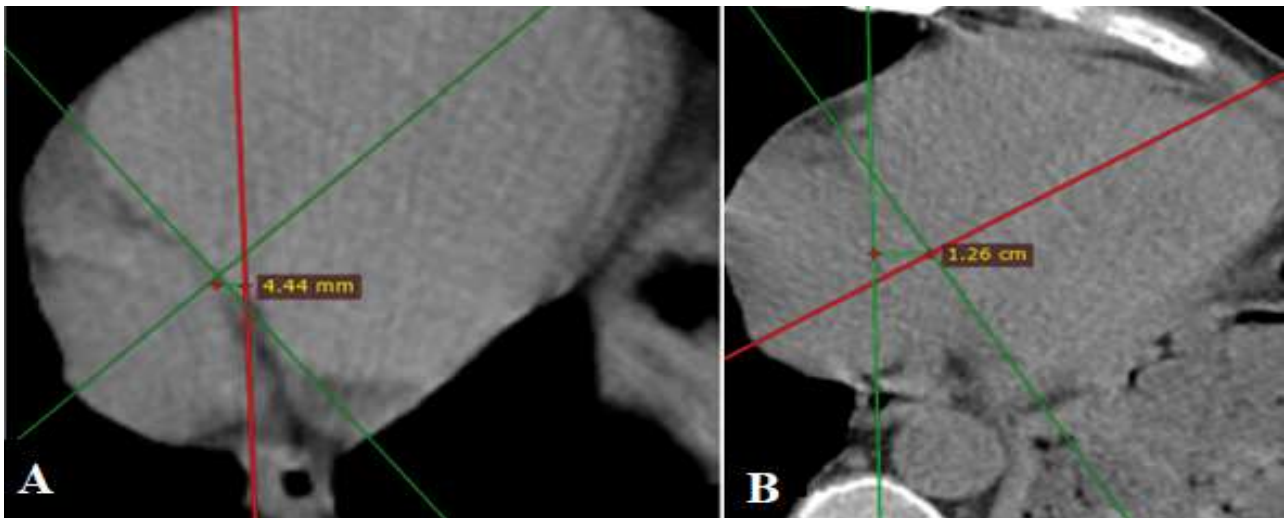


Figure 2. In a 60-year-old male patient who was operated due to left upper consolidated lung carcinoma, preoperative heart shift was 4.44 mm (A) to the right, while it was measured as 12.6 mm (B) to the left in the postoperative 2-year follow-up.

hypertrophy, and other possible changes were recorded. Net QRS electrical vectors were calculated based on the findings on D1 and D3 derivations. All patients underwent echocardiographic examination (Philips IE33 F Cart Echocardiography System) by the same cardiologist.

Statistical analysis

The continuous variables were expressed as mean and standard deviation and categorical

variables as frequencies and percentages. Repeated measures of ANOVA test (post-hoc: Bonferroni test) was used for comparison of the means of the groups before and after the procedure when the data were normally distributed, and otherwise Friedman test (post-hoc: Dunn's test) was used. The proportional differences of categorical variables between follow-ups were analyzed using the Cochran's Q test. The test was considered significant when

calculated p value is less than 0.05. IBM SPSS Statistics, version 23 for Windows (IBM Corporation, Armonk, NY, USA) was used for calculations.

Results

During the follow-up four patients in the first year and 24 others in the second year after the operation died and excluded from the study. The remaining seventy cases formed the study population. Male patients dominated the study group (64 cases, 91%) and the mean age of all patients was 55.51 ± 8.9 . Right pneumectomy was performed in 40 (57%) and left pneumectomy in 30 cases (43%) cases. All cases were followed for an average of 2 years. The angle of rotation did not change significantly in the first year after the operation when compared to the preoperative findings. In patients with right pneumectomy the amount of anatomical migration was statistically higher in the second year after the operation than the amount after the first year (17.73 ± 18.47 vs 24.73 ± 18.19 ; $P=0.001$). There was no

significant change regarding both the angle of rotation and the amount of pleural effusion between the findings of the second and first year after the operation (Table 1).

On ECG, the net QRS shift was tended to towards the same side in patients with pneumonectomy, but this trend did not show statistical significance (Table 2). The QRS shift was significantly more pronounced in patients with left pneumectomies than right pneumectomies ($p=0.001$). However, in both groups the QRS shift showed a tendency towards normal in the late period. In the late period on ECG right pneumectomy patients showed findings of right ventricular hypertrophy. When examined with echocardiography these cases showed right ventricular hypertrophy and increased pulmonary artery pressures in the second year when compared to the preoperative period. Left ventricle ejection fraction showed no differences in either groups when compared to the preoperative findings (Table 2).

Table 1. Chest CT findings before and after right and left pneumonectomy.

Parameters	Preoperative	Postoperative		<i>P value</i>	
		1 st year	2 nd year	<i>Preoperative vs 1st year</i>	<i>1st year vs 2nd year</i>
Angle of rotation R	69.80 ± 9.05	71.02 ± 9.82	70.45 ± 12.66	<i>0.391</i>	<i>0.822</i>
L	67.31 ± 7.07	74.47 ± 18.18	73.32 ± 19.41	<i>0.072</i>	<i>0.710</i>
Migration (mm) R	5.22 ± 13.40	17.73 ± 18.47	24.73 ± 18.19	<i>0.012</i>	<i>0.001</i>
L	7.41 ± 16.71	25.99 ± 13.41	31.96 ± 13.13	<i>0.001</i>	<i>0.086</i>
Pleural effusion (ml) R	1.61 ± 5.08	50.32 ± 35.09	42.40 ± 24.85	<i>0.001</i>	<i>0.247</i>
L	5.78 ± 14.40	47.34 ± 27.13	34.15 ± 22.40	<i>0.001</i>	<i>0.044</i>

Table 2. Heart rate and QRS vector shift parameters before and after right and left pneumonectomy.

Parameters	Preoperative	Postoperative		P value	
		1 st year	2 nd year	Preoperative vs 1 st year	1 st year vs 2 nd year
HR R L	49.80 ± 9.05	51.02 ± 9.82	50.45 ± 12.66	0.391	0.180
	47.31 ± 7.07	54.47 ± 18.18	53.32 ± 19.41	0.072	0.219
QRS shift R L	11.8±26.6	15.7±29.9	14.9±31.2	0.793	0.826
	5.22 ± 13.40	17.73 ± 18.47	14.73 ± 18.19	0.012	0.001
PAP (mmHg) R L	19.31±2.3	35.78±15	38±14	0.001	0.001
	18.26±3.1	29.43±9	32.25±11	0.001	0.001
LV EF R L	61±9	57±11	56±14	0.070	0.060
	63±8	59±10	58±12	0.090	0.060
R/S R L	5 (12.5%)	13 (32.5%)	16 (40.0%)	0.030	0.010
	4 (13.3%)	9/ (30.0%)	11 (36.7%)	0.200	0.090
AF R L	0	2 (5.0%)	0	0.500	0.500
	0	1 (3.3%)	1 (3.3%)	0.990	0.999
P pulmonale R L	0	2 (5.0%)	1 (2.5%)	0.500	0.910
	0	2 (6.7%)	1 (3.3%)	0.614	0.987

R: Patients with right pneumonectomy, L: Patients with left pneumonectomy, HR: Heart rate, PAP: Pulmonary artery pressure, LVEF: Left ventricular ejection fraction, AF: Atrial fibrillation

Discussion

In this study showed that [1] at the first year of visit thorax CT showed that the heart shifted to the site pneumonectomy. But interestingly at the second year instead of further shift, the heart moved slightly backwards possibly due to the collection of pleural effusion [2]. The rotational changes of the heart detected on the chest CT did not differ after the first year and second year compared to the preoperative findings. At the first postoperative year, the net QRS vector

which was dependent on the left ventricle shifted to the left and right after left and right pneumonectomy, respectively. However, at the second postoperative year there was no statistical difference in the net QRS vector between first and second year. The anatomical and functional changes of the heart, and the subsequent changes on the ECG after pneumonectomies due to various reasons were studied extensively in the literature. Decrease of pulmonary capacity and cardiac

derangements cause some signs and symptoms to occur after lung resections and it is sometimes difficult to understand the source whether cardiac or pulmonary. Routine outpatient visits after the operation with the use of accessible tools like chest CT, electrocardiogram, and echocardiography can make it possible to perceive the possible complications early [7-9].

There are only a few studies addressing the changes on ECG occurring due to shift of the heart and rotation of the heart around its axis after pneumonectomy [10]. In the current study four patients developed atrial fibrillation. The possible reason for atrial fibrillation could be the inflammation of the pulmonary veins and atrium developing during the early postoperative period. The increase in P wave dispersion which was reported on the literature could explain the situation [11]. Two limitations of our study were lack of P wave dispersion and atrial pressure measurements. Atrial fibrillation was the most frequent cardiac arrhythmia after pneumonectomy in the literature, and in 98% of the cases the situation resolves spontaneously or with medical therapy [12]. However, there might be some cases with atrial fibrillation that could not be detected or paroxysmal which could account for the unexplained symptoms. Holter monitoring or electrophysiological studies are required to detect the paroxysmal atrial fibrillation.

In the current study the height of p wave on ECG was increased significantly after the right pneumonectomy but the increase was not significant after the left pneumonectomy. The increase of the atrial pressure after right pneumonectomy could explain the increased height of p waves after right pneumonectomy. Another finding supporting this situation was the detection of the findings of right ventricular hypertrophy after the first and years of right

pneumonectomy. The systolic pulmonary pressures of these cases were recorded higher on preoperative echocardiography than postoperative echocardiography. The most likely explanation for this increase could be decrease in pulmonary vascular bed and subsequent increase of vascular resistance. However, the study could not validate this theory because either hemodynamic studies or cardiac magnetic resonance imaging was not performed. In contrast to the findings of patients with right pneumonectomy there was no statistical difference in systolic pulmonary artery pressures or right ventricular dimensions before and after the operation. These findings were consistent with the results of Foruolis et al. [13] but neither study had the hemodynamic data that could account for the differences of pulmonary artery pressures before and after pneumonectomy.

Several strengths and limitations of this study need to be acknowledged. First strength is the wide number of sample population. Moreover, in this study the changes of the heart after pneumonectomy were analyzed by combination of thorax CT, ECG, and echocardiography. However, there were some significant restrictions. First, this study was observational in design. Second limitation was that the follow-up duration was limited by two years. At the end, the authors hope that this study will be a call for future randomized controlled studies.

Conclusions

The current study showed that many significant changes occurred in the electrocardiographic and echocardiographic parameters of the heart after pneumonectomy. A clinician should be aware of these changes and their possible consequences. Possible cardiac arrhythmias could be the reason for the unexplained resting and exertional dyspnea besides decreased

pulmonary capacity. Pulmonary hypertension and increased workload of the right heart especially after right pneumonectomy may cause right heart failure. Multidisciplinary approach is necessary to provide best diagnostic and therapeutic strategy to these patients.

Funding: *The author(s) received no financial support for the research, authorship, and/or publication of this article.*

Conflict of Interest: *The authors declare that they have no conflict of interest.*

Ethical statement: *The study was approved by the Local Ethics Committee of University (Date and decision no: 2019/1660), and written informed consent was obtained from each subject.*

Open Access Statement

This is an open access journal which means that all content is freely available without charge to the user or his/her institution under the terms of the Creative Commons Attribution Non-Commercial License (<http://creativecommons.org/licenses/by-nc/4.0>). Users are allowed to read, download, copy, distribute, print, search, or link to the full texts of the articles, without asking prior permission from the publisher or the author.

References

[1] James TW, Faber LP. Indications for pneumonectomy. Pneumonectomy for malignant disease. Chest Surg Clin N Am. 1999; 9(2):291-309.

[2] Conlan AA, Kopec SE. Indications for pneumonectomy. Pneumonectomy for benign disease. Chest Surg Clin N Am. 1999; 9(2):311-26.

[3] Deslauriers J, Ugalde P, Miro S, et al. Long-term physiological consequences of

pneumonectomy. Semin Thorac Cardiovasc Surg. 201;23(3):196-202.

[4] Nonaka M, Kadokura M, Yamamoto S, et al. Analysis of the anatomic changes in the thoracic cage after a lung resection using magnetic resonance imaging. Surg Today. 2000;30(10):879–85.

[5] Abbas AE, Liu P, Lee RW. Acquired post-pneumonectomy dextrocardia. Interact Cardiovasc Thorac Surg. 2004;3(1):25-27.

[6] Smulders SA1, Holverda S, Vonk-Noordegraaf A, van den Bosch HC, Post JC, Marcus JT, Smeenk FW, Postmus PE. Cardiac function and position more than 5 years after pneumonectomy. Ann Thorac Surg. 2007;83(6):1986-92.

[7] Nair AS, Macherla G, Sahoo RK, Verma S. Electrocardiographic changes after lung resection: Case report and brief review. Anesth Essays Res. 2015; 9(2): 263–65.

[8] Bazwinsky-Wutschke I, Paulsen F, Stövesandt D, et al. Anatomical changes after pneumonectomy. Ann Anat. 2011;193(2):168-72.

[9] Weg IL, Rossoff L, McKeon K, et al. Development of Pulmonary Hypertension after Lung Volume Reduction Surgery. Am J Respir Crit Care Med. 1999;159(2):552-56.

[10] Gould L, Gopaldaswamy C, Chandy F, et al. EKG changes after left pneumonectomy. N Engl J Med. 1983;308(24):1481-82.

[11] Chhabra L, Bajaj R, Chaubey VK, et al. Electrocardiographic impacts of lung resection. J Electrocardiol. 2013;46(6):697.e1-8.

[12] O Rena, E Papalia, A Oliaro, et al. Supraventricular arrhythmias after resection surgery of the lung. Eur J Cardiothorac Surg. 2001;20(4):688-93.

[13] Foroulis CN, Kotoulas CS, Kakouros S, et al. Study on the late effect of

pneumonectomy on right heart pressures using Doppler echocardiography. *Eur J Cardiothorac Surg.* 2004;26(3):508-14.

Could triglyceride to high density lipoprotein-cholesterol ratio predict hepatosteatosi s?

Ozge Kurtkulagi¹, Satilmis Bilgin¹, Gizem Bakir Kahveci¹, Burcin Meryem Atak Tel¹, Mehmet Ali Kosekli²

¹Department of Internal Medicine, Bolu Abant Izzet Baysal University, School of Medicine, Bolu, Turkey

²Department of Internal Medicine and Gastroenterology, Bolu Abant Izzet Baysal University, School of Medicine, Bolu, Turkey

ABSTRACT

Aim: The triglyceride / HDL cholesterol (TG/HDL-c) ratio is increased in a variety of diseases including, coronary heart disease and type 2 diabetes mellitus. However, its role in non-alcoholic hepatosteatosi s is not well understood. In present study, we aimed to compare the TG/HDL-c levels of the patients with non-alcoholic hepatosteatosi s to those of the healthy subjects.

Methods: Medical data of the patients with non-alcoholic hepatosteatosi s whom presented to the outpatient internal medicine clinics of our institution were retrospectively analyzed. Healthy subjects whom admissions to our clinics were due to check up were enrolled to the study as control group. TG/HDL-c of the groups compared.

Results: TG/HDL-c level of the liver steatosi s group (5 (2-22) %) was higher than the control group (2.7 (1-8) %), (p<0.001). TG/HDL-c was significantly and positively correlated with fasting blood glucose (r=0.31, p<0.001), C - reactive protein (r=0.25, p<0.001) and LDL-cholesterol (r=0.3, p<0.001) levels. A TG/HDL-c value greater than 3.1% has 91% sensitivity and 77% specificity in detecting hepatosteatosi s.

Conclusions: We suggest that TG/HDL-c ratio could be a useful marker of non-alcoholic hepatosteatosi s due to its inexpensive and easy to assess nature.

Key words: Liver steatosi s, hepatosteatosi s, inflammation, triglyceride, HDL cholesterol.

✉ Dr. Ozge Kurtkulagi

Department of Internal Medicine, Bolu Abant Izzet Baysal University, School of Medicine, Bolu, Turkey

E-mail: ozgekurtkulagi@gmail.com

Received: 2021-01-14 / Revisions: 2021-01-30

Accepted: 2021-02-09 / Published online: 2021-07-01

Introduction

Liver steatosi s, as known as hepatosteatosi s, is defined as abnormal lipid accumulation in liver cells. The pathogenesis of the hepatosteatosi s includes inflammation, metabolic disorder and hyperlipidemia. Possible contributing factors to non-alcoholic hepatosteatosi s are metabolic

syndrome, dyslipidemia, obesity, type 2 diabetes mellitus and insulin resistance.

Recent researches studied numerous inflammatory and metabolic indices in patients with non-alcoholic hepatosteatosi s. These include; C - reactive protein, mean platelet volume, platelet distribution width, mean platelet volume to platelet count ratio and neutrophil/lymphocyte ratio [1-5]. Novel studies pointed out the relationship between triglyceride/ HDL cholesterol (TG/HDL-c) ratio in various conditions. Elevated TG/HDL-c level was considered as a risk factor for coronary heart disease in male population [6].

In a study from Japan, authors introduced TG/HDL-c ratio as a useful tool in predicting small LDL particles [7]. Moreover, it has been suggested that increased TG/HDL-c levels in young adults may serve as a predictor of insulin resistance and higher cardiometabolic risk [8]. In present study, we aimed to compare the TG/HDL-c levels of the patients with non-alcoholic hepatosteatosis to those of the healthy subjects.

Materials and methods

After receiving ethical approval from the local ethics committee (Date and decision no: 2020/311), medical data of the patients with non-alcoholic hepatosteatosis whom presented to the outpatient internal medicine clinics of our institution between October 2018 and October 2020 were retrospectively analyzed. Healthy subjects whom admissions to our clinics were due to check up within the same time period were enrolled to the study as control group. Exclusion criteria were as follows: hepatitis, alcohol consumption, active inflammatory diseases, hyperlipidemic syndromes, recent infection and those with a history of lipid lowering drug use. Hepatosteatosis was determined by ultrasound scan.

Age, gender, body weight, height, fasting blood glucose (FBG), serum creatinine, LDL cholesterol, HDL cholesterol, triglyceride, aspartate and alanine transaminases (AST and ALT) and c-reactive protein (CRP) levels were obtained and recorded from the institutional database and patients' files. Biochemical analyses were held with Architect c8000 analyzer (Abbott Inc. Lake Forest, IL, USA). White blood cell count (WBC), hemoglobin (Hb), hematocrit (Htc) and platelet count (plt) were also recorded. Automatic analyzer of LH 780 model of Beckman Coulter device (Beckman Coulter Inc.; Bre CA) was used for

complete blood count analyses. A TG/HDL-c level was obtained by the ratio of triglyceride/HDL-cholesterol. Body mass index is calculated by the division of weight by the square of height. Data of the patients with liver steatosis and the control subjects were compared.

Statistical analysis

Data were analyzed with SPSS software (SPSS 15.0; SPSS Inc., Chicago, IL, USA). Kolmogorov-Smirnov test was used in observing the distribution (normal or not) of the variables in study and control groups in terms of normal analyzed with. Variables with normal distribution were compared with independent samples t test and expressed as mean \pm standard deviation (SD). Mann-Whitney U test is used in comparison of the variables without normal distribution and these variables were expressed as median (min.-max.). Chi-square test is used in comparison of categorical variables between study and control subjects. Correlation between studies variables were conducted with Pearson's correlation analysis. Receiver Operative Characteristics (ROC) analyze used in determination of cut-off values of study variables in predicting NAFLD. Statistical significance was set when the p value was lower than 0.05.

Results

A total of 496 subjects, 267 in liver steatosis and 229 in control group, were enrolled to the study. Mean ages of the liver steatosis and control groups were 45.5 ± 12 years and 44 ± 10 years, respectively ($p=0.09$). 131 (49%) were women and 136 (51%) were men in the liver steatosis group whereas 96 (42%) were women and 133 (58%) were men in control group. Gender of the liver steatosis and control groups were not statistically different ($p=0.11$).

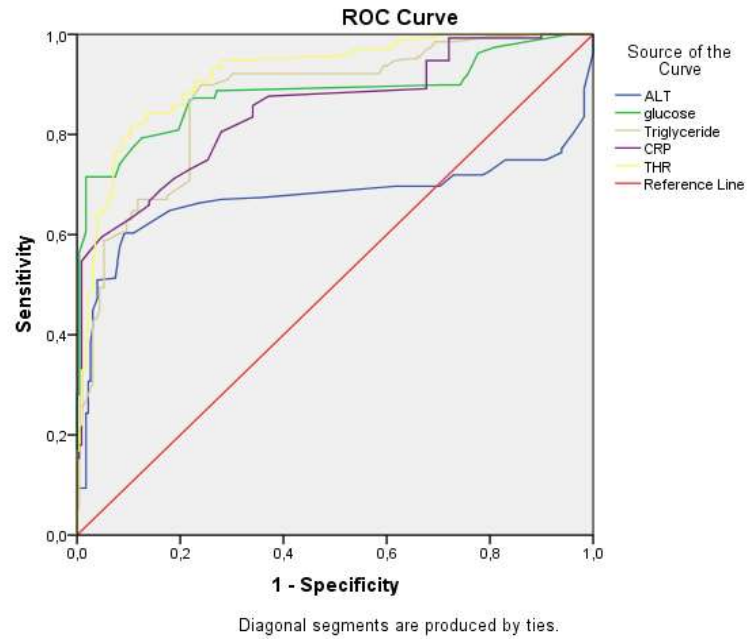


Figure 1. ROC curves of ALT, fasting glucose, triglyceride, CRP, and THR in determination of liver steatosis

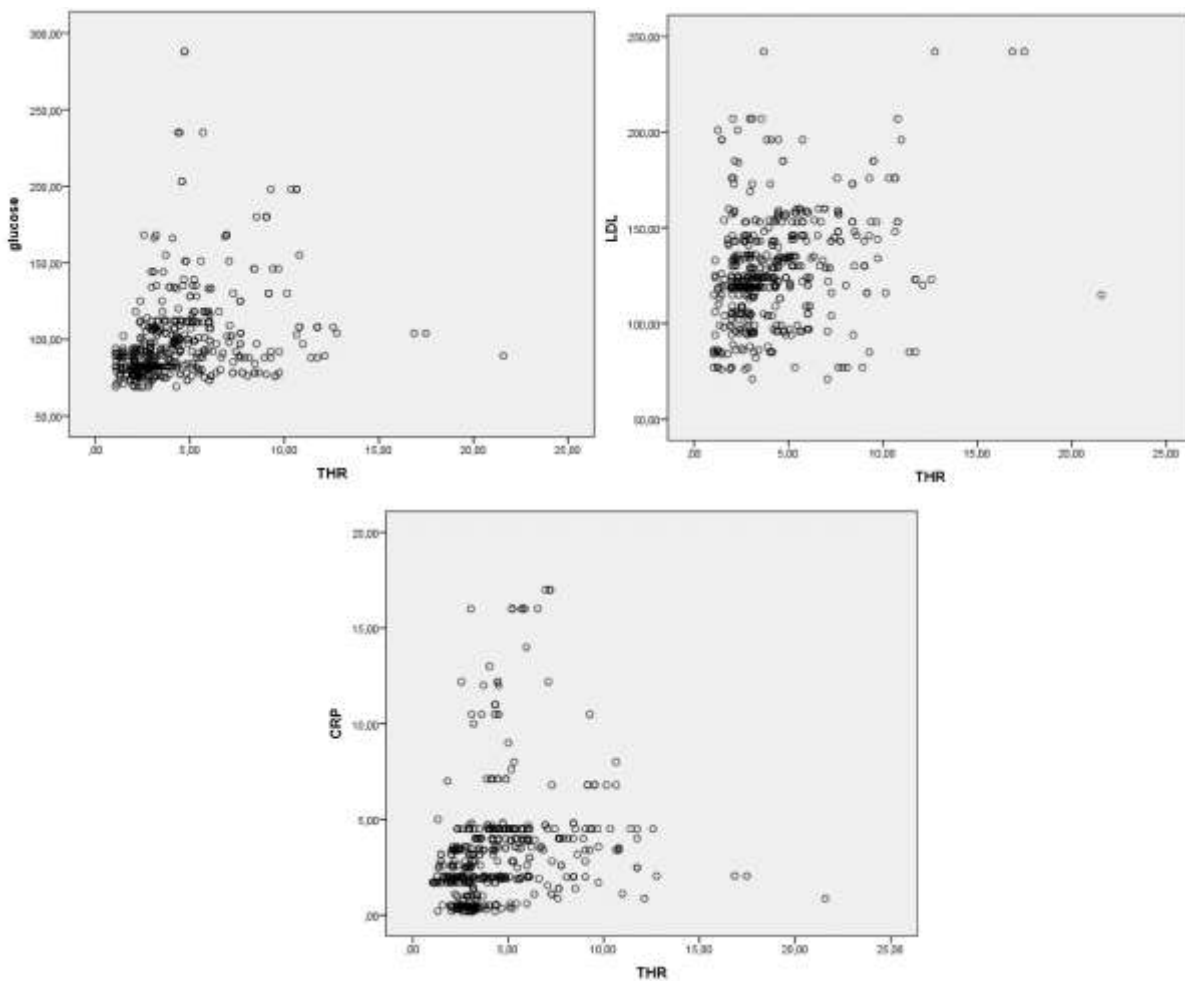


Figure 2. Correlations of THR with fasting glucose, LDL- cholesterol and CRP level.

The WBC ($p=0.11$), Hb ($p=0.26$), Htc ($p=0.08$), PLT ($p=0.19$), serum creatinine ($p=0.1$) and AST ($p=0.54$) levels of the liver steatosis and control groups were not statistically different.

The ALT ($p<0.001$), FPG ($p<0.001$), triglyceride ($p<0.001$), LDL-cholesterol ($p<0.001$) and CRP ($p<0.001$) levels were significantly increased and HDL-cholesterol ($p<0.001$) was significantly decreased in liver steatosis group compared to the control subjects. TG/HDL-c level of the liver steatosis group [5 (2-22) %] was higher than the TG/HDL-c level of the control group [2.7 (1-8) %], and this difference was statistically significant ($p<0.001$).

In Roc analysis test, a TG/HDL-c value greater than 3.1% have 91% sensitivity and 77% specificity in detecting hepatosteatosi, which is better than other variables, i.e., ALT, FPG, triglyceride and CRP (Figure 1).

In Pearson's correlation analysis test, TG/HDL-c was significantly and positively correlated with FPG ($r=0.31$, $p<0.001$), CRP ($r=0.25$, $p<0.001$) and LDL-cholesterol ($r=0.3$, $p<0.001$) levels (Figure 2).

Discussion

Main finding of present retrospective study is that TG/HDL-c ratio could be a promising indicator of liver steatosis in general population. Since it has significant correlation with inflammatory (CRP) and metabolic (FPG and LDL-cholesterol) markers of hepatosteatosi, and has stunning sensitivity and specificity in determination of the disease, it may have substantial utility in clinical practice.

Recent studies in literature focused on the usefulness of TG/HDL-c ratio in various clinical conditions. Authors suggested the TG/HDL-c ratio as a novel prognostic marker

in patients receiving peritoneal dialysis treatment since elevated THR was correlated with worse survival in this population [9]. Chronic renal insufficiency, like liver steatosis, is a condition characterized with increased inflammatory burden. Therefore, increased levels of TG/HDL-c were noted in patients with liver steatosis compared to controls in present work.

The role of TG/HDL-c ratio has been studied in gestational diabetes mellitus, too. A Chinese study reported that elevated first trimester TG/HDL-c levels could predict the development of gestational diabetes mellitus [10]. Both pregnancy, and gestational diabetes mellitus are characterized with insulin resistance and increased inflammation. Liver steatosis is also associated with insulin resistance and increased inflammatory burden. Therefore, elevated TG/HDL-c levels which reported in our study is a compatible finding with current medical literature.

Increased level of TG/HDL-c has been found to be a risk factor for inflammatory breast cancer in Schairer et al's study, which reported a 1.7 odds ratio for the THR level greater than 2.5% [11]. Cancer is also promoted by inflammatory reactions and cause chronic, low grade, continuous inflammatory load. Therefore, as an inflammatory condition, liver steatosis caused an elevation in TG/HDL-c levels in our study. The TG/HDL-c ratio has been proposed as a prognostic tool in coronary artery disease [6,12]. Moreover, high TG/HDL-c levels were associated with abnormal heart rate recovery, which is a marker of decreased parasympathetic activity and a predictor of all-cause mortality [13].

High TG/HDL-c ratio is associated with deteriorated insulin sensitivity [14]. Elevated TG/HDL-c is suggested to be a predictor of incident type 2 diabetes mellitus in male

subjects [15]. A similar association between diabetes mellitus and increased TG/HDL-c has been reported in obese postmenopausal women [16]. Since liver steatosis is associated with insulin resistance and inflammation, as diabetes mellitus do, increased levels of TG/HDL-c in patients with liver steatosis is not a coincidental finding.

Retrospective design and moderately large study population are two possible limitations of our work. However, to the best of our knowledge, this is the first study reported high sensitivity and specificity of TG/HDL-c ratio in detecting liver steatosis.

In conclusion, we suggest that TG/HDL-c ratio could be a useful marker of liver steatosis due to its inexpensive and easy to assess nature.

Funding: *The author(s) received no financial support for the research, authorship, and/or publication of this article.*

Conflict of Interest: *The authors declare that they have no conflict of interest.*

Ethical statement: *The study was approved by the Local Ethics Committee of University (Date and decision no: 2020/311), and written informed consent was obtained from each subject.*

Open Access Statement

This is an open access journal which means that all content is freely available without charge to the user or his/her institution under the terms of the Creative Commons Attribution Non-Commercial License (<http://creativecommons.org/licenses/by-nc/4.0>). Users are allowed to read, download, copy, distribute, print, search, or link to the full texts of the articles, without asking prior permission from the publisher or the author.

References

- [1] Keenan T, Blaha MJ, Nasir K et al. Relation of uric acid to serum levels of high-sensitivity C-reactive protein, triglycerides, and high-density lipoprotein cholesterol and to hepatic steatosis. *Am J Cardiol.* 2012; 110 (12): 1787-92.
- [2] Aktas G, Alcelik A, Tekce BK et al. Mean platelet volume and red cell distribution width in hepatosteatois. *Natl J Med Res.* 2013; 3 (3): 264-66.
- [3] Aktas G, Duman TT, Kurtkulagi O et al. Liver Steatosis is Associated Both with Platelet Distribution Width, Neutrophil/Lymphocyte and Monocyte/Lymphocyte Ratios. *Prim Health Care Open Access.* 2020; 10 (4): 1-4.
- [4] Kosekli MA, Erkus E, Kocak MZ. Mean Platelet Volume to Platelet ratio as a promising marker of hepatosteatois. *Exp Biomed Res.* 2018; 1 (2): 55-59.
- [5] Rodak AP, Kiciak S, Tomaszewicz K. Neutrophil-lymphocyte ratio and mean platelet volume as predictive factors for liver fibrosis and steatosis in patients with chronic hepatitis B. *Ann Agricul Environ Med.* 2018; 25 (4): 690-92.
- [6] Hadaegh F, Khalili D, Ghasemi A et al. Triglyceride/HDL-cholesterol ratio is an independent predictor for coronary heart disease in a population of Iranian men. *Nutr Metab Cardiovasc Dis.* 2009; 19 (6): 401-08.
- [7] Maruyama C, Imamura K, Teramoto T. Assessment of LDL particle size by triglyceride/HDL-cholesterol ratio in non-diabetic, healthy subjects without prominent hyperlipidemia. *J Atheroscleros Thrombos.* 2003; 10 (3): 186-91.
- [8] Murguía-Romero M, Jiménez-Flores JR, Sigríst-Flores SC et al. Plasma triglyceride/HDL-cholesterol ratio, insulin resistance, and cardiometabolic risk in

- young adults. *J Lipid Res.* 2013; 54 (10): 2795-99.
- [9] Xia W, Yao X, Chen Y et al. Elevated TG/HDL-C and non-HDL-C/HDL-C ratios predict mortality in peritoneal dialysis patients. *BMC Nephrol.* 2020; 21 (1): 324.
- [10] Liu PJ, Liu Y, Ma L et al. The Predictive Ability of Two Triglyceride-Associated Indices for Gestational Diabetes Mellitus and Large for Gestational Age Infant Among Chinese Pregnancies: A Preliminary Cohort Study. *Diab Metab Syndr Obes: targets and therapy* 2020; 13: 2025-35.
- [11] Schairer C, Laurent CA, Moy LM et al. Obesity and related conditions and risk of inflammatory breast cancer: a nested case-control study. *Breast Cancer Res Treat.* 2020; 183 (2): 467-78.
- [12] da Luz PL, Favarato D, Faria-Neto JR, Jr. et al. High ratio of triglycerides to HDL-cholesterol predicts extensive coronary disease. *Clinics (Sao Paulo, Brazil)* 2008; 63 (4): 427-32.
- [13] Shishehbor MH, Hoogwerf BJ, Lauer MS. Association of triglyceride-to-HDL cholesterol ratio with heart rate recovery. *Diabetes Care* 2004; 27 (4): 936-41.
- [14] Gonzalez-Chavez A, Simental-Mendia LE, Elizondo-Argueta S. Elevated triglyceride/HDL-cholesterol ratio associated with insulin resistance. *Cirugia y cirujanos.* 2011; 79 (2): 126-31.
- [15] Vega GL, Barlow CE, Grundy SM et al. Triglyceride-to-high-density-lipoprotein-cholesterol ratio is an index of heart disease mortality and of incidence of type 2 diabetes mellitus in men. *J Invest Med.* 2014; 62 (2): 345-9.
- [16] Karelis AD, Pasternyk SM, Messier L et al. Relationship between insulin sensitivity and the triglyceride-HDL-C ratio in overweight and obese postmenopausal women: a MONET study. *Appl Physiol Nutr Metab.* 2007; 32 (6): 1089-96.

Relationship between intracellular pathogens *Toxoplasma gondii* and *Borrelia burgdorferi* infections and migraine

Murat Yilmaz¹, Aysen Tugba Canbasoglu Yilmaz², Handan Teker¹, Sule Aydin Turkoglu¹, Serpil Yildiz¹

¹Department of Neurology, Bolu Abant Izzet Baysal University, School of Medicine, Bolu, Turkey

²Department of Neurology, Bolu Private Cagsu Hospital, Bolu, Turkey

ABSTRACT

Aim: In this study, the serological values of our patients followed up with a diagnosis of migraine were compared with the results of healthy controls in terms of possible association with intracellular pathogens, *Toxoplasma gondii* and *Borrelia burgdorferi*.

Methods: Fifty patients with migraine, randomly selected among migraine patients without any additional disease, who applied to Bolu Abant Izzet Baysal Training and Research Hospital between January 1, 2015 and August 31, 2019 were included in the study. Fifty subjects without headache were included as control group. The history of infectious diseases of the patient and control groups (*Toxoplasma gondii*, *Borrelia burgdorferi*-causing Lyme disease) was determined by serological diagnostic methods.

Results: The study group consisted of 64 women with a mean age of 45.5±13.1 (15-76) years. Migraine and control groups were found to be similar in terms of age (p=0.059) and gender (p=0.211) distributions. The frequency of *Toxoplasma gondii* positivity in the migraine group was 28% (n=14) and 10% (n=5) in the control group. The frequency of Lyme was 19.6% (n=11) in the migraine group and 14.3% (n=8) in the control group. The frequency of *Toxoplasma gondii* positivity was statistically significantly higher in the migraine group (p=0.022), while the frequency of Lyme was found to be similar in the migraine and control groups (p=0.450).

Conclusion: The results of our study suggest that there are statistically significant differences between migraine and control groups only in terms of *Toxoplasma gondii* positivity rates, not Lyme. However, we believe that larger sample studies are needed to determine the detailed relationship between migraine and *Toxoplasma gondii* infection.

Key words: Migraine disorders, *Toxoplasma gondii*, *Borrelia burgdorferi*, Lyme, serum immunoglobulins.

✉ Dr. Murat Yilmaz

Department of Neurology, Bolu Abant Izzet Baysal University, School of Medicine, Bolu, Turkey

E-mail: dryilmazmurat@gmail.com

Received: 2021-04-16 / Revisions: 2021-05-25

Accepted: 2021-05-29 / Published online: 2021-07-01

Introduction

Migraine is a form of recurrent headache experienced by approximately 10% of the population, with a 3:1 female-to-male ratio [1].

It is renowned for severely disabling headache attacks which last 4–72 hours, are often unilateral, and are exacerbated by routine physical activity. These attacks can also be associated with nausea, photophobia or phonophobia [2].

Many factors, like foods, psychosocial stress, lifestyle factors and smoking have been suggested to trigger migraine [3]. More interestingly, it has been emphasized that some

infections, such as *Toxoplasma gondii* (causing Toxoplasmosis), can be associated with migraine and it has also been reported that some infections can mimic the clinical features of migraine [4-6]. Therefore, screening patients diagnosed with migraine in terms of these infections may be beneficial for diagnosis and treatment in migraine. Although the relationship between *Toxoplasma gondii* and migraine has been studied relatively more frequently, there are very few studies examining the relationship between migraine and other diseases caused by intracellular pathogens, such as Lyme [5,6]. Lyme disease, usually caused by infection with the spirochete *Borrelia burgdorferi*, is a multisystem disease caused by the body's immune response to infection [7]. These patients may present with physical findings such as headache, meningismus and cranioneuropathy as a sign of aseptic meningitis [7,8].

In this study, the serological values of our patients followed up with a diagnosis of migraine were compared with the results of healthy controls in terms of possible association with intracellular pathogens, *Toxoplasma gondii* and *Borrelia burgdorferi*.

Materials and methods

Patient and control groups

In this study, patients with migraine who had applied to the Neurology Clinic of Bolu Abant Izzet Baysal Training and Research Hospital, between January 1, 2015 and August 31, 2019 were included. A healthy control group comprised of patients who had applied to the clinic in the study period were also included. Between the specified dates, a total of 50 patients with migraine attended follow-up or were newly diagnosed. Additionally, patients without migraine who had been admitted for other symptoms but were not diagnosed with

any neurological condition were included as healthy controls. Among these, patients with any other chronic diseases, history of surgery or malignancy, those with other neurological or psychiatric diagnoses, and individuals who refused to participate in the study were excluded from the analyses. A final total of 50 patients with migraine and 50 controls had undergone serological analyses for Toxoplasmosis and Lyme.

Necessary permissions were obtained from the Clinical Research Ethics Committee of Bolu Abant Izzet Baysal University to conduct the study. (Approval number: 2020/245, Approval date: 13/10/2020) and all the patients were informed about the study and their written informed consents were obtained.

Serological method

The infectious disease history of the patient and control groups (*Toxoplasma gondii*, Lyme) was determined by serological diagnostic methods. A commercial ELISA kit (Bio-Rad, France) was used for the detection of *Toxoplasma gondii* IgG and IgM antibodies. The presence of Lyme disease serology was assessed via ELISA (Anti-Borrelia IgG and IgM Generic Assay, Germany) in serum samples. All detection procedures were performed according to the manufacturer's instructions. Presence of either or both IgG and IGM antibodies was accepted seropositive

Sample size and statistical analysis

For the sample size, it was determined that at least 50 subjects should be included in each group according to power analysis performed with the following parameters: 5% error margin, 80% power, an expected odds ratio of 3 with a 50% frequency distribution of infection.

The SPSS version 20 program was used for the analysis of all data. The Shapiro-Wilk test was

used to evaluate compliance with normal distribution. For continuous data, median, lowest and highest values (min-max) and/or mean \pm standard deviation were preferred for the description of data, with respect to normality of distribution. The Mann Whitney U or Student's t-test was used for the comparison of continuous data between groups in the presence of non-normal and normal distribution, respectively. Pearson Chi-Square test was used for the comparison of categorical data. The $p < 0.05$ threshold was defined as the level of significance.

Results

The study group consisted of 64 females and mean age was 45.5 ± 13.1 (min-max: 15–76) years. The migraine and control groups were similar in terms of age ($p=0.059$) and gender distribution ($p=0.211$).

Toxoplasma gondii positivity was detected in 14 (28%) patients in the migraine group and in 5 (10%) subjects in the control group. The frequency of *Toxoplasma gondii* positivity was statistically significantly higher in the migraine

group compared to the control group ($p=0.022$).

Lyme positivity was detected in 11 (19.6%) patients in the migraine group and in 8 (14.3%) subjects in the control group. There was again no significant difference between the groups ($p=0.450$) (Table 1).

Discussion

The present study, in which we aimed to determine whether there were relationships between migraine presence and intracellular pathogens, demonstrated that there was no difference between the migraine and control groups in terms of Lyme positivity frequency. However, of note, the frequency of *Toxoplasma gondii* positivity was higher in the migraine group compared to controls.

In previous studies, *Toxoplasma gondii* has been shown to be a neurotrophic pathogen and is associated with neurological and neuropsychiatric symptoms [9-11]. In addition, the relationship between migraine, headache and *Toxoplasma gondii* has also received relatively high interest [5,8,12]. It has been

Table 1. Age and gender characteristics and infection positivity frequencies of the study.

Parameters	Control group n=50	Migraine group n=50	p-value
Age, years, mean \pm SD	44.3 \pm 15.23	47.5 \pm 10.8	0.059
Gender, n (%)			0.211
Female	29 (58.0%)	35 (70.0%)	
Male	21 (42.0%)	15 (30.0%)	
<i>Toxoplasma gondii</i>, n (%)			0.022
Negative	45 (90.0%)	36 (72.0%)	
Positive	5 (10.0%)	14 (28.0%)	
Lyme (<i>Borrelia burgdorferi</i>), n (%)			0.275
Negative	44 (88.0%)	40 (80.0%)	
Positive	6 (12.0%)	10 (20.0%)	

reported that this infection affects the levels of specific cytokines, causing edema in the brain, which may manifest as headaches [13,14]. In addition, in a study by Koseoglu et al., it was reported that *Toxoplasma gondii* was associated with migraine and was concluded that this infection may cause a neuroinflammatory process in the brain, thereby triggering migraine [8]. In a study comparing 105 patients with headache and 105 non-headache subjects, it was reported that the case and control group were similar in terms of *Toxoplasma* seropositivity [15]; however, interestingly, the level of IgG for *Toxoplasma gondii* was suggested to be associated with headache—even when the patient group included other types of headaches in addition to migraine (39 patients with migraine in the 105 subjects). Since this infection is very prevalent among humans, has a chronic characteristic in an estimated 30% of individuals [16] and the fact that the infection may persist in the brain [17], have supported the rationale of studies aiming to determine a relationship (if any) between headache and *Toxoplasma gondii* infection. One such study even suggested the introduction of serological testing for *Toxoplasma gondii*, after demonstrating that 11% of children with recurrent headaches had IgG positivity [12]. In a study from Brazil, wherein 261 cases with acute toxoplasmosis were investigated, headache frequency was reported to be the second most frequent symptom (after fever), and perhaps more interestingly, the distribution among sexes demonstrated a female-to-male ratio of 2.1 to 1 [18]. In the current study, to support the information in the literature, the frequency of *Toxoplasma gondii* positivity was significantly higher in patients with a diagnosis of migraine. We believe that these results indicate that the relationship between migraine and toxoplasmosis warrants further

investigation, preferably in population-based studies.

When *Borrelia burgdorferi*, the cause of Lyme disease, reaches the cerebral or spinal vessels, it attaches to endothelial cells. It has been reported that the direct and indirect effects of *B.burgdorferi* on the nervous system play a role in the formation of neuroborreliosis [19]. In a previous study, it was reported that *B. burgdorferi* invaded human neuronal and glial cells, remained alive and had no cytopathic effect on the host cell for up to seven days. It has been reported that this situation can lead to the escape of bacteria from the immune system and to long-term infections [20]. Various mechanisms have been reported in the literature regarding the transmission and action mechanisms of bacteria to the nervous system. Grab et al. reported that with the in vitro blood brain barrier model containing microvascular endothelial cells of the human brain, the passage of bacteria through the barrier depends on the ability of the bacteria to affect the Ca ++ signaling system in endothelial cells [21]. Cepok et al. reported that the early stage of *B. burgdorferi* meningoradiculitis is characterized by a well-coordinated immune response involving specific cytokine release and plasma cell uptake, followed by a prolonged, antigen-specific B cell response in the central nervous system [22]. In the study of Rupprecht et al, it has been reported that chemokines (CXCL13) play a key role in attracting other immune cells to the inflammatory focus in Lyme neuroborreliosis, B cell migration to infection sites [23]. In the animal study of Pachner et al., Cytokines such as IL-6 have been reported to be important amplification molecules for cerebrospinal fluid inflammation in Lyme neuroborreliosis [24]. In Lyme disease, as a result of these changes in the central nervous system, it is expected that Lyme positivity in

migraine patients is higher than in the control group. It has been reported that Lyme disease causes various neurological symptoms such as headache and 15% of patients have neurological involvement [25,26]. Chronic headache associated with Lyme disease is difficult to diagnose and can be confused with primary or analgesic overuse headaches. However, it is important to make the correct diagnosis because when this symptom is associated with borreliosis, it tends to regress with antibiotic therapy [27-30]. In the study of Scelsa et al., it was reported that the incidence of new-onset headache was 53.06% and the incidence of migraine was 18.37% among patients hospitalized for recurrent neurological Lyme disease. In addition, it has been reported that all patients with meningitis or encephalitis requiring intravenous antibiotics have not only headache but also focal neurological findings or cognitive abnormalities [28]. In the current study, the migraine and control groups were similar in terms of Lyme disease frequency. However, few studies have investigated the possible relationship between Lyme disease and migraine. We believe it is very important to point out that the initial design and strength of the study may not be sufficient for such a post-hoc analysis, and therefore we suggest that future studies should consider this possibility. The research has several limitations. One of its limitations is that the research is not community-based and has a single center. On the other hand, questioning the chronology of the onset of migraine and the positivity of these pathogens (*Toxoplasma gondii*, *Borrelia burgdorferi*) could enable us to see the relationship between migraine and the positivity of these pathogens more clearly. Despite these, this study is valuable because it is one of the few studies evaluating the relationship between migraine and Lyme

disease and it shares results that support the relationship between *Toxoplasma gondii* and migraine.

Conclusion

In terms of the infections studied in the study group, there was statistically significant difference was found between patients with migraine and controls. However, further studies that enable comparisons by ensuring an infection distribution similar to that of the population are required.

Funding: *The author(s) received no financial support for the research, authorship, and/or publication of this article.*

Conflict of Interest: *The authors declare that they have no conflict of interest.*

Ethical statement: *The study was approved by the Local Ethics Committee of University (Date: 13/10/2020, approval number: 2020/245), and written informed consent was obtained from each subject.*

Open Access Statement

This is an open access journal which means that all content is freely available without charge to the user or his/her institution under the terms of the Creative Commons Attribution Non-Commercial License (<http://creativecommons.org/licenses/by-nc/4.0>). Users are allowed to read, download, copy, distribute, print, search, or link to the full texts of the articles, without asking prior permission from the publisher or the author.

References

- [1]Stovner L, Hagen K, Jensen R, et al. The global burden of headache: a documentation of headache prevalence and disability worldwide. *Cephalalgia*. 2007; 27(3):193-210.

- [2] Society HCCOTIH. The international classification of headache disorders, (beta version). *Cephalalgia*. 2013; 33(9):629-808.
- [3] Schoonman GG, Schytz HW, Ashina M. Migraine trigger factors. *Oxford Textbook of Headache Syndromes*. 2020:67.
- [4] Ferrigno G, Mazza M, Morelli M, et al. Chronic migraine as unusual presentation of syphilis. *Xlvii Congresso Nazionale 22-25 Ottobre 2016 – Venezia*.
- [5] Nayeri T, Sarvi S, Moosazadeh M, Hosseini Z, Amouei A, Daryani A. Association between *Toxoplasma gondii* infection and headache: a systematic review and meta-analysis. *Infect Disord Drug Targets*. 2020. doi: 10.2174/1871526520666200617135851.
- [6] Koseoglu E, Yazar S, Koc I. Is *Toxoplasma gondii* a causal agent in migraine? *Am J Med Sci*. 2009;338(2):120-22.
- [7] Feder HM Jr. Lyme disease in children. *Infect Dis Clin North Am*. 2008;22(2):315-26.
- [8] Centers for Disease Control and Prevention. Lyme Disease: Diagnosis and Testing. CDC. Available at <http://www.cdc.gov/lyme/diagnosis/testing/LabTest/TwoStep/index.html>. November 20, 2019; Accessed: March 30, 2021.
- [9] Flegr J. Neurological and neuropsychiatric consequences of chronic *Toxoplasma* infection. *Curr Clin Micro Rpt*. 2015; 2(4):163-72.
- [10] Abo-Al-Ela HG. Toxoplasmosis and Psychiatric and Neurological Disorders: A Step toward Understanding Parasite Pathogenesis. *ACS Chem Neurosci*. 2020 Aug 19;11(16):2393-2406.
- [11] Tedford E, Mcconkey G. Neurophysiological changes induced by chronic *Toxoplasma gondii* infection. *Pathogens*. 2017; 6(2):19.
- [12] Prandota J, Gryglas A, Fuglewicz A, et al. Recurrent headaches may be caused by cerebral toxoplasmosis. *World J Clin Pediatr*. 2014;3(3):59-68.
- [13] Akturk HK, Sotello D, Ameri A, et al. *Toxoplasma* Infection in an Immunocompetent Host: Possible Risk of Living with Multiple Cats. *Cureus*. 2017;9(3):e1103.
- [14] Prandota J. Recurrent headache as the main symptom of acquired cerebral toxoplasmosis in nonhuman immunodeficiency virus-infected subjects with no lymphadenopathy: the parasite may be responsible for the neurogenic inflammation postulated as a cause of different types of headaches. *Am J Ther*. 2007; 14(1):63-105.
- [15] Alvarado-Esquivel C, Del Rosario Rico-Almochantaf Y, Sanchez-Anguiano LF, et al. *Toxoplasma gondii* Infection and Headache: A Matched Case-Control Study in a Public Hospital in Durango City, Mexico. *J Clin Med Res*. 2018; 10(1):27-31.
- [16] Schlüter D, Däubener W, Schares G, et al. Animals are key to human toxoplasmosis. *Int J Med Microbiol*. 2014; 304(7):917-29.
- [17] Mendez OA, Koshy AA. *Toxoplasma gondii*: Entry, association, and physiological influence on the central nervous system. *PLoS Pathog*. 2017; 13(7):e1006351.
- [18] Silva CS, Neves Ede S, Benchimol EI, et al. Postnatal acquired toxoplasmosis patients in an infectious diseases reference center. *Braz J Infect Dis*. 2008; 12(5):438-41.
- [19] Kazak E, Helvacı NY, Helvacı S. Nöroborrelyoz. *Uludağ Üniversitesi Tıp Fakültesi Dergisi*. 2013; 39(2):137-45.
- [20] Livengood JA, Gilmore RD. Invasion of human neuronal and glial cells by an infectious strain of *Borrelia burgdorferi*. *Microbes Infect*. 2006; 8(14-15):2832-40.

- [21] Grab DJ, Nyarko E, Nikolskaia OV, et al. Human brain microvascular endothelial cell traversal by *Borrelia burgdorferi* requires calcium signaling. *Clin Microbiol Infect.* 2009; 15(5):422-26.
- [22] Cepok S, Zhou D, Vogel F, et al. The Immune Response at Onset and During Recovery From *Borrelia burgdorferi* Meningoradiculitis. *Arch Neurol.* 2003; 60(6):849-55.
- [23] Rupprecht TA, Plate A, Adam M, et al. The chemokine CXCL13 is a key regulator of B cell recruitment to the cerebrospinal fluid in acute Lyme neuroborreliosis. *J Neuroinflammation.* 2009;6:42.
- [24] Pachner A, Amemiya K, Delaney E, et al. Interleukin-6 is expressed at high levels in the CNS in Lyme neuroborreliosis. *Neurology.* 1997; 49(1):147-52.
- [25] Rauer S, Kastenbauer S, Fingerle V, et al. Lyme neuroborreliosis. *Deutsches Ärzteblatt International.* 2018; 115(45):751.
- [26] Marques AR. Lyme neuroborreliosis. *CONTINUUM: Lifelong Learning in Neurology.* 2015; 21(6):1729-44.
- [27] Kowacs PA, Martins RT, Piovesan EJ, et al. Chronic unremitting headache associated with Lyme disease-like illness. *Arq Neuropsiquiatr.* 2013;71(7):470-73.
- [28] Scelsa SN, Lipton RB, Sander H, Herskovitz S. Headache characteristics in hospitalized patients with Lyme disease. *Headache.* 1995;35(3):125-30.
- [29] Brinck T, Hansen K, Olesen J. Headache resembling tension-type headache as the single manifestation of Lyme neuroborreliosis. *Cephalalgia.* 1993; 13(3):207-9.
- [30] Moses JM, Riseberg RS, Mansbach JM. Lyme disease presenting with persistent headache. *Pediatrics.* 2003; 112(6):e477-e9.

COVID-19 Pandemic: A comparison of adult and pediatric populations

Muhammed Emin Demirkol¹, Musa Kaya², Mehmet Balci³, Emine Ozsari⁴

¹Department of Internal Medicine, Bolu Abant Izzet Baysal University, Faculty of Medicine, Bolu, Turkey

²Department of Emergency Medicine, Zonguldak Ataturk State Hospital, Zonguldak, Turkey

³Department of Infectious Diseases, Izzet Baysal State Hospital, Bolu, Turkey

⁴Department of Chest Diseases, Bolu Abant Izzet Baysal University, Faculty of Medicine, Bolu, Turkey

ABSTRACT

Aim: Couple of pneumonia cases were reported in a short period in Wuhan, China. The cases were revealed to be associated with a different coronavirus type was named SARS-CoV-2 and the disease was identified as Covid-19. It is known that the disease occurs in all age groups. We aimed to evaluate the differences in clinical and laboratory features between adult and pediatric patients.

Method: The study is a retrospective cross-sectional study and consists of 206 patients with a definitive diagnosis of Covid-19 confirmed by a positive real-time reverse-transcriptase polymerase chain reaction (RT-PCR) testing for SARS-CoV-2. They hospitalized in health institutions connected to City Health Administrative of Bolu, Turkey between 11.03.2020 and 19.04.2020. The number of the pediatric patients (0-17 age group) was 106, that of the adult patients (18 and above age group) was 100. Data concerning the patients consisted of age, symptoms, laboratory parameters such as hemogram, biochemistry, coagulation.

Results: The mean values of platelet (PLT), platocrit (PCT), percentage of monocytes (MONO %) and MONO in the “0-17” age group were found to be significantly higher than the mean values in the “18 and above” age group. The hemoglobin (HGB) mean value of the “0-17” age group was significantly lower than that of the “18 and above” age group. The mean C - reactive protein (CRP) value of the “0-17” age group (4.55; min: 1.20 – max: 11.80) was significantly lower than that of the “18 and above” age group (5.35; min 1.25- max: 19.77) with no statistically significance. In pediatric group, the most common symptoms were other symptoms like diarrhea, vomiting and joint pain whereas the adult patients had fever and cough often with statistically significant.

Conclusion: Clinical findings and laboratory abnormalities in Covid-19 are less common in children. Although it seems that Covid-19 is less symptomatic in children, they are also affected by the disease. Performing RT-PCR test based on the contact history of the children may help to minimize morbidity with an early diagnosis. Multicenter studies with more numbers of patients should be performed.

Key words: COVID – 19, SARS-CoV-2, adolescent, adult, child.

✉ Dr. Emine Ozsari

Department of Chest Diseases, Bolu Abant Izzet Baysal University, Faculty of Medicine, Bolu, Turkey

E-mail: dreminedemirok@hotmail.com

Received: 2021-01-04 / Revisions: 2021-01-16

Accepted: 2021-04-19

Published online: 2021-07-01

Introduction

In December 2019, a couple of pneumonia cases were reported in a short period in Wuhan, China [1]. The cases were revealed to be associated with a different coronavirus type was named SARS-CoV-2 and the disease it caused was identified as Covid-19 [2]. While

other types of coronavirus such as SARS-CoV and MERS-CoV do not lead to severe diseases, SARS-CoV-2 have caused millions of deaths [3,4].

It is known that Covid-19 occurs not only in adults but also in children [5]. However, children represent a very small proportion of cases and prior studies have shown that the mortality rate is much lower in them [6,7]. Moreover, it has been determined that the clinical picture in children is considerably milder than in adults [8]. The disease is diagnosed mostly with fever, cough, sneezing, sore throat, myalgia, pharyngeal erythema and runny nose. However, symptoms such as diarrhea, nausea, vomiting and malaise can also be seen [9]. Compared to adults, frequent laboratory abnormalities such as elevated CRP and procalcitonin levels and lymphopenia were found to be quite low in children diagnosed with Covid-19 [10]. In this study, we aimed to evaluate the differences in clinical and laboratory features between adult and pediatric patients to diagnose more effectively.

Materials and methods

The study is a retrospective cross-sectional study and consists of 206 patients with a definitive diagnosis of Covid-19 confirmed by a positive RT-PCR test after hospitalized in health institutions connected to City Health Administrative of Bolu, Turkey between 11.03.2020 and 19.04.2020. Ethical approval of the study was obtained from Bolu Abant İzzet Baysal University Clinical Research Ethics Committee (Date: 12.05.2020, Number: 2020/92). Data was obtained by scanning the patients from the Public Health Management System of City Health Administrative and Hospital Information Management System. Information about the patients consisted of age, symptoms, results of laboratory parameters

such as white blood cell count (WBC), hemoglobin (HGB), hematocrit (Htc), lymphocyte count (LYM), platelet count (PLT), red blood cell (RBC), basophil (BASO), platocrit (PCT), neutrophil (NEU), monocyte (MONO), D-DIMER, C-Reactive protein (CRP) and lactate dehydrogenase (LDH). Clinical findings categorized as fever, cough and other symptoms like diarrhea, vomiting, anosmia, headache, joint pain and sore throat. Patients who didn't apply during the mentioned dates were not included the study. Also pregnant women and patients with immunosuppressions, diabetes mellitus, chronic lung and kidney diseases, and hypertension were excluded.

Statistical analyses

For all statistical analyses, the 20.0 version of SPSS (Statistical Package for the Social Sciences) for Windows, (Chicago, Illinois, USA) was used. The numerical data were expressed as mean \pm standard deviation. The difference between the study and the control groups was evaluated by Student t-test for data which were normally distributed. For the data which were not normally distributed Mann-Whitney's U-test was used. Chi-Square test was used in the analysis of categorical data. The correlation between EFT and MS was evaluated using Spearman's correlation analysis. A *p-value* < 0.05 was considered as significant.

Results

There were 206 patients in the study; 106 patients between 0-17 years, 100 patients aged 18 and above. The mean age was 13.52 (min: 1-max: 17) in the "0-17" age group and 45.43 (min: 18-max: 85) in the "18 and above" age group (*p=0,000*).

The mean values of PLT, PCT, MONO% and MONO in the "0-17" age group were found to

be significantly higher than the mean values in the “18 and above” age group ($p < 0.05$). The HGB mean value of the “0-17” age group was significantly lower than that of the “18 and above” age group ($p < 0.05$) (Table 1). The mean CRP value of the “0-17” age group (4.55; min: 1.20 – max: 11.80) was significantly lower than that of the “18 and above” age group (5.35; min 1.25- max: 19.77) with no statistically significance ($p = 0.461$) (Table 1).

The percentages of the clinical findings were calculated for both age groups. In the “0- 17” age group, the most common symptoms were other symptoms (54.8%) like diarrhea, vomiting, anosmia, sore throat and joint pain. ($p = 1.153$) The presence of fever (69%) and cough (69.9%) symptoms was significantly higher in the 18 and above age group ($p = 0.000$) (Table 2).

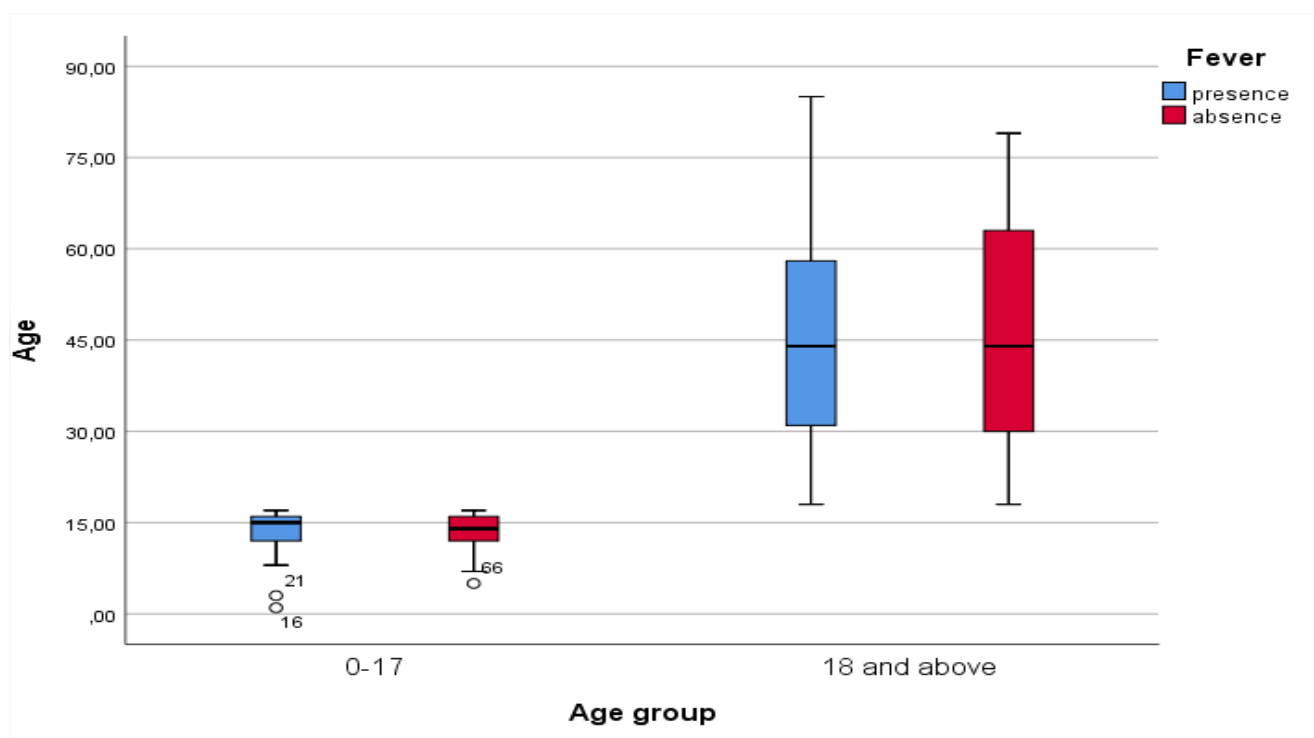
Table 1. Laboratory results of age groups.

Comparison of laboratory results between age groups				
Parameters	“0-17” age group (n=106;%51.5)	“18 and above” age group (n=100; 48.5)	All Patients	p-value
	Median (Q1-Q3)**			
WBC	5.83 (4.77-7.39)	5.50 (4.50-6.59)	5.76 (4.57-7.03)	0.062
LYM	1.49 (1.01-2.00)	1.45 (1.15-1.93)	1.45 (1.1-1.96)	0.931
HGB	13.50 (13.00-14.40)	14.25 (12.80-15.40)	13.70 (13-14.90)	0.024*
BASO	0.02 (0.01-0.03)	0.034 (0-0.06)	0.03 (0.01-0.05)	0.390
PLT	253.5 (216-293)	207.5 (172.5-247.0)	228.5 (196-273)	0.000*
PCT	0.25 (0.22-0.29)	0.17 (0.14-0.21)	0.21 (0.17-0.26)	0.000*
NEU	3.44 (2.40-5.00)	3.46 (2.41-4.60)	3.44 (2.4-4.76)	0.514
D-DİMER	0.29 (0.21-0.58)	0.37 (0.22-0.59)	0.32 (0.21-0.58)	0.566
LDH	234 (207-283)	222.5 (185-273.5)	230 (196-276)	0.073
CRP	4.55 (1.20-11.80)	5.35 (1.25-19.77)	4.84 (1.2-14.7)	0.461
$\bar{X} \pm ss^{***}$				
Age	13.52±3.15	45.43±17.26	29.01±20.11	0.000*
RBC	4.88±0.45	4.86±0.55	4.87±0.49	0.728
LYM%	27.09±13.41	28.47±10.98	27.76±12.28	0.419
MONO%	11.31±3.85	8.75±3.50	10.07±3.89	0.000*
NEU%	59.98±14.56	61.39±12.02	60.66±13.37	0.447
MONO	0.70±0.28	0.50±0.25	0.61±0.28	0.000*
*a value of $p < 0.05$ was taken statistically significant				
** Mann-Whitney U test ***Independent Sample t test				

Table 2. Chi-Square analysis of clinical findings according to age groups.

Parameters	“0-17” age group (n:106; %51.5)	“18 and above” age group (n:100; %48.5)	All Patients (n:206)	p-value	χ^2 value
Fever positive	48 (%39.3)	74 (%69.0)	122 (%59.2)	0.000*	17.572
negative	58 (%60.7)	26 (%31.0)	84 (%40.8)		
Cough positive	27 (%29.0)	79 (%69.9)	93 (%45.1)	0.000*	34.129
negative	66 (%71.0)	34 (%30.1)	113 (%54.9)		
Other symptoms positive	63 (%54.8)	52 (%47.3)	115 (%55.8)	0.326	1.153
negative	43 (%45.2)	48 (%52.7)	91 (%44.2)		

a value of $p < 0.05$ was taken statistically significant * Chi-Square test

**Figure 1.** Relationship between age groups and fever.

Discussion

In this study, we aimed to reveal the differences in clinical and laboratory features between adult and pediatric patients and tried to emphasize that children are also at risk for Covid-19 as different manifestations.

It was observed that only 1.7% of the cases reported in United States of America (USA)

until April 2020 were children. Despite the low incidence compared to adult patients, SARS-CoV-2 is also seen in children and has been shown to be associated with milder clinical symptoms [11-13]. Of 206 patients in our study, 106 (%51.5) were children, and the proportion was found to be quite higher according to USA data. We attributed this to the fact that children

were scanned and caught at the stage without symptoms. While none of pediatric patients needed intensive care, 3 of the adult patients were followed up in intensive care unit. Among 100 adult patients 1 (1%) death occurred, but no death was seen in children.

A study in China revealed that children had mild clinical symptoms and less need for intensive care compared to adults. In this study, the most common symptoms were cough (48.5%), pharyngeal erythema (46.2%) and fever (41.5%). It was reported that only 3 of 171 patients needed intensive care and all of them had underlying diseases.[14] In our study, fever (39.3%), cough (29.0%) and other symptoms (54.8%) like diarrhea, vomiting, anosmia, joint pain and sore throat were recorded in children (Figure 1) On the other hand, major symptoms of adults were fever (69%) and cough (69.9%) while other symptoms (47.3%) noticed lower than children (Figure 2) In a Chinese study, 8 of 10 pediatric patients had fever and 6 of them had cough confirming most common symptoms in children were similar to those in adults [15]. In a study performed by Yang et al. [16] with 134 pediatric patients, the fever was found to be the most common symptom with 76.1%.

In a study conducted by Chen et al. [17] with 505 patients of whom 12 were children, it has been shown that lymphopenia seen in only 2 patients was less common than adults. In our study, lymphopenia was similar in children as adults (mean LYM value in children: 1.49 – mean LYM value in adults 1.45). (Table 1) Moreover, it has been shown that the mean LYM value was lower in adults compared to pediatric patients. Xia et al. [18] researched that; 70% of pediatric patients had normal WBC count, 20% had leukopenia and 10% had leukocytosis. Additionally, lymphopenia (35%), elevated alanine aminotransferase (ALT) (25%), elevated CRP (45%) and

elevated procalcitonin (80%) were the other laboratory abnormalities. In our pediatric patients; WBC, RBC, MONO, PLT, PCT and LDH were higher than adults whereas Hb, BASO, NEU, D DIMER and CRP were lower than adults. Among these findings, while the increase of PLT, PCT, MONO% and MONO and the decrease of Hb in the “0-17” age group were statistically significant. ($p < 0.05$) (Table 1).

There may some explanations for the reasons between the differences in clinical features between adults and children. One of the study has been suggested that the virus in children is the second, third and sometimes fourth generation because of the transmission of the disease from adults, and compared to the first generation one it is more difficult for the virus to replicate, mutate and survive before it is recognized by the immune system [19]. Furthermore, it has been argued that natural immunity in children is more ready against such pathogens and immune system functions decrease with aging [19,20]. Considering that there is a curfew for people under 20 years of age since the beginning of the outbreak in Turkey, it can be concluded that children get the disease from adult members of the family. In addition to this, the children had a history of indirect contact and the disease in children was less symptomatic, the above-mentioned opinions seem to be reasonable.

Conclusion

Clinical findings and laboratory abnormalities in Covid-19 are less common in children. Although it seems that Covid-19 is less symptomatic in children, they are also affected by the disease. Performing RT-PCR test based on the contact history of the children may help to minimize morbidity with an early diagnosis. Multicenter studies with more numbers of

patients should be performed for more accurate outcomes.

Funding: *The author(s) received no financial support for the research, authorship, and/or publication of this article.*

Conflict of Interest: *The authors declare that they have no conflict of interest.*

Ethical statement: *The study was approved by Bolu Abant İzzet Baysal University Clinical Research Ethics Committee (Date: 12.05.2020, Number: 2020/92), and written informed consent was obtained from each subject.*

Open Access Statement

This is an open access journal which means that all content is freely available without charge to the user or his/her institution under the terms of the Creative Commons Attribution Non-Commercial License (<http://creativecommons.org/licenses/by-nc/4.0>). Users are allowed to read, download, copy, distribute, print, search, or link to the full texts of the articles, without asking prior permission from the publisher or the author.

References

- [1]Zhu N, Zhang D, Wang W, et al. China Novel Coronavirus Investigating and Research Team. A Novel Coronavirus from Patients with Pneumonia in China, 2019. *N Engl J Med.* 2020;382(8):727-33.
- [2]World Health Organization. Novel coronavirus—China2020 (At <https://www.who.int/csr/don/12-january-2020-novel-coronavirus-china/en/>).
- [3]Huang C, Wang Y, Li X, et al ; Clinical features of patients infected with 2019 novel coronavirus in Wuhan, China. *Lancet.* 2020;395(10223):497-506.
- [4]Chen N, Zhou M, Dong X, et al. Epidemiological and clinical characteristics of 99 cases of 2019 novel coronavirus pneumonia in Wuhan, China: a descriptive study. *Lancet.* 2020;395 (10223):507- 13.
- [5]Ludvigsson JF. Systematic review of COVID-19 in children shows milder cases and a better prognosis than adults. *Acta Paediatr.* 2020 Jun;109(6):1088-1095.
- [6]Novel Coronavirus Pneumonia Emergency Response Epidemiology Team. The Epidemiological Characteristics of an Outbreak of 2019 Novel Coronavirus Diseases (COVID-19) in China. *Zhonghua Liu Xing Bing Xue Za Zhi.* 2020;41(2):145–151.
- [7]Livingston E, Bucher K. Coronavirus Disease 2019 (COVID-19) in Italy. *JAMA.* 2020;323(14):1335.
- [8]Dong Y, Mo X, Hu Y, Qi X, Jiang F, Jiang Z, Tong S. Epidemiology of COVID-19 Among Children in China. *Pediatrics.* 2020;145(6):e20200702.
- [9]Henry BM, Lippi G, Plebani M. Laboratory abnormalities in children with novel coronavirus disease 2019. *Clin Chem Lab Med.* 2020;58(7):1135-38.
- [10]Weiss SR, Leibowitz JL. Coronavirus pathogenesis. *Adv Virus Res.* 2011;81:85-164.
- [11]Zaki AM, van Boheemen S, Bestebroer TM, et al. Isolation of a novel coronavirus from a man with pneumonia in Saudi Arabia. *N Engl J Med.*2012;367(19):1814-20.
- [12]Special Expert Group for Control of the Epidemic of Novel Coronavirus Pneumonia of the Chinese Preventive Medicine Association. [An update on the epidemiological characteristics of novel coronavirus pneumonia (COVID-19)]. *Zhonghua Liu Xing Bing Xue Za Zhi.* 2020;41(2):139-144.
- [13]CDC COVID-19 Response Team. Coronavirus Disease 2019 in Children -

- United States, February 12-April 2, 2020. *MMWR Morb Mortal Wkly Rep.* 2020;69(14):422-26.
- [14] Lu X, Zhang L, Du H, et al. Chinese Pediatric Novel Coronavirus Study Team. *N Engl J Med.* 2020; 382(17):1663-65.
- [15] Jiehao C, Jin X, Daojiong L, et al. A Case Series of Children With 2019 Novel Coronavirus Infection: Clinical and Epidemiological Features. *Clin Infect Dis.* 2020;71(6):1547-51.
- [16] Yang P, Liu P, Li D, Zhao D. Corona Virus Disease 2019, a growing threat to children? *J Infect.* 2020;80(6):671-93.
- [17] Chen J, Zhang ZZ, Chen YK, et al. The clinical and immunological features of pediatric COVID-19 patients in China. *Genes Dis.* 2020;7(4):535-541.
- [18] Xia W, Shao J, Guo Y, et al. Clinical and CT features in pediatric patients with COVID-19 infection: Different points from adults. *Pediatr Pulmonol.* 2020 ;55(5):1169-74.
- [19] Su L, Ma X, Yu H, et al. The different clinical characteristics of corona virus disease cases between children and their families in China - the character of children with COVID-19. *Emerg Microbes Infect.* 2020;9(1):707-13.
- [20] Ruggiero A, Attinà G, Chiaretti A. Additional hypotheses about why COVID-19 is milder in children than adults. *Acta Paediatr.* 2020;109(8):1690.

The evaluation of the effect of vitamin D replacement on the symptoms of carpal tunnel syndrome in patients with low vitamin D levels

Ayşe Gul Korkut¹, Sebnem Koldas Dogan², Meral Bilgilişoy Filiz², Naciye Fusun Toraman²

¹Department of Physical Medicine and Rehabilitation, Kepez State Hospital, Antalya, Turkey

²Department of Physical Medicine and Rehabilitation, Health Science University, Antalya Training and Research Hospital, Antalya, Turkey

ABSTRACT

Aim: To evaluate the effect of vitamin D replacement on carpal tunnel syndrome (CTS) symptoms and signs in CTS patients with low vitamin D levels.

Methods: This study was designed prospective observably. The patient population was admitted to the EMG (electromyography) laboratory in a tertiary hospital's Physical Medicine and Rehabilitation Department between 1 January and 31 July 2018. Initially, 55 patients were included in the study. The patients were categorized into two groups as group 1 (<10 ng / ml) and group 2 (10-20 ng / ml) according to the vitamin D levels. A total of 39 patients and 63 wrists, 17 patients in group 1 (28 wrists) and 22 patients in group 2 (35 wrists), were included in the analysis.

Results: There was a statistically significant decrease in visual analogue scale and quick arm-shoulder-hand disability score in two groups when compared before treatment. In two groups, there was a significant improvement in grip and pinch strength after treatment. At the same time, after treatment we showed that there was a statistically significant increase in median nerve sensory amplitude in two groups. The increase in median nerve sensory velocity was significant in group 2 whereas it was not statistically significant between group 1 vs group 2.

Conclusions: Vitamin D replacement can improve symptoms, functional status and electrophysiological findings in CTS patients with low vitamin D levels.

Key words: Carpal tunnel syndrome, vitamin D, median nerve, neuropathy, visual analog scale, electrophysiology.

✉ Dr. Ayşe Gul Korkut

Department of Physical Medicine and Rehabilitation,
Kepez State Hospital, Antalya, Turkey

E-mail: draysegulkorkut07@gmail.com

Received: 2021-03-12 / Revisions: 2021-04-10

Accepted: 2021-06-20/ Published online: 2021-07-01

Introduction

Carpal tunnel syndrome (CTS) is characterized by chronic compression of the median nerve through the carpal tunnel at the wrist. Most of

the causes are idiopathic but diabetes mellitus (DM), thyroid disease, gout and pregnancy are known as the risk factors [1].

Conservative treatment options for CTS include avoiding repetitive hand activities; splinting; local corticosteroid injections, oral corticosteroid treatment; physical therapy modalities; nerve gliding exercises [2]. Carpal tunnel release surgery is recommended for patients with severe CTS whose symptoms

have not improved with conservative treatment [3].

Vitamin D (Vit D) is a steroid-like compound that can have hormone-like effects. Despite being known as a vitamin, it is distinguished from other vitamins as it can be synthesized in the body. Serum 25 hydroxyvitamin D (25(OH)D) levels indicate the adequate Vit D levels[4].

In recent years, the neuroprotective effects of Vit D have been emphasized in the literature. Although the mechanism of this neuroprotective effect has not been fully elucidated yet, Vit D has been shown to have an antioxidant effect and this effect may play a role in preventing neuronal necrosis, and increasing myelination by reducing the release of free radicals and blocking calcium channels [5]. Animal studies have reported that Vit D has protective effects on neurons and decreases neuronal toxicity and damage [6]. Low level of Vit D levels in CTS are reported in small number of studies however, studies in which evaluating whether CTS symptoms and signs improve after Vit D replacement is limited[1].

In this study it is aimed to evaluate the symptoms and signs of CTS after Vit D replacement in mild-to-moderate CTS patients with low Vit D levels. The study hypothesizes that both the clinical and electrophysiological findings in CTS cases with low Vit D levels will improve in the third month following the initiation of Vit D replacement therapy.

Materials and methods

This research was designed as a single-center prospective observational study. An informed consent form was signed by and obtained from all patients who volunteered to participate in the study. The study was approved by the Ethics Committee of Health Sciences University, Clinics of Physical Medicine and Rehabilitation

with the decision number 5/1, date 08/03/2018, and research number 2018-030.

Vitamin D level < 20 ng/mL was considered to be low vitamin D level. Patients aged 18–65 years with a VitD level of <20 ng/mL, who were admitted to the outpatient clinic with CTS symptoms and signs within the period from January 2018 to July 2018, were evaluated in terms of eligibility for the study.

The diagnosis of CTS was clarified based on clinical and electrodiagnostic criteria published jointly by the American Association of Electrodiagnostic Medicine (AAEM), American Academy of Neurology (AAN), and American Academy of Physical Medicine and Rehabilitation (AAPMR) in 2002 [7].

Patients, who met all clinical criteria and had electrophysiological findings supporting median neuropathy at the wrist, were accepted as definite CTS. Among patients, who received the definite CTS diagnosis and were evaluated to be mild-to-moderate CTS based on their electrophysiological findings, were included in the study. Both wrists were considered as separate patients.

Inclusion criteria of the study were being 18–65 years of age, and having mild-to-moderate CTS with a VitD level below 20 ng/mL.

Patients who were <18 and >65 years old; patients with normal VitD levels; severe or very severe CTS; comorbidities including DM, chronic renal failure, chronic liver disease, thyroid disease, rheumatoid arthritis, systemic lupus erythematosus, scleroderma, gout, polymyositis, dermatomyositis, polyneuropathy, cervical radiculopathy, brachial plexopathy, and thoracic outlet syndrome; vitamin B12 or folic acid deficiency a history of trauma; and previous carpal tunnel surgery were excluded (Figure 1).

The patients were divided into two groups according to their VitD level. In Group 1

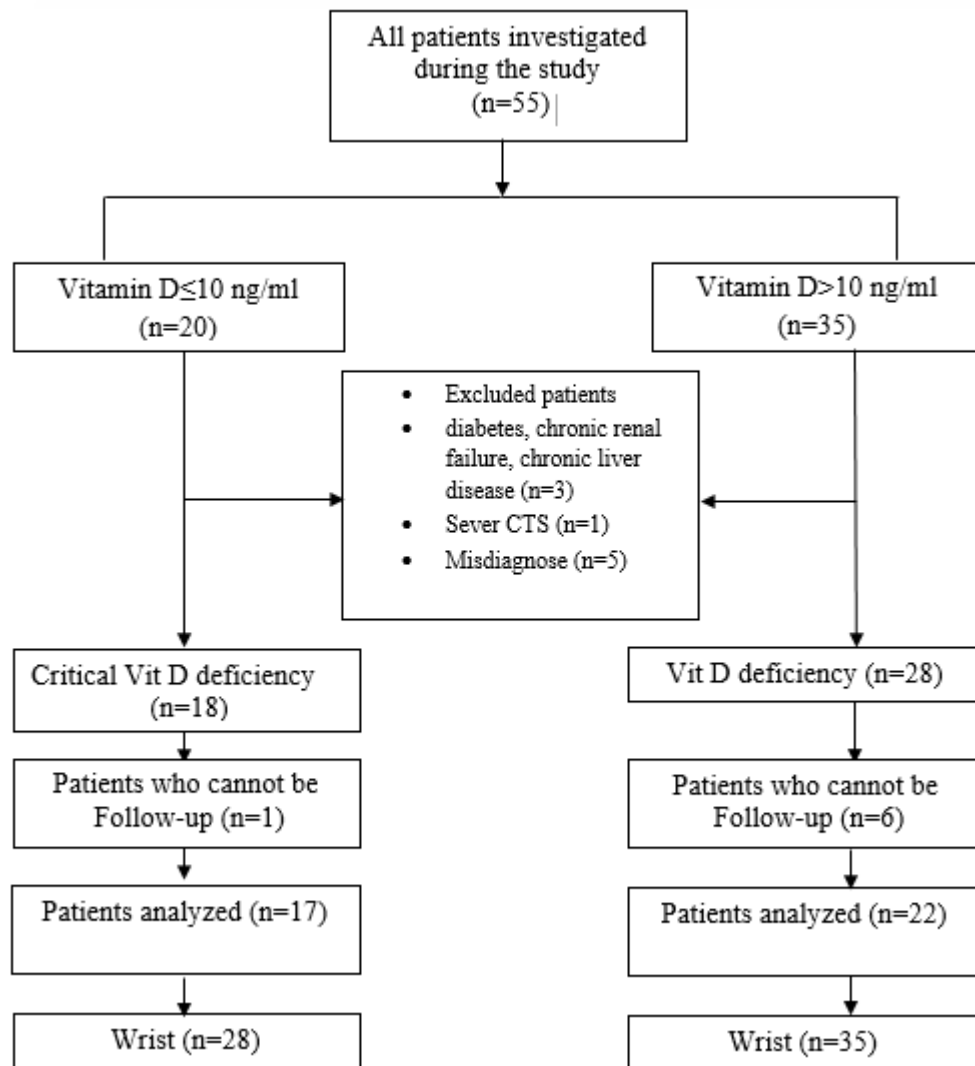


Figure 1. Patient flow chart.

patients with a VitD level of <10 ng/mL (Critical VitD deficiency) and in Group 2 patients with a VitD level of 10–20 ng/mL (VitD deficiency) were included. Splinting is recommended for all patients and VitD replacement therapy were applied in both groups. Cholecalciferol (vitamin D3) were given orally at a loading dose of 50,000 IU/week for eight weeks as VitD replacement therapy. Afterward, the maintenance dose was given as 3000–6000 IU/day. During the 3-month follow up period, patients did not receive any physical therapy or median nerve injection therapy.

Biochemical analysis

Laboratory examinations, including a screening analysis of 25(OH)D levels, were performed using venous blood specimens. All serum 25(OH)D (ng/mL) concentrations were analyzed using electrochemiluminescence immunoassay (ECLIA) technique with LIAISON analyzer (DiaSorin, Stillwater, MN).

Evaluation of peripheral neuropathy and pain

At baseline sociodemographic characteristics (age, gender, weight, height, occupation, hand dominance, disease duration) of the patients were recorded. (Table 1). The quick disabilities

of the arm, shoulder, and hand questionnaire (QuickDASH) was used to assess symptom severity, pain, and functional capability in the hand, while the pain intensity was assessed by visual analog scale (VAS). Patients completed these questionnaires at the beginning of the study and in the third month following the initiation of replacement therapy.

Visual analogue scale (VAS)

Patients were asked to rate their severity of hand or wrist pain on a 10-cm-long straight line with numbers, ranging from 0 to 10. Before the application, it was explained that the value 0 represented no pain and the value 10 represented the most severe pain they had ever felt.

Quick disabilities of the arm, shoulder, and hand questionnaire (QuickDASH)

This self-reported questionnaire was developed by the American Academy of Orthopaedic Surgeons (AAOS) in 1994 based on the model developed by the World Health Organization (WHO). It measures physical function and symptoms of patients suffering from upper extremity problems. The questionnaire contains disability/symptom scale (11 items) and 2 optional scales (work (4 items) and sports/performing arts (4 items)). Each question is scored between 1 and 5. Each subscales ranged between 0 (no disability) and 100 (most severe disability). The reliability and validity of the Turkish version of the questionnaire in patients with CTS was conducted by Koldaş Doğan Ş et al.[8] among patients with CTS. It is completed in about five to seven minutes, with moderate ease of scoring [9].

Measurement of grip and pinch strength

Grip and pinch strengths were measured at the beginning of the study and at the third month of

treatment. An electronic hand dynamometer [Electronic Hand Dynamometer (HS-005), China] was used to measure grip strength whereas finger grip strength was measured using a manual pinchmeter (Sammons Preston, Inc. Bolingbrook, IL 60440-4989). The results were recorded in kilograms (kg). Handgrip strength measurements were performed while the patient was in the sitting position, the arm was in adduction, the forearm was in 90° flexion and neutral position, and the wrist was in 0–30° extension and 0–15° ulnar abduction position. Patients were asked to give full maximum voluntary effort grip [10]. In the test procedure, a total of three measurements were made by taking a break between each measurement for grip and pinch strengths and their averages were recorded [11, 12].

Electrophysiological evaluation

All electrophysiological evaluations were performed using Nihon Kohden Neuropack S1 MEB-9400K EMG Device (Tokyo, Japan). All patients were evaluated electrophysiologically at the beginning of the treatment and at the third month of treatment. All nerve conduction studies were performed by the same physician using bipolar superficial electrodes, the same device, and standard technique, in accordance with the relevant guidelines. Median and ulnar sensory nerve conduction and distal (wrist) and proximal (elbow) motor nerve conduction were studied on the one hand, and median sensory nerve conduction and distal and proximal motor nerve conduction were studied on the other hand [13, 14].

Statistical analysis

Statistical analysis was performed using SPSS version 20.0 software (IBM Corporation, Armonk, NY, USA). Using the G-Power analysis, the sample size was calculated by

taking the power as 90%, alpha value as 0.05, and effect value as 0.2. To the best of our knowledge, there were no studies evaluating Vit D replacement therapy in line with the purpose of this study. Therefore, studies comparing the VAS score and CTS severity of mild-to-moderate CTS patients with low and normal Vit D levels were utilized to calculate the effect value. The Shapiro–Wilk test was used to determine whether the groups followed a normal distribution. Descriptive data were

expressed as mean, standard deviation, median, highest and lowest values, frequency, and ratio. The means of variables following normal distribution were compared using Student's t-test. In variables not following a normal distribution, the Wilcoxon signed-rank test was used for dependent groups whereas the Mann–Whitney U test test was used for independent groups. Chi-Square and McNemar tests were used in categorical variables. A *p* value of <0.05 was considered statistically significant.

Tablo 1. Demographic status of the patients.

Parameters	Group 1 Critical Vit D deficiency (n=17)	Group 2 Vit D deficiency (n=22)	P
Wrist	28	35	
Age (years) (mean±SD)	47.82±8,47	46.14±8,46	0.541 ^a
Gender (n, %)			0.202 ^b
Female	17 (100)	20 (90.9)	
Male	0 (0.0)	2 (9.1)	
Working status (n, %)			0.907 ^b
Work	5 (29.4)	7 (31.8)	
Not working	11 (64.7)	13 (59.1)	
Retired	1 (5.9)	2 (9.1)	
Length (cm) (mean±SD)	158.59±6.12	159.18±6,58	0.775 ^a
Weight (kg) (mean±SD)	72.12±12.22	70.59±14.23	0.460 ^c
BMI (kg/m ²) (mean±SD)	28.49±5.63	27.62±4.07	0.580 ^a
Symptom time (month) (mean±SD)	5.65±2.89	4.59±2.44	0.177 ^c
Dominant hand (n, %)			0.425 ^b
Right	13 (76.5)	19 (86.4)	
Left	4 (23.5)	3 (1.6)	
Symptomatic hand (n, %)			0.159 ^b
Right	6 (35.3)	5 (22.7)	
Left	0 (0.0)	4 (18.2)	
Bilaterally	11 (64.7)	13 (59.1)	

a; Student T test was used. Mean±Standart deviation (SD) was shown. b; Chi-square test was used.

c; Mann-Whitney U was used. Mean±Standart deviation (SD) was shown.

Results

At the initial phase of the study, a total of 55 patients meeting the inclusion criteria were included. Nine patients were excluded due to the presence of exclusion criteria and seven patients were excluded from the study because they did not come for post-treatment controls.

A total of 63 wrists were included in the analyses. All of these patients were given Vit D replacement. The patient flow chart is shown in Figure 1. The mean age of the patients was 46.87 ± 8.39 years. The symptom duration of the patients was 5.65 ± 2.89 and 4.59 ± 2.44 months in Group 1 and Group 2, respectively. Demographic characteristics of the patients were given in Table 1

In both groups, Vit D levels were observed to be statistically significantly increased in posttreatment compared to baseline ($p=0.000$ and $p=0.000$ for Group 1 and Group 2, respectively). Similarly, there were statistically significant decreases in VAS scores in both groups after treatment (VAS day/night $p=0.021$, $p=0.012$, $p=0.000$, and $p=0.000$ for Group 1 and Group 2, respectively). In both

groups, statistically significant decreases were found in the QuickDASH symptom and job subscores measured after treatment compared to pre-treatment ($p=0.000$ and $p=0.002$; $p=0.000$ and $p=0.000$ for Group 1 and Group 2, respectively). There were also statistically significant differences between groups in terms of grip and pinch strengths after treatment compared to pre-treatment ($p=0.026$ and $p=0.030$). At Post-treatment grip strengths of both groups were increased compared to pre-treatment values ($p=0.003$ and $p=0.000$ for Group 1 and Group 2, respectively). There was no statistically significant difference in the pinch strengths ($p=0.892$ and $p=0.079$ for Group 1 and Group 2, respectively) between the groups. The rate of patients whose VitD levels returned to normal after treatment was 10.7% in Group 1 and 22.7% in Group 2. This improvement rate was found to be statistically significant ($p=0.012$ and $p=0.039$ for Group 1 and Group 2, respectively). The pre and posttreatment values of the pain severity and functional status of the patients were given in Table 2.

Table 2. Comparison between the patients of functional and pain scores before and after vitamin D replacement.

Parameters	Group 1 Critical Vit D deficiency (n=17)		Group 2 Vit D deficiency (n=22)		P1	P2	P3	P4
	Before Treatment (BT)	After, Treatment (AT)	Before Treatment (BT)	After, Treatment (AT)				
Variable (mean \pm SD)					Group1 BT vs AT	Group2 BT vs AT	Group 1vs Group 2 for BT	Group 1 vs Group 2 for AT
Vit. D Level (ng/mL)	7.29 \pm 1.96	19.52 \pm 4.72	17.09 \pm 3.11	25.62 \pm 5.35	0.000 ^b	0.000 ^b	0.000 ^a	0.001 ^a
Quick Dash Score	55.86 \pm 9.12	48.77 \pm 8.95	51.55 \pm 8.93	44.70 \pm 10.41	0.000 ^b	0.002 ^b	0.148 ^a	0.207 ^a
Quick Dash work model	46.69 \pm 11.92	42.77 \pm 9.80	43.58 \pm 12.50	36.65 \pm 12.98	0.000 ^b	0.000 ^b	0.438 ^a	0.114 ^a
Grip strengths (kg)	20.36 \pm 5.72	22.50 \pm 4.76	22.86 \pm 5.58	25.63 \pm 5.84	0.003 ^b	0.000 ^b	0.086 ^a	0.026 ^a
Pinch strengths (kg)	5.48 \pm 1.52	5.43 \pm 1.50	5.71 \pm 1.99	6.26 \pm 1.45	0.892 ^b	0.079 ^b	0.613 ^a	0.030 ^a
VAS (morning)	2.88 \pm 0.99	2.35 \pm 0.77	2.95 \pm 1.09	1.91 \pm 1.31	0.021 ^d	0.000 ^d	0.906 ^c	0.930 ^c
VAS (Night)	5.35 \pm 1.06	4.59 \pm 0.80	5.41 \pm 1.14	4.05 \pm 1.53	0.012 ^d	0.000 ^d	0.342 ^c	0.325 ^c
Mild CTS (n, %)	12(42.9)	3 (10.7)	16(45.7)	8 (22.7)	0.012 ^c	0.039 ^c	0.821 ^c	0.354 ^e
Moderate CTS (n, %)	16(57.1)	7 (25.0)	19(54.3)	10 (28.6)				
Improved CTS (n, %)		18 (64.3)		17 (48.6)				

a; Student T test was used. b;T test was used at the dependent groups. c;Mann-Whitney U was used. d;Wilcoxon Test was used. e: Chi-square and Mc Nemar test test was used. CTS: Carpal Tunnel Syndrome Mean \pm Standart deviation (SD) was shown.

There was no statistically significant difference between the two groups in terms of pre-treatment and post-treatment electrophysiological findings. Only median nerve sensory amplitude (SA) and sensory conduction velocity (SCV) were increased in both groups. A statistically significant increase was found in the median nerve SA after treatment compared to before treatment in both groups ($p=0.043$ and $p=0.017$ for Group 1 and Group 2, respectively). The increase in median nerve SCV was significant in Group 2 whereas it was not statistically significant in Group 1 ($p=0.168$ and $p=0.036$ for Group 1 and Group 2, respectively). Table 3 shows the changes in electrophysiological findings before and after treatment.

Discussion

Several studies have shown that patients with CTS have lower Vit D levels. While Vit D deficiency has been reported to increase the severity of pain in CTS cases in a study, low Vit D levels have been suggested to trigger CTS signs and symptoms in another study [15-17].

In a study by Nageeb et al. [18] involving 50 patients with CTS and 50 healthy individuals, in which the effects of Vit D level on CTS was investigated, the authors compared the Vit D levels of patients with severe CTS and patients with mild-to-moderate CTS and found that Vit D levels were significantly lower in those with severe CTS. There are studies indicating that Vit D has protective effects on neurons and decreases neuronal toxicity and damage by suppressing the cytokine pathway [19]. In a study by Shebab et al. [20] in 2015 investigating the effects of Vit D on peripheral neuropathy, 112 patients with type II DM accompanied by peripheral neuropathy were given 50,000 IU cholecalciferol once a week for eight weeks and the authors reported a significant increase in Vit D levels and a significant improvement in neuropathy symptom scores in the treatment group compared to the placebo group at the end of eight weeks.

In a recent study by Sacmaci et al. [21], Vit D values of patients with moderate CTS were reported to improve at the end of the third

Table 3: Comparison between the patients of the electrophysical evaluations before and after vitamin D replacement.

Parameters	Group 1 Critical vit.D deficiency (n=17)		Group 2 vit.D deficiency (n=22)		P1	P2	P3	P4
	Before Treatment (BT)	After, Treatment (AT)	Before Treatment (BT)	After, Treatment (AT)				
Median Nerve DML (ms)	4.03±0.80	4.17±0.72	37.72±4.49	39.14±6.02	0.061 ^c	0.277 ^c	0.857 ^b	0.323 ^b
Median nerve MA (m/s)	13.06±4.93	12.88±4.13	14.72±4.63	14.50±3.73	0.001 ^d	0.000 ^d	0.719 ^a	0.851 ^a
Median Nerve MCV (ms)	60.24±6.15	57.50±6.08	58.63±6.51	57.77±5.07	0.750 ^d	0.373 ^d	0.175 ^a	0.605 ^a
Median Nerve DSOL (ms)	3.20±0.42	3.24±0.47	3.27±0.47	3.30±0.51	0.707 ^c	0.353 ^c	0.538 ^b	0.771 ^b
Median Nerve SA(mV)	17.16±6.88	18.30±6.59	18.44±8.96	19.34±8.91	0.043 ^d	0.017 ^d	0.643 ^b	0.606
Median Nerve SCV (m/s)	38.18±3.89	39.03±3.78	3.96±0.70	4.03±0.75	0.168 ^c	0.036 ^c	0.841 ^b	0.934 ^b

a; Student T test was used. b; Mann-Whitney U was used. c; Wilcoxon Test was used. d; T test was used at the dependent groups. Mean ±Standard deviation (SD) was shown. DSOL: Distal Sensory Onset Latency. DML: Distal motor latency. MCV: Motor Conduction velocity. SCV: Sensory Conduction Velocity SA: sensory amplitude. MA: motor Amplitude.

month after replacement therapy compared to pre-treatment. Similar to this study, we found a statistically significant increase in post-treatment Vit D levels of both groups. Akyuz et al. [22] reported a significant improvement in pain and quality of life after eight-weeks of Vit D treatment in patients with chronic widespread pain; however, they further examined the patients electrophysiologically and did not identify any significant changes in nerve conduction studies following the Vit D supplementation. In a study by Sacmaci et al. [21] involving 50 female patients (45 wrists with mild CTS and 37 wrists with moderate CTS), an improvement was observed in both groups after treatment compared to pre-treatment. Consistent with these findings, in the present study, a statistically significant improvement was observed in both day and night VAS scores of both groups after the treatment.

Measuring the grip strength in CTS cases is important for the evaluation of the patients. Gumieiro et al. [23] showed that individuals suffering from Vit D insufficiency had insufficient grip strength. In the present study, the grip strength of patients in both groups was increased after treatment and increase in Group 2 is significantly greater than in Group 1 which can be interpreted as less muscle strength loss since patients in Group 2 have higher Vit D levels. Post-treatment pinch strength was observed to decrease in Group 1, whereas it increased in Group 2; however, this increase in Group 2 was not statistically significant. While the pre-treatment QuickDASH scores were similar in both groups, there were statistically significant decreases after treatment in both groups, and there was no significant difference between the groups.

In a study investigating the effect of Vit D on peripheral neuropathy, the authors divided

patients with DM accompanied by polyneuropathy into treatment and placebo groups and evaluated them electrophysiologically after eight weeks of Vit D treatment. The treatment group was observed to have lower values in median nerve motor and sensory distal latencies, higher values in median nerve SCV and median nerve motor and SAs, and lower values in the median nerve motor conduction velocity (MCV) compared to the placebo group. None of these differences were found to be statistically significant [20]. In a study examining Vit D levels of CTS patients, Vit D levels were found to have a positive correlation with MCV and a negative correlation with distal motor latency (DML). In the same study, CTS patients were classified as mild, moderate, and severe, and patients with severe CTS were observed to have the lowest Vit D levels [18]. A similar study was conducted by Tanik et al. [24], in which the authors found a positive correlation between the severity of Vit D deficiency and the severity of CTS. In a study by Sacmaci et al. [21], involving 50 female patients (45 wrists with mild CTS and 37 wrists with moderate CTS), an improvement in nerve conduction values was reported in both groups. Shortening in median nerve distal sensory onset latency (DSOL) and an increase in SCV were found to be statistically significant in the mild CTS group. In the moderate CTS group, an increase in SA and SCV and a shortening in DML were found to be significant. In the present study, an increase was found only in the median nerve SA and SCV in both groups. A statistically significant increase was found in the post-treatment median nerve SA in both groups. It was observed that SCV showed a statistically significant increase only in Group 2. The positive effect of Vit D on both myelination and axonogenesis, which has been shown in

animal studies, is compatible with the results presented here [6, 25]. However, we attribute the presence of a more significant increase in SCV only in Group 2 to the fact that the patients in this group have higher Vit D levels. In Group 1 with lower Vit D levels, mild and moderate CTS rates were 42.9% and 57.1%, respectively, whereas these rates were found to be 45.7% and 54.3% in Group 2, respectively. This difference between the two groups was not statistically significant. Post-treatment findings were found to be normal in 10.7% of Group 1 and 22.7% of Group 2. Similarly, the reason for the higher rate of normal findings in Group 2 may be that the patients in this group have higher Vit D levels.

One of the important limitations of this study is that as required by routine treatment, all patients were given hand-wrist splint in addition to Vit D replacement therapy. The absence of a control group that obtained either a hand-wrist splint or a placebo group makes evaluating the efficacy of Vit D difficult. Furthermore, the inclusion of a small number of patients and a short follow-up period are other limitations. There is a need for studies with longer follow-up periods, particularly for electrophysiological evaluations.

Conclusions

In CTS patients with low Vit D levels, Vit D replacement therapy can reduce symptoms and improve functional status, as well as electrophysiological findings. When the subgroups are evaluated according to the severity of Vit D deficiency, those with higher Vit D levels show more improvement in terms of pain, functional status, and electrophysiological findings. Prospective randomized-controlled trials with longer treatment and follow-up periods, in which the efficacy of Vit D in CTS patients is evaluated are needed.

Funding: *The author(s) received no financial support for the research, authorship, and/or publication of this article.*

Conflict of Interest: *The authors declare that they have no conflict of interest.*

Ethical statement:

The study was approved by Local Clinical Research Ethics Committee (Decision number 5/1, Date 08/03/2018, and Research number 2018-030), and written informed consent was obtained from each subject.

Open Access Statement

This is an open access journal which means that all content is freely available without charge to the user or his/her institution under the terms of the Creative Commons Attribution Non-Commercial License (<http://creativecommons.org/licenses/by-nc/4.0>). Users are allowed to read, download, copy, distribute, print, search, or link to the full texts of the articles, without asking prior permission from the publisher or the author.

References

- [1]Lee MH, Gong HS, Lee MH, et al. The Effect of Vitamin D Deficiency Correction on the Outcomes in Women After Carpal Tunnel Release. *J Hand Surg.* 2019;44(8):649-54.
- [2]Afşar Sİ, Sarıfakıoğlu B, Yalbuздаğ ŞA. Karpal Tünel sendromu tedavisinde fizik tedavi modalitelerinin yeri: Derleme. *Turkish J Osteoporosis.* 2014;20(3):125-31.
- [3]Ren Y-M, Wang X-S, Wei Z-J, et al. Efficacy, safety, and cost of surgical versus nonsurgical treatment for carpal tunnel syndrome: a systematic review and meta-analysis. *Medicine.* 2016;95(40):e4857.
- [4]Hastalıkları Mk. Osteoporoz Ve Metabolik Kemik Hastalıkları Tani Ve Tedavi Kilavuzu. 2016.

- [5] DeLuca G, Kimball S, Kolasinski J, et al. The role of vitamin D in nervous system health and disease. *Neuropathol Appl Neurobiol.* 2013;39(5):458-84.
- [6] Chabas J, Stephan D, Marqueste T, et al. Cholecalciferol (Vitamin D3) Improves Myelination and Recovery after Nerve. 2013. *PLOS ONE* 8(5): e65034.
- [7] Jablecki C, Andary M, Floeter M, et al. Practice parameter: electrodiagnostic studies in carpal tunnel syndrome: report of the American Association of Electrodiagnostic Medicine, American Academy of Neurology, and the American Academy of Physical Medicine and Rehabilitation. *Neurology.* 2002;58(11):1589-92.
- [8] Dogan SK, Ay S, Evcik D, et al. Adaptation of Turkish version of the questionnaire Quick Disability of the Arm, Shoulder, and Hand (Quick DASH) in patients with carpal tunnel syndrome. *Clinical rheumatology.* 2011;30(2):185-91.
- [9] Gummesson C, Ward MM, Atroshi I. The shortened disabilities of the arm, shoulder and hand questionnaire (Quick DASH): validity and reliability based on responses within the full-length DASH. *BMC Musculoskeletal Disorders.* 2006;7(1):1-7.
- [10] Narin S, Demirbüken İ, Özyürek S, et al. Dominant el kavrama ve parmak kavrama kuvvetinin önkol antropometrik ölçümlerle ilişkisi. *Dokuz Eylül Üniversitesi Tıp Fakültesi Dergisi.* 2009;23(2):81-85.
- [11] Mathiowetz V, Kashman N, Volland G, et al. Grip and pinch strength: normative data for adults. *Arch Phys Med Rehabil.* 1985;66(2):69-74.
- [12] Bircan C, El O, Akalin E, et al. Functional outcome in patients with zone V flexor tendon injuries. *Arch Orthop Trauma Surg.* 2005;125(6):405-9.
- [13] Medicine AAoE. AAEM Practice topic in electrodiagnostic medicine. *Muscle Nerve.* 2002;25:918-22.
- [14] Preston DC, Shapiro BE. *Electromyography and neuromuscular disorders e-book: clinical-electrophysiologic correlations (Expert Consult-Online): Elsevier Health Sciences;* 2012.
- [15] Demiryurek B, Gundogdu A. The effect of vitamin D levels on pain in carpal tunnel syndrome. *Orthop Traumatol Surg Res.* 2017;103(6):919-22.
- [16] Gürsoy AE, Bilgen HR, Dürüyen H, et al. The evaluation of vitamin D levels in patients with carpal tunnel syndrome. *Neurological Sciences.* 2016;37(7):1055-61.
- [17] Lee SH, Gong HS, Kim D, et al. Evaluation of vitamin D levels in women with carpal tunnel syndrome. *J Hand Surg. (European Volume).* 2016;41(6):643-7.
- [18] Nageeb RS, Shehta N, Nageeb GS, et al. Body mass index and vitamin D level in carpal tunnel syndrome patients. *Egypt J Neurol Psychiatr Neurosurg.* 2018;54(1):1-7.
- [19] Chabas J-F, Alluin O, Rao G, et al. Vitamin D2 potentiates axon regeneration. *J Neurotrauma.* 2008;25(10):1247-56.
- [20] Shehab D, Al-Jarallah K, Abdella N, et al. Prospective evaluation of the effect of short-term oral vitamin D supplementation on peripheral neuropathy in type 2 diabetes mellitus. *Med Princ Pract.* 2015;24(3):250-6.
- [21] Sacmaci H, Tanik N, Balbaloglu Ö, et al. Electrophysiological evaluation of carpal tunnel syndrome female patients after vitamin D replacement. *Arq Neuropsiquiatr.* 2020;78(4):224-9.
- [22] Akyuz G, Sanal-Toprak C, Yagci I, et al. The effect of vitamin D supplementation on pain, quality of life, and nerve conduction

studies in women with chronic widespread pain. *Int J Rehabil Res.* 2017;40(1):76-83.

[23] Gumieiro DN, Rafacho BPM, Pereira BLB, et al. Vitamin D serum levels are associated with handgrip strength but not with muscle mass or length of hospital stay after hip fracture. *Nutrition.* 2015;31(7-8):931-34.

[24] Tanik N, Balbaloglu Ö, Ucar M, et al. Does vitamin D deficiency trigger carpal tunnel syndrome? *J Back Musculoskelet Rehabil.* 2016;29(4):835-39.

[25] Montava M, Garcia S, Mancini J, et al. Vitamin D3 potentiates myelination and recovery after facial nerve injury. *Eur Arch Otorhinolaryngol Suppl.* 2015;272(10):2815-23.

Relationship between osteoarthritis findings in knee radiography and meniscus lesion in magnetic resonance imaging in symptomatic knee pain cases

Melike Elif Kalfaoglu,  Zeliha Cosgun,  Emine Dagistan 

Department of Radiology, Bolu Abant Izzet Baysal University, Faculty of Medicine, Bolu, Turkey

ABSTRACT

Aim: Knee osteoarthritis is a very common joint disease in the community. However, some meniscus lesions are asymptomatic. Studies show that a significant number of individuals with knee pain without radiographic osteoarthritis findings show meniscus injury on magnetic resonance imaging (MRI). Our study aimed to evaluate the relationship between meniscus lesions and the presence of radiographic knee osteoarthritis in individuals over 50 years of age with knee pain complaints.

Methods: Radiographic and MRI results of two hundred and forty patients who applied to our hospital with the complaint of knee pain between August 2018 and January 2020 were analyzed. Radiographic grading for knee osteoarthritis was performed using the Kellgren Lawrence scale. Classification of meniscus lesions in MRI was made as per the criteria defined by the British Knee Meniscus Surgery Association. Intergroup results were evaluated statistically.

Results: Osteoarthritis was detected in 110 (45.8%) of 240 knee radiographs. In 78.3% of all cases, meniscus lesions were detected in 96.4% of those with osteoarthritis and 63% of those without osteoarthritis. In patients with osteoarthritis, the prevalence of surgically targeted and possible target lesions was found to be significantly higher than those with no arthritis findings.

Conclusions: According to our study results, meniscus lesions were found quite common in individuals with knee pain, especially those with osteoarthritis. Particularly in patients with radiographic osteoarthritis findings, surgical targets and possible target meniscus lesions were more common than those without osteoarthritis findings. Therefore, MRI, in addition to direct radiography, should not be overlooked when determining treatment.

Key words: Osteoarthritis, meniscus lesions, radiography, magnetic resonance imaging.

✉ Dr. Melike Elif Kalfaoglu

Department of Radiology, Bolu Abant Izzet Baysal University, Faculty of Medicine, Bolu, Turkey

E-mail: melikekalfaoglu@hotmail.com

Received: 2021-05-18

Accepted: 2021-06-16/ Published online: 2021-07-01

Introduction

Osteoarthritis (OA) is very common in the population. It is a significant cause of morbidity, especially in the elderly population, and the knee is one of the most commonly

affected joints. Osteoarthritis causes loss of working time by making it difficult to do many daily activities and is among the top ten causes of disability [1,2]. Approximately 25% of people over the age of 50 suffer from knee pain due to degenerative knee disease [3]. In daily practice, non-traumatic knee pain of a middle-aged or elderly patient is often associated with knee OA. However, some meniscus lesions have been reported asymptomatic in this age group [4].

Extensive scientific research performed in recent years has revealed the anatomical, biomechanical, and functional importance of the meniscus in the knee joint. As a vital part of the joint, it acts to prevent the disruption and degeneration of articular cartilage and the onset and development of OA [6]. Studies show that an *Magnetic resonance imaging (MRI)* reveals meniscus injury in a significant number of individuals with knee pain without radiographic OA findings [6,7]. Menisci are rarely normal in patients with knee OA, and there is a strong relationship between knee OA and meniscus pathologies. The relationship between meniscus damage and knee OA is complex. Meniscus lesions developing in a healthy knee may eventually lead to OA. Meniscus lesions may result from knee OA or might be the cause [8,9]. The distinctive structural feature of OA is the loss of joint cartilage. Although there is a weak correlation between the findings and clinical symptoms, direct radiographs are the first choice for OA imaging, including follow-up. However, since the narrowing of the joint distance is an indirect indicator of the state of the articular cartilage and radiographs are two-dimensional, they provide limited information in evaluating three-dimensional joint structures [10,11]. Studies have shown that OA is a disorder involving other knee joint tissues, such as subchondral bone, ligaments, synovial membrane, muscle, and meniscus. Therefore, with its cross-sectional imaging, high spatial resolution, high tissue contrast, and multiplanar imaging features, MRI allows the evaluation of all pathologies belonging to the structures that make up the knee joint [12,13].

Our study aimed to evaluate the relationship between OA findings in knee radiography and meniscus lesions in MRI in symptomatic knee pain cases.

Materials and methods

The Abant Izzet Baysal University, Clinical Research Local Ethics Committee (27.10.2020: 2020/253) provided ethical approval. The examinations of 318 patients between the ages of 50 and 79 who had knee radiography and knee MRI and were admitted to our hospital between August 2018 and January 2020 with pain complaints were examined.

The study included 240 cases and excluded seventy-eight cases with a history of knee trauma (n=26), Body mass index (BMI) of >30 (n=19), anterior cruciate ligament tear (n=16), and previous knee surgery (n=17). The demographic data of the patients were evaluated retrospectively using the PACS system (picture archiving and communication system) of our hospital. A radiologist with ten years of experience interpreted antero-posterior knee radiographs and knee MRIs obtained in standing positions.

Radiographic grading for knee OA was performed using the Kellgren Lawrence scale (KL) [14]. The levels were Grade 0: Normal; Grade 1: Suspected joint narrowing, possible osteophytic sharpening; Grade 2: Possible joint narrowing, marked osteophytes; Grade 3: Definite joint distance narrowing, mild sclerosis, small pseudocystic areas, multiple osteophytes; and Grade 4: Severe narrowing of the joint distance, intense sclerosis and irregularity in the joint surface, and large osteophytes.

Cases with a degree of ≥ 2 according to KL were considered positive for OA. All MRI examinations were performed with a 1.5 T MRI device (Symphony; Siemens, Erlangen, Germany). Section thickness was 4 mm. Images were obtained as T1-weighted images (repeat time (TR)/echo time (TE) = 473/14 ms), T2-weighted images (TR/TE = 3760/68 ms),

and PD-weighted images (TR/TE=2760/23 ms).

Classification of meniscus lesions in MRI was made as per the criteria defined by the British Knee Meniscus Surgery Association. Accordingly, meniscus lesions were classified as: 1) target lesion (surgically treatable): bucket handle tear, displaced meniscus tear, meniscus root insufficiency; 2) possible target lesion (unclear; may require surgical treatment): radial tear, horizontal tear ± cyst, complex tear, short longitudinal tear; and 3) non-target lesion (possibly untreatable, meniscus surgery is not necessary): contour abnormality, isolated meniscus extrusion.

Statistical analysis

Data were analyzed using the SPSS 15.0 program. The Mann-Whitney U test compared the numerical data of the two independent groups, and the Pearson chi-square test evaluated the relationship between categorical variables. A p-value of <0.05 was considered statistically significant.

Results

A total of 240 patients were involved in the study. One hundred forty-nine of the patients were female, and 91 were male. The mean age of those with radiographic findings of OA was 60±6.7 years, and the mean age of those without OA findings was 54±5.4 years.

Osteoarthritis was detected in 110 (45.8%) of 240 knee radiographs. We detected meniscus lesions in 96.4% (n=106) of those with OA and 63% (n=82) of those without OA, in 78.3% of all cases (Table 1). In patients with knee OA, the prevalence of surgically targeted and possible target lesions was significantly higher than those with no OA findings (Figure 1). Target and possible target lesions were detected in approximately 49% of the cases without radiographically discovered OA. The most common lesions observed were horizontal and complex meniscus tears, respectively (Figure 2 and 3).

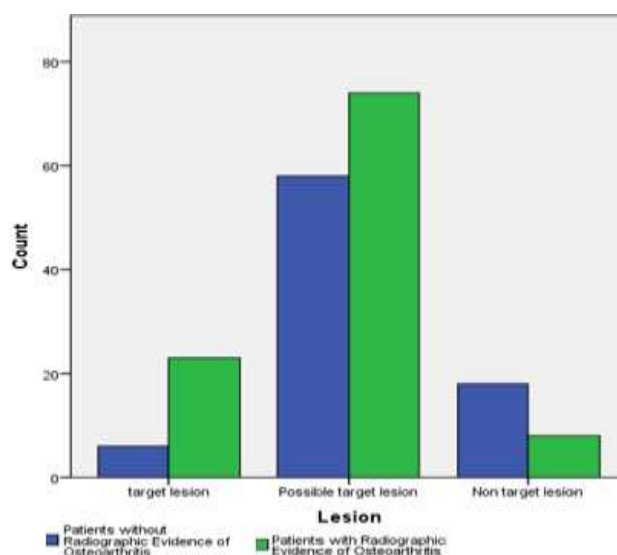


Figure 1. The prevalence of the meniscus lesion types according to the presence or absence of radiographic evidence of the knee osteoarthritis.

Table 1. The distribution of the meniscal lesions according to whether there is radiographic evidence of the knee osteoarthritis or not.

MRI meniscus lesion types	Patients with Radiographic evidence of osteoarthritis (n=110)	Patients without Radiographic evidence of osteoarthritis (n=130)	P Value
Target lesion	23 (20.9)	6 (4.6)	0.001
Possible target lesion	74 (67.3)	58 (44.6)	0.001
Non-target lesion	9 (8.2)	18 (13.8)	0.166
Total	106 (96.4)	82 (63.07)	0.001

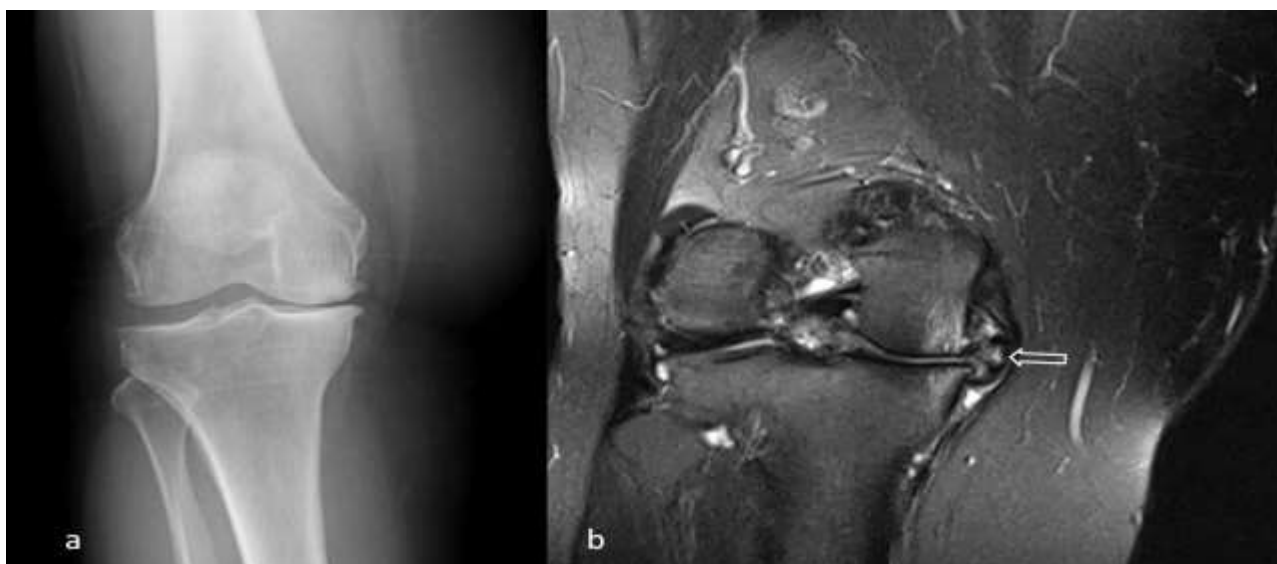


Figure 2. Anteroposterior radiograph of the right knee of a 54-year-old woman with knee pain shows Kellgren Lawrence grade 3 changes (a). A displaced medial meniscus tear (open arrow) is seen on the coronal T2 weighted magnetic resonance image of the same patient (b).



Figure 3. Anteroposterior radiograph of the right knee of a 52-year-old woman with knee pain shows Kellgren Lawrence grade 1 changes (a). A Horizontal tear and meniscus cyst (open arrow) are seen on the coronal T2 weighted magnetic resonance image of the same patient (b).

Discussion

Our study found the prevalence of surgical target and possible target lesions to be higher in patients over 50 years of age with radiographic knee OA compared to those without OA. The most common target lesion observed in patients with and without OA was meniscus root insufficiency, and possible target lesions were

horizontal and complex meniscus tears, respectively. The rate of meniscus tears was high in both groups. These findings show us that MRI should be performed in addition to direct radiography when determining treatment. Root tear was the most common lesion we found, with 13.6% of those having radiographic OA findings. Root tears have been shown to

disrupt knee joint dynamics by causing meniscus extrusion and OA [16]. The low incidence of root tears in our group without radiographic OA supports this finding.

Meniscus tears are asymptomatic in elderly individuals and quite common in those with knee OA and correlated with the degree of OA. Studies have shown that meniscus tears do not significantly affect pain and function in patients with OA. Meniscus tears have been reported in up to 65% of asymptomatic individuals evaluated by MRI [17]. Controversial results have been obtained regarding whether knee pain is secondary to OA or meniscus tear. Englund et al. showed that meniscus lesions are quite common in individuals with knee pain, especially those with OA, increasing with age [4,17]. Our study detected meniscus lesions in 63% of those without OA and 96% of those with OA. According to the literature, the reason for our higher meniscus lesion rates may be our higher mean age. These results suggest that knee OA increases meniscus injury.

The frequency of meniscus injuries in the general population is approximately 12-14%. Although traumatic meniscus tears are associated with sports injuries in younger age groups, age-related degenerative tears constitute 30% of meniscus tears and, unlike acute tears, may be unrelated to trauma [18]. Meniscus tears can be treated with conservative treatment, surgical repair, or partial or complete meniscectomy [19]. The general tendency is to apply physical therapy/rehabilitation and non-surgical treatment, especially in the OA group. It is essential to define the morphology of the tear well with MRI as it will affect the decision regarding surgical treatment.

While surgical repair is possible in horizontal tears, meniscus root tears—which are relatively rare in the general population—are lesions that constitute approximately 10.1% of arthroscopic

meniscectomies. An MRI is usually required to identify root tears. In our study, the most common target lesion we detected in patients with radiographic OA was meniscus root tear, and it was observed in 13.6% of the patients. Root tears may cause extrusion of the meniscus body relative to the joint and also significantly weaken the ability of the meniscus to dissipate circumferential stress. As a result, it increases contact forces along the joint, causing OA and predisposing the patient to the development of cartilage damage [16]. In our study, statistically more root tears were observed in patients with OA, which is consistent with the literature's information.

The literature reports that meniscus extrusion is associated with the development and progression of OA [20].

Studies show that meniscus extrusion is evident in middle-aged individuals without knee OA [21]. These results suggest that meniscus extrusion is common not only in individuals with knee OA but also in those without OA findings. In line with these data, we found that meniscus extrusion was the most common non-target lesion in our patient population, both in the group with and without knee OA.

The most important limitation of this study is that the imaging findings were not evaluated together with clinical findings, and the imaging findings were evaluated by a single radiologist. Therefore, more comprehensive studies that evaluate clinical and radiological findings together are needed to support the findings of the present study.

Conclusions

The menisci play a critical role in the knee joint. Meniscus tears can cause knee OA, and knee OA can also cause a meniscus tear. Although radiographs are the first imaging methods used to evaluate knee OA, MRI is required for

evaluating meniscus lesions and defining tear morphology. A meniscus lesion detected in a middle-aged or elderly patient may be an indication of early-stage OA. There are different approaches in the treatment of meniscus tears depending on the type of tear. Detection of meniscus lesions on MRI and a good definition of the tear type constitute critical parameters in determining conservative or surgical treatment.

Magnetic resonance imaging of the knee is widely used to diagnose meniscus injury, and clinicians often use MRI findings as a factor in determining whether a person should undergo an arthroscopic meniscectomy. However, there is a lack of epidemiological data on the prevalence of meniscus tears in the general population.

Funding: *The author(s) received no financial support for the research, authorship, and/or publication of this article.*

Conflict of Interest: *The authors declare that they have no conflict of interest.*

Ethical statement:

The study was approved by Local Clinical Research Ethics Committee (Decision number: 2020/253, Date: 27.10.2020), and written informed consent was obtained from each subject.

Open Access Statement

This is an open access journal which means that all content is freely available without charge to the user or his/her institution under the terms of the Creative Commons Attribution Non-Commercial License (<http://creativecommons.org/licenses/by-nc/4.0>). Users are allowed to read, download, copy, distribute, print, search, or link to the full texts of the articles, without asking prior permission from the publisher or the author.

References

- [1] Murray CJL, Vos T, Lozano R, et al. Disability-adjusted life years (DALYs) for 291 diseases and injuries in 21 regions, 1990-2010: A systematic analysis for the Global Burden of Disease Study 2010. *Lancet*. 2012;380(9859):2197–223.
- [2] Bortoluzzi A, Furini F, Scirè CA. Osteoarthritis and its management - Epidemiology, nutritional aspects, and environmental factors. *Autoimmun Rev*. 2018;17(11):1097-104.
- [3] Nguyen USDT, Zhang Y, Zhu Y, et al. Increasing prevalence of knee pain and symptomatic knee osteoarthritis: Survey and cohort data. *Ann Intern Med*. 2011;155(11):725–32.
- [4] Englund M, Guermazi A, Gale D, et al. Incidental Meniscus Findings on Knee MRI in Middle-Aged and Elderly Persons. *N Engl J Med*. 2008;359(11):1108–15.
- [5] Makris EA, Hadidi P, Athanasiou KA. The knee meniscus: Structure-function, pathophysiology, current repair techniques, and prospects for regeneration. *Biomaterials*. 2011;32(30):7411–31.
- [6] Guermazi A, Niu J, Hayashi D, et al. Prevalence of abnormalities in knees detected by MRI in adults without knee osteoarthritis: Population-based observational study (Framingham Osteoarthritis Study). *BMJ*. 2012;345(7874).
- [7] Kumm J, Turkiewicz A, Zhang F, et al. Structural abnormalities detected by knee magnetic resonance imaging are common in middle-aged subjects with and without risk factors for osteoarthritis. *Acta Orthop*. 2018;89(5):535–40.
- [8] Chambers HG, Chambers RC. The Natural History of Meniscus Tears. *J Pediatr Orthop*. 2019;39(6):53–5.

- [9]Englund M, Guermazi A, Lohmander SL. The Role of the Meniscus in Knee Osteoarthritis: a Cause or Consequence? *Radiol Clin North Am.* 2009;47(4):703–12.
- [10]Kornaat PR, Bloem JL, Ceulemans RY, et al. Osteoarthritis of the Knee : Association between Clinical Features and MR Imaging Findings. *Radiology.* 2006;239(3):811–7.
- [11]Jacobson JA, Girish G, Jiang Y et al. Radiographic Evaluation of Arthritis : Degenerative Joint Disease and Variations. *Radiology.* 2008;248(3):737–47.
- [12]Hayes CW, Jamadar DA, Welch GW, et al. Osteoarthritis of the Knee : Comparison of MR Imaging Findings with Radiographic Severity Measurements and Pain in Middle-aged Women. *Radiology.* 2005;237(3):998-1007.
- [13]Nguyen JG, Smet AA De, Graf BK, et al. MR Imaging-based Diagnosis and Classification of Meniscus Tears. *RadioGraphics.* 2014;34(1):981-99.
- [14]Kellgren JH, Lawrence JS. Radiological Assessment of Osteo-Arthrosis. *Ann Rheum Dis.* 1957;(3):494–502.
- [15]Abram SGF, Beard DJ, Price AJ, et al. The Knee National consensus on the definition, investigation, and classification of meniscus lesions of the knee. *The Knee.* 2018;25(5):834-40.
- [16]Russ P, Kilcoyne RF, Russ PD, et al. MR imaging patterns of displaced meniscus injuries of the knee. *Am J Roentgenol.* 1998;17(1):63–7.
- [17]Bhattacharyya T, Gale D, Dewire P, et al. The clinical importance of meniscus tears demonstrated by magnetic resonance imaging in osteoarthritis of the knee. *J Bone Jt Surg.* 2003;85(1):4–9
- [18]Fox AJS, Wanivenhaus F, Burge AJ, et al. The human meniscus : a review of anatomy, function, injury, and advances in treatment. *Clin Anat.* 2014;28(2):269-87.
- [19]Fox MG. MR imaging of the meniscus : review, current trends, and clinical implications. *Radiol Clin North Am.* 2007;45(6):1033–53.
- [20]Guermazi A, Hayashi D, Jarraya M, et al. Medial posterior meniscus root tears are associated with development or worsening of medial tibiofemoral cartilage damage : the multicenter osteoarthritis study. *Radiology.* 2013;268(3):814-21.
- [21]Svensson F, Felson DT, Zhang F, et al. Meniscus body extrusion and cartilage coverage in middle-aged and elderly without radiographic knee osteoarthritis. *Eur Radiol.* 2019;29(4):1848-54.